Technical University of Denmark

DTU

Matrix changes and side effects induced by electrokinetic treatment of porous and particulate materials

Skibsted, Gry; Ottosen, Lisbeth M.; Jensen, Pernille Erland; Elektorowicz, Maria

Publication date:
2013

Document Version
Publisher's PDF, also known as Version of record

Link back to DTU Orbit

DTU Library
Technical Information Center of Denmark

Matrix changes and side effects induced by electrokinetic treatment of porous and particulate materials

PhD-thesis, 2013

Gry Skibsted

BYG DTU - Department of Civil Engineering

Technical University of Denmark

Front page:
Removed amounts of Al, Fe and Si during electrodialytic remediation (EDR)
of soil (Soil 1 in Appendix A)

Title: Matrix changes and side effects induced by electrokinetic treatment
of porous and particulate materials.

(c) Gry Skibsted, 2013

Publisher: BYG·DTU – Department of Civil Engineering
Building 118, 2800 Kgs. Lyngby, Denmark

Preface

This thesis is submitted in the completion of my PhD study at the Technical University of Denmark (DTU). The work has been carried out in the section for Building Materials at the Department of Civil Engineering (BYG-DTU). The main supervisor was associated professor Lisbeth M. Ottosen (BYG-DTU) and co-supervisors were Researcher Pernille E. Jensen (BYG-DTU) and Professor Maria Elektorowicz (Concordia University, Montreal, Canada). The PhD study was funded by The Danish Agency for Science Technology and Innovation (Project no. 09-065880, Fundamentals of Electrokinetics in In-Homogenous Matrices).

I would like to thanks my colleagues in the group of Building Materials for a friendly and supportive working environment, my PhD-student colleagues for moral support and the "Electrochemistry Group" for inspiration, great discussions and eager to share knowledge. Especially, I would like to thanks Lisbeth M. Ottosen and Pernille E. Jensen for scientific discussions, positive comments and for having confidence in my work and Maria Elektorowicz for visiting DTU several times, for discussions of clay and matrix changes and for the scientific support and advice. I would like to thank Henryk Sobczuk for introduction and close collaboration on testing Time-Domain Reflectometry (TDR in combination with electrokinetic treatment. For assistance with experimental work and sample measurements I would like to thanks laboratory technicians Sabrina Madsen, Louise Gammeltoft and Christina Winther Dufke and especially I would like to thanks Ebba C. Schnell for her coordinating role and supervision with the practical work. I am grateful to Louise Josefine Belmonte and Gunvor M. Kirkelund for support in conducting XRD analysis and to Inge Rörig-Dalgaard and emeritus Anders Nielsen for instructions in managing the light microscope according to analysis of thin sections.

Finally I would like to thank my family and friends and especially my husband and our children for support, understanding and cheering during my work.

Gry Skibsted
December 2013

Abstract

Transport of ions in an applied electric field holds many applications within both civil and environmental engineering, e.g. for removal of chlorides from concrete to hinder reinforcement corrosion, remediation of heavy metals from soils and other waste materials and recently for desalination of porous stone materials to hinder decay. However, in addition to the removal of target ions in these systems, matrix changes may occur during the electrochemical treatment. For a broader implementation of the electrokinetic methods it is important to understand changes in the matrix composition for different types of materials. *The overall aim of this PhD-project is to evaluate matrix changes and side effects induced by electrokinetic treatment of porous and particulate materials.*

During electro-remediation protons are produced at the anode and hydroxyl ions are produced at the cathode. The consequent pH changes may influence the matrix of the treated materials. *The main research objectives were to identify matrix changes during electro-remediation, to investigate the impact of induced matrix changes on the removal of target elements and finally to evaluate the extent of Al dissolution during electrodialytic remediation and the impact on the implementation of soil remediation, e.g. concerning the toxicity of residual soluble Al in the soil matrix.*

Electrokinetic treatment was carried out as electrodialytic remediation (EDR) of three particulate matrices (soils and clay) and electrochemical desalination (ED) of three different porous matrices (brick and sandstones). The degree of impact of the induced side effects by electro-remediation on the different types of matrices is related to the subsequent purpose of the treated material. For electrochemical desalination of a porous matrix e.g. sculpture from cultural heritage, the properties of the matrix must remain unaffected by the treatment. Irreversible treatments of such matrices are unacceptable, e.g. in case of increased porosity, the materials is increasingly vulnerable to environmental exposure. The present work has investigated potential pH, chemical and porosity changes of the matrix during ED. In EDR it is not crucial to avoid matrix changes as in ED, but it is important to know which matrix changes are taking place, as these may influence the overall remediation result. In addition, the overall toxicity of the soil must not increase during the treatment e.g. concerning the concentration of soluble Al.

EDR experiments with the three particulate matrices showed that soil weathering occurred during EDR by dissolution of minerals. Pb mobilization was initiated after acidification due to dissolution and removal of calcite from the matrix. In addition to Pb mobilization, acidification caused dissolution of Al from the matrix. Mobilization of Al during EDR was not found to be problematic for the two tested soil matrices, as the mobilization of Al was slower than the electromigration out of the matrix. However, for the clay mineral matrix (illite) the concentration of acid soluble Al increased in the matrix during EDR. The illite matrix was negatively affected by the EDR treatment. Thus the risk of increasing soluble Al

in the matrix has to be evaluated in each specific case before implementation of soil remediation.

From X-ray powder diffraction it was found that calcite was decomposed in the EDR treated soil. No new mineral phases were developed and no other phases than calcite were fully decomposed. Since dissolution of Al, Fe and Si minerals was observed, it was thus concluded that these elements were dissolved by partial decomposition of soil minerals.

The porous matrices studied in this work were Red Brick, Nexø sandstone and Gotland sandstone. The Red Brick and the Nexø sandstone is considered relatively inert matrices while the Gotland sandstone is a limestone and thus adversely affected by acid. To avoid the observed matrix change of dissolution of the bonding material ($CaCO_3$) resulting in an increased porosity during ED it is important to use a $CaCO_3$-containing poultice for neutralizing the acid produced at the anode. This generates electromigration of Ca^{2+} from the anode towards the cathode. The ED removal rate of SO_4^{2-} is observed lower than for Cl^- and NO_3^-. The reason was precipitation of gypsum when SO_4^{2-} reacts with Ca^{2+} from the poultice. Precipitation of gypsum did not prevent desalination of SO_4^{2-}, although the ED removal rate was reduced.

Resumé

Transport af ioner i et elektrisk spændingsfelt har mange anvendelsesmuligheder inden for både bygge og miljøområdet, f.eks. til fjernelse af klorid ioner fra beton for at forhindre korrosion af armeringsjernet, til fjernelse af tungmetaller fra jord og andre affaldsmaterialer og senest til afsaltning af porøse sten materialer for at forhindre nedbrydning. I tillæg til fjernelse af de målrettede ioner, kan der ske matrix ændringer under den elektrokemiske behandling. For en bredere implementering af de elektrokinetiske metoder er det vigtigt at forstå ændringer i sammensætningen af matricen for de forskellige typer af materialer. *Det overordnede formål med dette ph.d.-projekt er at evaluere matrixændringer og sideeffekter induceret af elektrokemisk behandling af porøse og partikulære materialer.*

Ved elektrokemisk rensning dannes der protoner ved anoden og hydroxyl ioner ved katoden. De medfølgende pH ændringer kan påvirke matricen af det behandlede materiale. *De forskningsmæssige hovedformål med studiet er at identificere matrixændringer ved elektrokemisk rensning, at undersøge indvirkningen af inducerede matrixændringer på fjernelsen af de målrettede ioner og endelig at evaluere omfanget af Al opløsning under elektrodialytisk rensning og betydningen for implementeringen af jord rensning, f.eks. vedrørende giftigheden af tilbageværende opløst Al i jord matricen.*

Det eksperimentelle arbejde er baseret på elektrodialytisk rensning (EDR) af tre partikulære materialer (jord og ler) og elektrokemisk saltfjernelse (ED) af tre forskellige porøse materialer (mursten og sandsten). Hvor kritiske de inducerede side effekter fra elektrokemisk behandling er for de forskellige matricer afhænger af den efterfølgende brug af matricen. For elektrokemisk saltfjernelse fra porøse materialer som f.eks. skulpturer fra vores kulturarv, skal egenskaberne forblive upåvirkede af behandlingen. En irreversibel behandling af en sådan matrix er uacceptabel, f.eks. i tilfældet af en øget porøsitet vil matricen blive mere sårbar overfor miljømæssige påvirkninger. I dette arbejde er mulige pH-, kemiske- og porøsitetsændringer for matricen undersøgt under ED. Ved EDR er det ikke vitalt at undgå matrixændringer som ved ED, men det er vigtigt at kende til de matrixændringer der sker, da de kan påvirke rensningsresultatet. I tillæg må giftigheden af jorden ikke øges under behandlingen, f.eks. ved en øget koncentrationen af opløseligt Al.

EDR eksperimenter med de tre partikulære matricer viste at jordforvitring forekom under EDR ved opløsning af mineraler. Pb mobiliseringen startede efter kalciumkarbonat var opløst og fjernet fra matricen, hvorefter jorden blev forsuret. I tillæg til Pb mobiliseringen, medførte forsuringen også opløsning af Al fra matricen. Al mobiliseringen under EDR blev ikke fundet problematisk for de to testede jordmatricer, da mobiliseringen af Al var langsommere end elektromigrationen ud af matricen. For ler mineral matricen (illite) derimod, forøgedes koncentrationen af syreopløseligt Al under EDR behandlingen. Derfor bør risikoen for en øget opløselighed af Al i matricen evalueres i hvert specifikt tilfælde før implementering af jordrensning.

Ved analyse med røntgen pulver diffraktion blev det fundet at kalciumkarbonat var fjernet fra jorden under EDR. Der var ikke dannet nye mineralfaser og ikke andre faser end kalciumkarbonat var fjernet totalt. Eftersom opløsning af Al, Fe og Si mineraler blev observeret, konkluderes det at disse grundstoffer er opløst ved en delvis nedbrydning af jord mineraler.

De porøse matricer, som blev undersøgt i dette studie var Rød mursten, Nexø sandsten og Gotland sandsten. Den røde mursten og Nexø sandstenen betragtes som relativt inerte matricer hvorimod den Gotlandske sandsten er en kalksten og dermed negativt påvirket af syre. For at forhindre den observerede matrixændring ved opløsning af bindingsmaterialet ($CaCO_3$), som resulterer i en øget porøsitet under ED, er det vigtigt at anvende et $CaCO_3$-holdig materiale for at neutralisere den producerede syre ved anoden. Dette skaber en transport af Ca^{2+} fra anoden mod katoden. ED hastigheden hvormed SO_4^{2-} blev fjernet var lavere end for Cl^- og NO_3^-. Årsagen var at SO_4^{2-} reagerede med Ca^{2+} fra buffermaterialet, hvorved der blev udfældet gips. Udfældning af gips forhindrede ikke afsaltning af SO_4^{2-} selvom ED hastigheden for fjernelsen blev reduceret.

Table of contents

Appendix – list

A   Long-term electrodialytic soil remediation – Soil weathering (Paper)

B   Long-term electrodialytic soil remediation – Effect on removal efficiency of lead (Paper)

C   The possibility of using electrokinetics for desalination of sandstone with low porosity (Paper published in: Proceedings from the 8th fib international PhD Symposium in Civil Engineering, DTU, Denmark June 20-23 2010, pp 455-460)

D   Electrochemical desalination of bricks – removal of Cl, NO_3 and SO_4 (Paper submitted)

E   Electrochemical desalination of limestone contaminated with Na_2SO_4 – the importance of buffering anode produced acid (Paper)

F   Electrodialytic decomposition of the clay mineral illite (Additional experimental data)

Conference contributions

- 8th Symposium in Civil Engineering, 2010, DTU, Denmark. (Paper, Appendix C).

- EREM 2010, 9th symposium in electrokinetics, Taiwan. Title: The impact of the pore volume in sandstone on the electrochemical desalination rate. (Poster: Electrochemical desalination of sulfate from stone and the impact of calcium ions).

- Annual meeting of the Danish Electrochemical Society, October 2010, DTU, Denmark. Title: The impact of calcium ions on the electrokinetic desalination of sulfate from stone: Preliminary results. (Poster: The impact of calcium ions on the electrokinetic desalination of sulfate from stone: Preliminary results).

- EREM 2011, 10th symposium in electrokinetics, Belgium. Title: Test of a non-destructive method for determination of moisture changes in particulate materials during electrokinetic treatment. (Poster: Test of a non-destructive method for determination of moisture changes in particulate materials during electrokinetic treatment).

1. Introduction

Electrokinetic treatment has been recognized as a promising technology for different purposes in both civil and environmental engineering. The technique utilizes the application of an electric DC field for transportation of ions (electromigration) and liquid (electroosmosis). In the field of *civil engineering* the applied electric field is used for removal of chlorides from concrete to hinder reinforcement corrosion (Bertolini et al. 1996, Mietz 1998, Hosseini and Khaloo 2005, Fajardo et al. 2006), and in recent research for desalination to hinder salt induced decay of bricks (Ottosen and Rörig-Dalgaard 2007 and 2009, Rörig-Dalgaard et al. 2012, Kamran et al. 2012[a]), natural sandstones (Ottosen and Christensen 2012, Petersen et al. 2010) and tiles (Ottosen et al. 2010[a], Ferreira et al 2011). In addition, electromigration has been tested for in-situ impregnation of heritage wood (Ottosen et al. 2010[b]). In the field of *environmental engineering* electro-remediation of polluted soils has been investigated (Lageman et al. 1989). Electrokinetic treatment has also been applied for remediation of other materials, e.g. fly ashes and impregnated wood waste (Ottosen et al. 2003). The main focus of research in electrokinetic treatment has so far been on optimizing the transport of target elements in different matrices, and in general electrokinetics is found powerful as solution to the many different problems. However, few studies have investigated the potential side effects induced by the electrokinetic treatment.

During electro-remediation protons are produced at the anode and hydroxyl ions are produced at the cathode. The consequent pH changes may influence the matrix of the treated materials. For electrochemical desalination of a porous matrix e.g. sculpture from cultural heritage, the properties of the matrix must remain unaffected by the treatment and changes in e.g. porosity are not accepted. Some porous stone matrices are sensitive to acid attack and thus neutralization of the produced acid from the anode is important to prevent damage. Placement of the electrodes in $CaCO_3$ rich clay poultice can be a solution for neutralizing the formed acid, whereby Ca-ions are released. The influence of free Ca-ions on the removal efficiency of target elements needs to be evaluated.

Acidification is important in electrokinetic remediation of heavy metal polluted soil. Heavy metals are adsorbed strongly to soil particles, but are in general mobilized by acidification. However, acidification is undesirable for the soil matrix. The acids will significantly alter the soil geochemistry as well as the soil microstructure (Alshawabkeh 2009). To mobilize the heavy metals from the soil, the soil must be acidified and this means that the buffering capacity of the soil must be overcome, before the remediation process starts. Dissolution of e.g. calcite is thus important before mobilization of heavy metals is initiated, but the low pH reached can also initiate dissolution of Al-minerals, which is undesirable due to the toxicity of soluble Al. For implementation of the electrokinetic methods it is important to understand changes of the matrix composition for the different types of materials.

The overall aim of this PhD-project is to evaluate matrix changes and side effects induced by electrokinetic treatment of porous and particulate materials. The work builds on the following main research objectives:

- Identification of matrix changes during electrodialytic remediation (EDR) and electrochemical desalination (ED), with focus on dissolution of minerals, potential development of new minerals and compositional changes in the pore structure.

- Investigation of the impact of induced matrix changes on the removal of target elements.

- Evaluation of the extent of Al dissolution during EDR of particulate soil matrices and the potential impact on implementation of soil remediation, e.g. concerning toxicity of residual soluble Al.

The thesis is primarily written as papers, focusing on the listed research topics. The thesis is written according to the guidelines from DTU for a paper based PhD-thesis with a summary of the background and major findings from the experimental work.

2. Background

The present work is focusing on electrodialytic remediation of Pb polluted soil and salt extraction from porous stone materials. To evaluate the impact of the induced matrix change on the removal of target elements, it is important to understand the different characteristics of the matrices. The target elements are bound differently in the matrices, which can influence how easily the elements are mobilized.

2.1 Soil and heavy metals in soils

Soil is a complex heterogeneous medium composed of solid minerals (e.g. rock fragments, phyllo-silicates, clay minerals, oxides of Fe, Al and Mn and carbonates), organic solids, aqueous and gaseous components (Adriano 1986). Heavy metals are part of the terrestrial ecosystem, as they are in the earth's geological basic material and are released by weathering of the soil minerals. Heavy metals will thus always to some extent be present in soil (Jensen et al. 1996).

Geochemically, heavy metals introduced into the soil may end up in one or more of the following phases; (1) dissolved in the soil solution, (2) linked to exchange sites of organic solids or inorganic constituents and consequently named as the exchangeable fraction, (3) fixed into soil minerals, (4) precipitated with other components in the soil or (5) incorporated into the biological material. The first two phases are mobile forms and phyto-available, the last three are immobile and sometimes become mobile and phyto- available with time (Adriano 1986). Darmawan and Wada (1999) observed from sequential extraction of soil spiked with soluble salts of Cu, Pb and Zn, that Cu and Pb in the exchangeable fraction decreased at prolonged incubation time and the part in the oxide bond fraction increased. From sequential extraction of kaolinite and forest soil, both spiked with Cu, Ottosen et al. (2006) showed that aging is important for the adsorption strength of Cu. In the study Ottosen et al (2006) observed a tendency for Cu to be found in higher steps of sequential extraction after 30 days compared to 2 days of incubation time.

Mobilization of heavy metal ions is required for the electro-remediation methods to work. In general, heavy metal cations are most mobile under acidic conditions and increasing the pH usually reduces their bioavailability (Alloway 1995). Thus desorption of heavy metal cations is more feasible at reduced pH. There are however exceptions to this tendency; As, Mo, Se and some valence states of Cr are commonly more mobile under alkaline conditions (Adriano 1986). Other factors than pH are also impacting the mobility of heavy metals in soils. Jensen et al. (2007) evaluated the importance of Pb speciation and the soil composition such as organic matter, for the feasibility of EDR, and observed that Pb speciation is of primary importance. The speciation of Pb in industrially polluted soils depended on the stability of the original speciation of Pb and the contamination level, while the soil characteristics were of secondary importance (Jensen et al. 2006). Ottosen et al. (2006) showed that even though the soil types were very similar then Cu was adsorbed stronger in an industrially polluted soil

than in a spiked soil. The stronger adsorption reduced the removal efficiency by electrochemical treatment. In general, the removal efficiency of electrochemical treatment is much higher for spiked matrices than from industrially polluted (Table 1 in Appendix B).

In industrially polluted soils heavy metals are strongly bound and desorption/mobilization of the heavy metals requires acidification, which might also cause weathering of the soil minerals. Clear signs of matrix decomposition due to electro-remediation have been reported, e.g. removal of Al, Fe and Si from polluted soil or clay minerals (Kliem 2000, West et al. 1999, Roy 1049, Caldwell and Marshall 1942), removal of Ca, Mn, Mg and Fe from soil (Ottosen et al. 2001) and removal of cations from pure mineral matrices (Cameron and Bell 1905, Mattson 1926, Hla 1945). However, little knowledge about the potential side effects induced by electrokinetic soil remediation is available and therefore more research is needed before implementation.

2.2 Salt decay

Salt induced decay is an important issue in the weathering of porous stone materials. Dissolved salts penetrate the porous matrix together with moisture and due to continuous evaporation and supply of salt solution; the solution inside the porous matrix can become supersaturated and cause salt precipitation (Lewin 1982). The crystal formation can generate a pressure on the pore walls, which can result in cracking and blistering of the material surface (Winkler 1987; Rodriguez-Navarro and Doehne 1999; Ruedrich and Siegesmund 2007).

The origin of the salts varies; most comes from de-icing roads with NaCl, from groundwater rising through masonry, from salts entrapped in the masonry, from salts in ocean aerosols, and from desert dust (Winkler 1987). NaCl, $NaNO_3$, Na_2SO_4 and $MgSO_4$ are among the most common salts in building materials (Steiger 2005).

The impact of salts on weathering depends on the salt type, on the size and shape of the capillary system, on the moisture gradient in the material, and the exposure to solar radiation (Winkler 1987). The location where the salt crystallizes is determined by the dynamic balance between the rate of evaporation of water from the surface and the rate of resupply of solution to that site (Lewin 1982). Two different salt crystallization mechanisms can take place: If the rate of resupply of solution to the surface is sufficient to compensate the rate of evaporation, the solution deposits on the surface and the pattern is named efflorescence. If the rate of transport of solution through the pores of the masonry does not bring fresh liquid to the surface as rapidly as the liquid evaporates, a dry zone develops beneath the surface and the crystallization occurs within the pores of the stone; named subflorescence (Lewin 1982). Efflorescence is primarily a visual problem as it can be removed mechanically from the surface, while subflorescence is the more damaging mechanism, see examples in Figure 1.
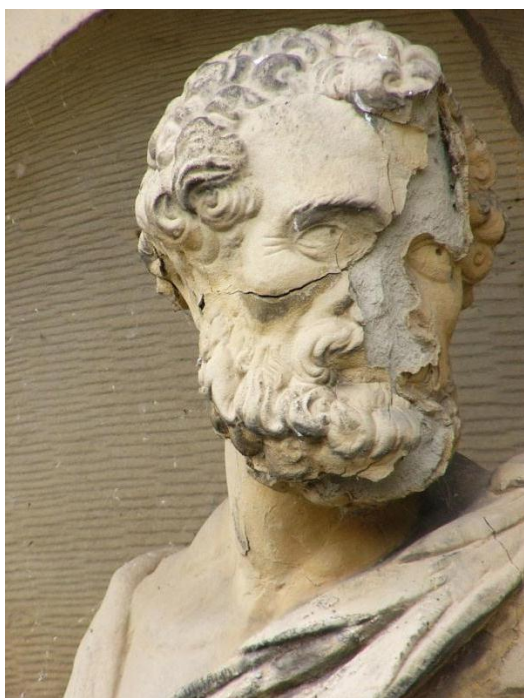
Sculpture. Picture: Lisbeth M. Ottosen (2007)

Monument. Picture: Lisbeth M. Ottosen (2007)

Portuguese tiles. Picture: Lisbeth M. Ottosen (2011)

Masonry. Picture: Lisbeth M. Ottosen (2007)

Figure 1: Examples of subflorescence salt decay.

Currently, most methods for preventing salt damage problems are aimed at reducing the salt content in the material, where one of the most common *in situ* approaches is to use a poultice (Pel et al. 2010). In the poultizing method soluble salts are extracted through the application of a moistened absorbing material (poultice/plaster) on the surface of the object. Electrochemical desalination (ED) is an alternative method, where an applied electric DC field promotes the removal of salt ions in the pore solution of a porous, moist material (Ottosen and Rörig-Dalgaard 2009).

Salt crystals in porous stone are not adsorbed to the matrix as heavy metals are in soils. Thus mobilization depends on dissolution of salt crystals which only need a soft treatment compared to desorption of heavy metals from soil.

2.3 Principles of electro-remediation

Electro-remediation of target elements from either solid or particular porous materials is based on the fundamentals of electrolysis, where charged species are transported towards the oppositely charged electrodes under the action of an applied electric field. The primary electrode reactions are (1) oxidation of water at the anode, generating acid and (2) reduction of water at the cathode, producing an alkaline front.

$$H_2O \rightarrow 2H^+ + \frac{1}{2}O_2(g) + 2e^- \qquad (1)$$

$$2H_2O + 2e^- \rightarrow 2OH^- + H_2(g) \qquad (2)$$
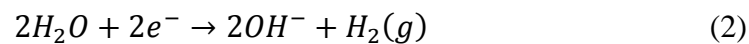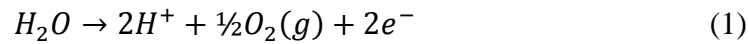
The principal mechanisms by which element transport takes place under the action of an electric field are electromigration, advection of elements by electroosmotic flow and electrophoresis (Probstein & Hicks, 1993), and diffusion due to the generated concentration gradients.

- Electromigration: Movement of charged species in a solution caused by an electric field.
- Electroosmosis: Movement of liquid relative to a stationary charged surface caused by an electric field.
- Electrophoresis: Movement of charged particles (e.g. colloides, clay particles, and organic particles) relative to a stationary liquid caused by an electric field.
- Diffusion: Movement of elements in solution caused by concentration gradient.

Several compositional and external variables affect the contribution of each transport mechanism to the total mass flux: soil mineralogy; pore fluid composition and conductivity; electrochemical properties of the species in the pore fluid; and porosity and tortuosity of the porous medium (Acar and Alshawabkeh 1993).

The flux of the ions is a product of the driving force (gradient) and a constant for each transport mechanism. For electromigration the constant is the ionic mobility, for electroosmosis it is the electroosmotic mobility, for the electrophoretic flux the constant is the electrophoretic mobility and for the diffusion flux it is the diffusion coefficient. The ionic mobility for heavy metals, and common salt ions in soil are usually of the order $10^{-8}\text{m}^2/(\text{V}\cdot\text{s})$ (Table 1).

Table 1: Ionic mobility for selected anions and cations in free electrolytes at 25 °C

Element	Ionic mobility (10^{-8} m^2/V·s)	Reference	Element	Ionic mobility (10^{-8} m^2/V·s)	Reference
H^+	36.23	Atkins 1998	OH^-	20.64	Atkins 1998
Al^{3+}	6.32	Lide 1997	Cl^-	7.19	Atkins 1998
Ca^{2+}	6.17	Atkins 1998	CO_3^{2-}	7.46	Atkins 1998
Cd^{2+}	7.36	Lide 1997	NO_3^-	7.40	Atkins 1998
Cr^{2+}	6.94	Lide 1997	SO_4^{2-}	8.29	Atkins 1998
Cu^{2+}	5.56	Atkins 1998			
Fe^{3+}	5.6	Lide 1997			
K^+	7.62	Atkins 1998			
Na^+	5.19	Atkins 1998			
Pb^{2+}	7.36	Lide 1997			
Zn^{2+}	5.47	Atkins 1998			

The ionic mobility for H^+ and OH^- are significant higher than for the other ions, and is relevant to have in mind when working with electrochemical treatment, as a part of the current will be used on transporting those two ions. Acar and Alshawabkeh (1993) demonstrated by the principles of species transport under the action of an electric field that ionic migration (electromigration) was the most significant component of mass transport in electrokinetic remediation in most soils.

The average electroosmotic mobility in soil is usually in the order of $5 \cdot 10^{-9}$ m^2/(V·s) (Lageman et al. 1989). This is an order of magnitude lower than the ionic mobility for heavy metals in soils (Table 1). Electroosmosis in a pore occurs because of the drag interactions between the bulk of the liquid in the pore and the thin layer of charged fluid (electric double layer) next to the pore wall that, like a single ion, is moved under the action of the electric field in a direction parallel to it (Probstein and Hicks, 1993). Both counter and co-ions will be transported with the electroosmotic flow (electroosmotic advection). In desalination of bricks the electroosmotic effect on ion transport is expected to be almost absent at high salt concentrations because of high conductivity in the pore water outside the electric double layer which means that current preferentially passes here. It is only at low salt concentrations electroosmosis is expected to play a role (Ottosen & Rörig-Dalgaard 2009).

The order of electrophoretic mobility in soils varies between 10^{-10} and 10^{-9} m^2/(V·s) (Lageman et al. 1989). This is lower than both the electroosmotic mobility and the ionic mobility. Electrophoresis becomes significant in electrokinetic remediation when e.g. surfactants are introduced in the processing fluid to form micelles (charged particles) with other spices or when the technique is employed in remediating slurries (Acar and Alshawabkeh 1993). Electrophoresis is of high importance in some electrokinetic systems, e.g. for removal of Cd from sewage sludge, where severe fouling was seen at the anion exchange membrane (Jakobsen et al. 2003). However, Colloidal particle transport by electrophoresis is of little importance in compacted soils (Probstein and Hicks 1993).

The diffusion coefficient for charged species in soils is often at least 1 order of magnitude less than the ionic mobility of the same species (Acar and Alshawabkeh 1993). In addition, the ionic mobility of an ion in a unit electric field is about 40 times per charge higher than the diffusion coefficient, which means that electromigration contributes more than diffusion in the ion transport in an electric field (Acar and Alshawabkeh 1993). The relation between the ionic mobility and the diffusion coefficient, can be calculated from the Einstein relation in Equation 3 (Atkins 1998) , where F is the Faraday constant, R the gas constant, T is the temperature and z is the valence of the ion (i). For a monovalent ion at 298 K, the ionic mobility of the ion is thus 38.9 V^{-1} times higher than the diffusion coefficient of the same ion.

$$u_i = \frac{z \cdot D_i \cdot F}{R \cdot T} \qquad (3)$$

In a free electrolyte, the diffusion coefficients for Cl^-, Na^+, H^+ and OH^- are in the order of $(0.33 - 5.30) \cdot 10^{-9} m^2$/s (Atkins 1998), but in porous materials the effective diffusion coefficient are lower than that of free electrolytes. Based on the concept Binary Salt Diffusion[1], Ahl (2004) measured the effective diffusion coefficient in new Finish red bricks to vary between $(2.71 - 5.44) \cdot 10^{-10} m^2$/s for 0.05 M salt solutions of KCl, $NaNO_3$, $CaCl_2$, Na_2SO_4, $MgCl_2$ and Na_2CO_3. In three different types of red bricks the result for the diffusivity of 0.05 M NaCl solution were $(3.37 - 4.99) \cdot 10^{-10} m^2$/s (Ahl 2003). The relationship between the effective diffusion in porous materials and the diffusion of free electrolytes is affected by both the porosity and the tortuosity factor of the material. However, the impact of the porosity and tortuosity factor is the same for diffusion and electromigration (Acar and Alshawabkeh 1993).

Electromigration is expected to be the major mechanism for transport of the ions in the matrices selected for this study, but diffusion and electroosmosis might also contribute to the total mass flux. Likewise, the effect of electrophoresis is believed of limited importance in the selected matrices, since no surfactants were added and the experiments were made with stationary matrices and not slurries.

2.4 Electrodialytic remediation

In electrodialytic remediation (EDR), ion-exchange membranes are used to separate the particulate matrix from the electrode compartments with electrolytic solutions and to avoid hydroxyl ions from the cathode to enter the matrix (Jensen et al. 1994) (Figure 2). Due to the net-negatively charged surface of soil particles and thus less free anions than cations in the pore solution, the limiting current of the anion exchange membrane is lower than for the

---

[1] In binary salt diffusion, where only one electrolyte, e.g. NaCl is present, the highly mobile chloride and the slower sodium ions are constrained by electrostatic forces to move at the same rate and the flux of sodium chloride is characterized by a single diffusion coefficient (Ahl 2003).

cation exchange membrane. During EDR the limiting current for the anion exchange membrane is exceeded, thus an acid-front is generated due to water-splitting, and this front will move through the soil towards the cathode (Ottosen et al. 2000). Thus pH in the soil solution decreases, which in general is an advantage for the mobilization of adsorbed heavy metals, but it can also affect the original soil matrix. The amount of ions available for electromigration in the soil solution is controlled by both desorption/adsorption and precipitation/dissolution processes.
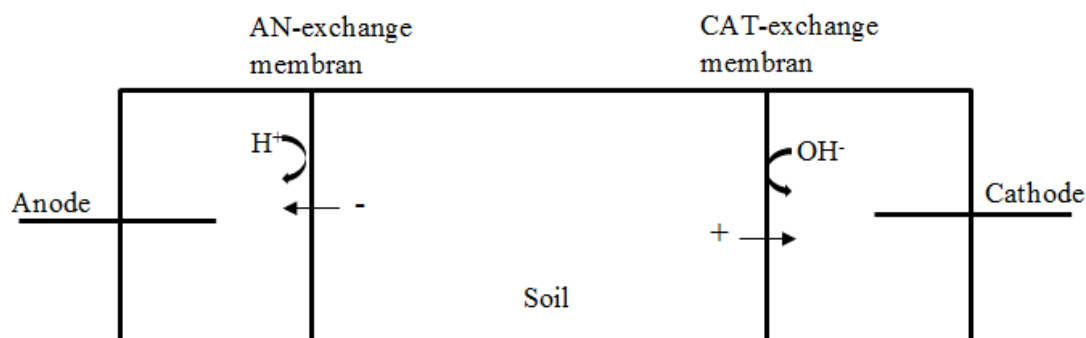

Figure 2: Illustration of electrodialytic soil remediation (EDR). The anode compartment at the left (with the anode), center compartment for the soil and the cathode compartment (with the cathode) at the right. The three compartments are separated with ion-exchange membranes.

A stirred setup (with stirring of the soil solution) was more efficient for removal of heavy metals from harbor sediments compared to a stationary setup (compacted soil without stirring) (Nystrøm et al. 2004). In the stationary setup the mobilization occurred in the regions of the matrix, where the acid front had caused acidification. This enabled evaluation of regional profiles in the soils and thus the stationary setup was selected for the present work.

2.5 Electrochemical desalination

Electrochemical desalination is based on application of an electric DC field over the salt contaminated stone and utilization of electromigration as transport mechanism for free ions out of the sample (Ottosen & Rörig-Dalgaard 2007). By electromigration the ions are transported in the pore solution towards the electrode of opposite polarity. In ED (Figure 3) the electrodes are placed in external electrode compartments filled with a $CaCO_3$ rich clay poultice. A reason for using poultice instead of liquid in the electrode compartments, as used in EDR, is the high risk of leakage at the joints between stone and electrode compartment with electrolytic solutions. Furthermore capillary suction of electrolytic solution into the stone is reduced by the use of clay poultice. Finally, the poultice (1) act as storage location for ions removed from the material matrix, (2) ensures buffering of the acid at the anode and to some extent hydroxyl ions produced at the cathode, and (3) creates contact between the electrodes and the contaminated matrix (Ottosen and Rörig-Dalgaard 2009).
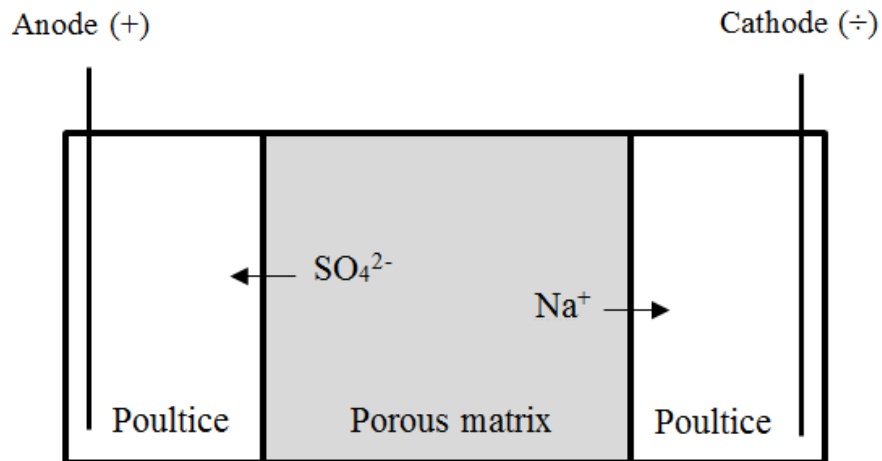
Figure 3: Principle of the electrochemical desalination method with separate compartments for electrodes.

Acidification is a potential damaging mechanism for porous matrices. Radeka (2007) observed an increased porosity in roofing tiles when exposed to 4 % acetic acid. ED experiments conducted without buffering at the electrodes have underlined that the buffering poultice is vital to the method and visible damage of limestone due to the acid generated at the anode has been reported (Herinckx et al. 2011). In addition, it has been shown that electromigration of target ions in an inert matrix was inhibited due to an extremely high potential drop caused by collision of the alkaline and acidic fronts in the stone, as this zone was depleted of ions (Kamran et al. 2012[b]).

A clear advantage of the ED method compared to the poultice method without application of an electric field, is that the electrodes (placed in poultice) do not have to cover the whole surface of the desalination object. The electric field will be strongest where the conductivity is highest and that is where the ion concentration is highest.

In relation to this study the focus will be on the potential side effects from neutralizing the acid with $CaCO_3$ containing poultice during ED.

3. Major findings from the experimental work

3.1 Overview of the studied matrices

The thesis is based on experimental work on both particulate and porous matrices (Figure 4).
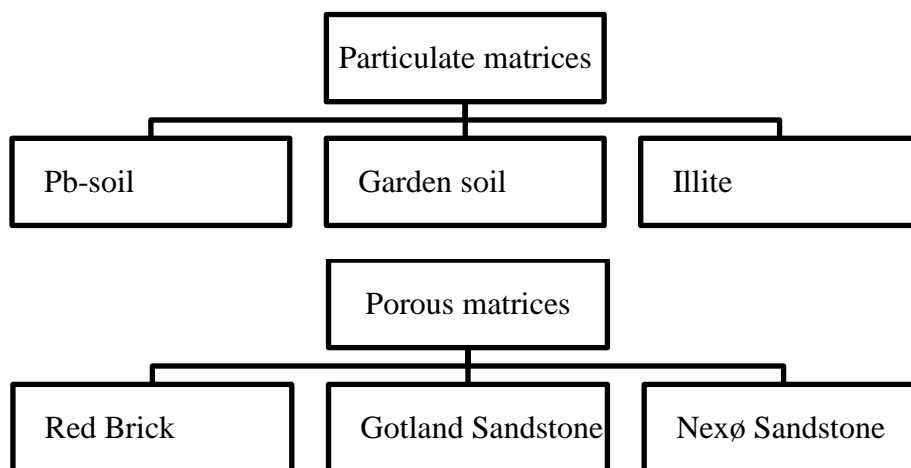
Figure 4: Overview of the studied matrices.

The following provides a short description of each of the studied matrices:

Pb-Soil: An industrially Pb contaminated soil was collected from an excavated pile at KMC (Kalvebod Miljøcenter), which is a disposal site for polluted soil in Denmark. It contained 9.1 % $CaCO_3$ and 3.3 % organic matter.

Garden soil: An unpolluted soil sample was collected from a garden in the north of Zealand, Denmark. It was sampled below 10 cm depth and contained 0.2 % $CaCO_3$ and 6.4 % organic matter.

Illite: This clay shale matrix only contains minerals and was obtained from Ward's Natural Science. Before use the material was crushed to a fine powder. Illite is not a specific mineral name, but the name for the group of minerals with composition between smectite and muscovite and an abundance of interlayer K. The used illite matrix has a mixed-layer structure, meaning that it does not have a defined structure.

Red Brick: Danish red, baked clay bricks with the porosity 31.5 % and 0.6 % $CaCO_3$. It is the only tested factory made porous matrix.

Gotland and Nexø sandstones are from Kronborg Castle, Helsingør, Denmark. The Nexø sandstone was removed during a minor renovation, while the Gotland sandstones were unused stone samples.

Gotland: Limestone with $CaCO_3$ as bonding material. The porosity is about 20 % (Suenson 1942) and it contained 6.0 % $CaCO_3$.

Nexø: A violet/red sandstone. It was visually inhomogeneous and separate layers were visible by variations in color and grain size. The porosity was 8 %. Nexø sandstones consist of grains of mainly quartz and feldspar, and the bonding material is silicon (Suenson 1942).

The Red Brick and the Nexø sandstone are considered relatively inert matrices while the Gotland sandstone is a limestone and thus adversely affected by acid.

An overview of the experimental work carried out for evaluation of the research objectives is shown in Table 2.

Table 2: Overview of the experimental work documented in the appendixes

Appendix	Title	Matrix	Method	Contaminants	Current density (mA/cm^2)	Treatment time
A	Long-term EDR - Soil weathering	Pb-soil, Garden soil	EDR	Pb	0.1	842 days
B	Long-term EDR – effect on removal efficiency of lead	Pb-soil, Garden soil	EDR	Pb	0.1	842 days
C	The possibility of using electrokinetics for desalination of sandstone with low porosity	Nexø sandstone	ED	Na$_2$SO$_4$	0.1	72 hours
D	Electrochemical desalination of bricks – removal of Cl$^-$, NO$_3^-$ and SO$_4^{2-}$	Red Brick	ED	Na$_2$SO$_4$ NaNO$_3$ NaCl	0.2	0, 1,2,5,8 days
E	ED of limestone contaminated with Na$_2$SO$_4$ – the importance of buffering anode produced acid	Gotland sandstone	ED	Na$_2$SO$_4$	0.2	0, 8 days
F	Electrodialytic decomposition of the clay mineral illite	Illite	EDR	Non-polluted	0.2 and 0.4	8 days 35 days

(EDR) Electrodialytic Remediation, (ED) Electrochemical Desalination.

3.1 Matrix changes

The identification of matrix changes during electro-remediation was focused on mineral dissolution, development of new phases and porosity changes. The porosity changes are only relevant for ED of porous matrices.

3.1.1 Mineral dissolution

From the two soil matrices (Appendix A) and the illite matrix (Appendix F) reductions in the mass of solid matter and removal of Al, Fe and Si during EDR were observed. The removal of Al, Fe and Si from the illite matrix confirmed mobilization/dissolution of these elements from clay minerals during EDR. Since illite is a pure clay mineral matrix, the removed Al, Fe and Si must have originated from the mineral matrix.

The removed amounts of Al, Fe and Si for the three particulate matrices during EDR are shown in Table 3. Dissolution of Si containing minerals initiated immediately after the electric field was applied and continued during the entire treatment. The amount of removed Si constituted less than 0.5 % of the total initial Si content in every case. For the two soil matrices less than $3 \cdot 10^{-6}$ % of the current was carried by Si and thus the energy consumption used for Si removal was concluded to be negligible.

Acidification caused dissolution of first $CaCO_3$ followed by Al- and Fe-minerals (Appendix A). The Pb-soil had a higher $CaCO_3$ content than the Garden soil and correspondingly the buffering capacity against acid was highest for the Pb-soil. In accordance to this, the time for acidifying the matrix and reaching a pH low enough to start dissolution of Al- and Fe-minerals was thus shortest in the Garden soil. The result was a higher degree of dissolved Al and Fe in the Garden soil compared to the Pb-soil (Table 3).

Table 3: Removed fraction obtained of Al, Fe and Si during EDR of particulate matrices.

Appendix	Matrix	Current density (mA/cm^2)	Treatment time (days)	Removed (mg)	Fraction of total content
A	Garden soil	0.1	842	801 (Al)	3.5 % (Al)
				720 (Fe)	8.3 % (Fe)
				383 (Si)	0.2 % (Si)
A	Pb-soil	0.1	842	457 (Al)	1.1 % (Al)
				383 (Fe)	1.1 % (Fe)
				642 (Si)	0.3 % (Si)
F	Illite	0.4	35	798 (Al)	3.3 % (Al)
				2110 (Fe)	23 % (Fe)
				329 (Si)	0.5 % (Si)

There are no defined limit values for acid soluble Al in soils (*Miljø- og Energiministeriet 2010*). Therefore as target criteria it was argued that the concentration of acid soluble Al should be lower or identical to the initial conditions in the matrix, since the matrices were not toxic due to Al before EDR. The acid soluble concentrations of Al in the particulate matrices after EDR are presented in Table 4. For the Garden soil the acid soluble concentration of Al was reduced during EDR. For the Pb-soil the acid soluble concentration of Al was on average slightly increased. However, in 50 % of the matrix (the region closest to the anode) the concentration of Al was reduced by 24.6 % compared to the initial concentration. This indicated that in the two soil matrices the dissolution of Al from the minerals was slower than the electromigration towards the electrolytes and the soil toxicity from acid soluble Al was not increased.

The acid soluble Al increased in both EDR experiments with illite (Table 4). There was no significant deviation (<1 %) in Al concentration between the slices in the illite after EDR. This indicated that kinetic equilibrium was established between the dissolution and electromigration rates of Al.

Thus for the two soil matrices it was concluded that dissolution of Al was not critical during EDR, while for the illite matrix EDR resulted in an undesirable increase in the acid soluble concentration of Al.

Table 4: Acid soluble Al (DS 259) in the three particulate matrices

Appendix	Matrix	Current density (mA/cm^2)	Treatment time (days)	Initial acid soluble Al (mg/kg)	Final acid soluble Al (mg/kg)
A	Garden soil	0.1	842	4890	4390 ± 580
A	Pb-soil	0.1	842	4310	4610 ± 1650*
F	Illite	0.4	35	9660	17400 ± 190
F	Illite	0.2 and 0.4	2 and 6	9660	17500 ± 287

* In 50 % of the matrix (the region closest to the anode) the average value was 3250 mg/kg

3.1.2 Development of new mineral phases

From EDR of the Pb-soil visual signs of changes in the soil matrix were observed. A white hard layer had developed at the interface between the soil matrix and the cation-exchange membrane. SEM analysis showed that the precipitated layer was composed of 58 wt % (O), 25.4 wt % (Si), 11.7 wt % (Al) and 4.9 wt % (Fe). Based on the results from the SEM analysis and the color it was suggested to be a combination of natural soil constituents such as quartz, kaolinite and Fe-oxides. This indicated that dissolved cations of Al, Fe and Si migrated towards the cathode compartment and thus out of the soil matrix, where the elements

precipitated in a white layer at the membrane or passed into the catolyte. This can be characterized as a developed external phase during long-term EDR of the Pb-soil.

The two soil matrices and the Gotland sandstone (Appendix E) were analyzed by X-ray powder diffraction (XRD) before and after electro-remediation. Except for full dissolution of calcite in the two soil matrices, there was no sign of new developed phases or lack of crystalline minerals. From the XRD analysis it was not possible to evaluate if the concentration of the different mineral phases were changed during EDR. However, from the observation that Al, Fe and Si were removed (Table 3) and the fact that no specific minerals except calcite were fully decomposed it was concluded that only partial decomposition of soil minerals had occurred.

3.1.3 Porosity changes

ED of SO_4^{2-} from Gotland sandstone showed that buffering of acid produced at the anode was important to avoid decomposition of the stone seen as an increased porosity close to the anode due to dissolution of calcite (Appendix E). At the tested conditions, the used poultice was found to provide sufficient buffer capacity to hinder porosity changes in the Gotland sandstone.

3.2 Influence of induced matrix changes on remediation

Matrix changes induced by electro-remediation can influence the removal efficiency of the target ions. In the following the findings will be described for ED of salt from porous stone matrices and for EDR of Pb-polluted soil.

3.2.1 Electrochemical desalination

In the ED experiments it was found that SO_4^{2-} was reduced between 44 % and 89 % for the tested matrices (Table 5). The reduction of SO_4^{2-} in the Nexø Sandstone (porosity 8 %) showed that ED is effective even for a matrix with a low porosity. The removal of NO_3^- and Cl^- from the Red Brick by ED was more efficient than the removal of SO_4^{2-} (Table 5).

Table 5: Reduction of anions in different matrices by electrochemical desalination

Appendix	Matrix	Current density (mA/cm^2)	Treatment time (days)	Reduction (%)
C	Nexø Sandstone	0.1	4	44 % (SO_4^{2-})
D	Red Brick	0.2	8	99 % (Cl^-) 100 % (NO_3^-) 89 % (SO_4^{2-})
E	Gotland Sandstone	0.2	8	72 % (SO_4^{2-})

The ED removal rate of SO_4^{2-} was found to be 25 % lower than the ED removal rate for Cl^- and NO_3^- in the Red Brick (Appendix D). The lower ED removal rate for SO_4^{2-} can be linked to the use of $CaCO_3$ rich poultice for neutralizing acid produced at the anode, resulting in release of Ca-ions. This allows penetration of Ca^{2+} into the stone matrix by electromigration and precipitation of $CaSO_4$ in the pore solution, when the Ca^{2+} reacts with SO_4^{2-}. The gypsum formation is a side effect caused by the use of $CaCO_3$ rich poultice in the anode compartment. The poultice is required for buffering the anode produced acid and avoiding damage of the treated matrix e.g. resulting in an increased porosity (Appendix E).

For SO_4^{2-} extraction from Gotland sandstone by ED (Appendix E), gypsum formation in the region closest to the anode was not detectable by XRD. The highest possible amount of formed gypsum (calculated on basis of Ca^{2+} and SO_4^{2-} in the sample) was < 1 % which is below the detection limit for the XRD analysis. Although gypsum formation was not verified by XRD, chemical analysis of the treated matrix showed an increase in both the Ca^{2+} and SO_4^{2-} content in the region closest to the anode. For the Red Brick (Appendix D) the theoretically calculated concentrations of Ca^{2+} and SO_4^{2-} in the pore solution of the stone matrix closest to the anode were more than three orders of magnitude higher than the solubility of gypsum. These findings strongly indicated that gypsum formation was occurring and could be a reasonable explanation for the reduced ED removal rate of SO_4^{2-}.

In the Red Brick (Appendix D) the concentrations of Ca^{2+} and SO_4^{2-} in the region closest to the anode started to decrease after 5 days of ED. Thus precipitation of gypsum was not found to be a permanent problem and neutralization of acid with $CaCO_3$-containing poultice was evaluated to be suitable even when SO_4^{2-} is the target anion.

3.2.2 Electrodialytic soil remediation

In EDR of Pb-polluted soil (Appendix B), it was shown that the Pb mobilization was initiated after the buffering capacity from $CaCO_3$ was used up. Thus dissolution and removal of $CaCO_3$ was a necessary matrix change for initiating the mobilization of Pb. In addition to the mobilization of Pb, dissolution of soil minerals occurred when the soil was acidified. Pb was reduced in the soil by EDR, but with the undesired side effect of Al dissolution, which can be problematic for the implementation of soil remediation, e.g. concerning toxicity of residual soluble Al in the matrix. In Appendix B, the dissolution of Al continued for the remaining treatment time. For this specific soil matrix the mobilization of Al was not evaluated to be problematic since the mobilization of Al was slower than the electromigration out of the matrix. This is not the case for all matrices (se section 3.1.1) and thus the risk of increasing the soluble Al concentrations in the matrix by EDR has to be evaluated in each specific case before implementation of EDR.

In the part of the Pb-soil located closest to the anode more Pb was removed than the initial level of acid soluble Pb (Appendix B). This showed that part of the acid insoluble Pb, e.g. from the mineral matrix, was dissolved during EDR. In addition, the soil contained significant

levels of acid soluble Pb after EDR, indicating that EDR induced a redistribution of Pb from the acid insoluble fraction to the acid soluble fraction.

4. Conclusion

Experiments with electrodialytic remediation (EDR) of the three particulate matrices showed that soil weathering occurs during EDR by dissolution of minerals. In contrary to Al- and Fe-minerals, acidification was not required for mobilization of Si. Dissolution of Si containing minerals initiated immediately after the electric field was applied and continued during the entire treatment.

From X-ray powder diffraction of the soil matrices it was seen that EDR treatment resulted in total dissolution of the calcite. No new mineral phases were identified and no other phases than calcite were fully decomposed during the EDR treatment. Since dissolution of Al, Fe and Si minerals was observed, it was thus concluded that these elements were dissolved by partial decomposition of soil minerals.

During ED of limestone it was found to be important to use a buffering poultice for neutralizing the acid produced at the anode, to hinder dissolution of the bonding material ($CaCO_3$) resulting in an increased porosity.

ED was proven effective for the reduction of Cl^-, NO_3^- and SO_4^{2-}, but usage of the $CaCO_3$-containing poultice influenced the ED removal rate of SO_4^{2-}. The ED removal rate of SO_4^{2-} was observed to be lower than for Cl^- and NO_3^-, due to formation of gypsum when Ca^{2+} from the poultice at the anode precipitated with SO_4^{2-} in the matrix. Precipitation of gypsum was not found to be a permanent problem and use of the $CaCO_3$-containing poultice was evaluated to be suitable even when SO_4^{2-} is the target anion.

In EDR of Pb-polluted soil, it is known that dissolution of $CaCO_3$ is essential for initiating the mobilization of Pb. Dissolution of Al was initiated only when the soil was acidified. Concerning the toxicity of residual soluble Al in the matrix this can be problematic for the potential use of the soil after the treatment.

Mobilization of Al during EDR was not found to be problematic for the two soil matrices. The mobilization of Al was slower than the electromigration out of the matrix. However, for illite the concentration of acid soluble Al increased in the matrix during EDR. Thus the risk of increasing soluble Al in the matrix has to be evaluated in each specific case before implementation of soil remediation. The final acid soluble concentration of Al in the matrix depended on the kinetic equilibrium between the dissolution and the electromigration of Al towards the electrolytes.

EDR of heavy metal polluted soil is, in contrary to ED of porous materials, a method for upgrading the soil and thus matrix changes can be acceptable, as long as the soil is not becoming more toxic, e.g. with regards to acid soluble Al.

In addition to dissolution of Al, redistribution of Pb from the acid insoluble fraction to the acid soluble fraction was identified to occur during EDR treatment of the soil.

References

Acar YB, Alshawabkeh AN (1993). Principles of electrokinetic remediation. Environ Sci Technol 27: 2638-2647.

Adriano DC (1986). Trace elements in the terrestrial environment. Springer, New York.

Ahl J (2003). Salt diffusion in brick structures - Part I: Measurements with NaCl. Material Science 38: 2055-2061.

Ahl J (2004). Salt diffusion in brick structures - Part II: The effect of temperature, concentration and salt. Material Science 39: 4247-4254.

Alloway BJ (1995). Heavy Metals in Soils, 2nd edition. Blackie Academic & Professional, UK, Chapter 2.

Altin A, Degirmenci M (2005). Lead (II) removal from natural soils by enhanced electrokinetic remediation. Sci. Total Environment 337: 1-10.

Atkins PW (1998). Physical Chemistry, 6th edition. Oxford University Press, Oxford.

Atkins PW, Paula J de (2010). Physical Chemistry, 9th edition. W.H. Freeman and Company, New York.

Bertolini L, Yu SW, Page CL (1996). Effects of electrochemical chloride extraction on chemical and mechanical properties of hydrated cement paste, Advn Cement Res 8(31): 93–100.

Caldwell OG, Marshall CE (1942). A study of some chemical and physical properties of the caly minerals Nontronite, Attapulgite and Saponite. University of Missouri, Research Bulletin 354: 15-20.

Cameron FK, Bell JM (1905). The mineral constituents of the soil solution. U.S. Dept Agr Bureau of Soils Bul 30.

Darmawan, Wade S (1999). Kinetics of speciation of copper, lead, and zinc loaded to soils that differ in cation exchanger composition at low moisture content. Commun Soil sci plant anal 30: 2363-2375.

Fajardo G, Escadeillas G, Argiguie G (2006). Electrochemical chloride extraction (ECE) from steel-reinforced concrete specimens contaminated by "artificial" sea-water, Corros Sci 48: 110-125.

Ferreira CMD, Ottosen LM, Christensen IV, Brammer SH, Sveegaard DAF (2011). Evaluation of salt removal from Azulejo tiles and mortars using electrodesalination, In: Proceedings from the international conference on durability of building materials and components, XII DBMC, Porto, PORTUGAL, 2011.

Hla T (1945). Electrodialysis of mineral silicates: an experimental study of rock weathering. Mineral Mag 27: 137-145.

Hamed J, Acar YB, Gale RJ (1991). Pb(II) removal from kaolinite by electrokinetics. Geotechnical Engineering 117: 241-271.

Han SJ, Kim SS (2003). Application of enhanced electrokinetic extraction for lead spiked kaolin. Civil Engineering 7: 499-506.

Herinckx S, Vanhellemont Y, Hendrickx R, Roels S, De Clercq H (2011) Salt removal from stone building materials using an electric field. In: Proceedings from the international conference on salt weathering on building and stone sculptures, Limassol, Cyprus 19-22 October 2011, pp 357-364.

Hosseini A, Khaloo AR (2005). Study of electrochemical chloride extraction as a non-destructive repair method: Part I. Discrete test samples. Asian J Civ Eng (Building and Housing) 6(3), 167–182.

Jakobsen MR, Fritt-Rasmussen J, Nielsen S, Ottosen LM (2003). Electrodialytic removal of cadmium from wastewater sludge. Hazardous Materials 106B: 127-132.

Jensen JB, Kubes V and Kubal M (1994). Electrokinetic remediation of soils polluted with heavy metals. Removal of zink and copper using a new concept. Environmental Technology 15: 1077-1082.

Jensen J, Bak J, Larsen MM (1996). Tungmetaller i danske jorder. TEMA-rapport fra DMU, Miljø-og Energiministeriet, Danmarks Miljøundersøgelser, Silkeborg, Danmark. ISBN: 87-7772-235-3.

Jensen PE, Ottosen LM, Ferreira C, Villumsen A (2006). Kinetics of electrodialytic extraction of Pb and soil cations from a slurry of contaminated soil fines. Hazardous Materials B138: 493-499.

Jensen PE, Ottosen LM, Harmon TC (2007). The effect of soil type on the electrodialytic remediation of Lead-contaminated soil. Environ Eng 24: 234-244.

Kamran K, Pel L, Sawsy A, Huinink H, Kopinga K (2012a). Desalination of porous building materials by electrokinetics: an NMR study. Materials and structures 45: 297-308.

Kamran K, Van Soestbergen M, Huinink HP, Pel L (2012b). Inhibition of electrokinetic ion transport in porous materials due to potential drops induced by electrolysis. Electrochem Acta 78: 229-235.

Kim SO, Moon SH, Kim KW (2001). Removal of heavy metals from soils using enhanced electrokinetic soil processing. Water, air and soil pollution 125: 259-272.

Kim WS, Kim SO, Kim KW (2004). Enhanced electrokinetic extraction of heavy metals from soils assisted by ion exchange membranes. Hazardous Materials 118: 93-102.

Kliem BK (2000). Bonding of heavy metals in soil, PhD-thesis, Department of Geology and Geotechnical Engineering and Department of Chemistry, Technical University of Denmark.

Lageman R, Pool W, Seffinga G (1989). Electro-Reclamation - Theory and Practice. Chemistry and industry 18: 585-590.

Lewin SZ (1982). The mechanism of masonry decay through crystallization, In: Conservation of Historic Stone Buildings and Monuments, Washington, D.C.: National Academy of Sciences, pp. 120-144.

Li RS, Li LY (2000). Enhancement of electrokinetic extraction from lead-spiked soils. Environ Eng 126: 849-857.

Lide DR (1997). CRC Handbook of Chemistry and Physics, CRC Press, New York.

Mattson S (1926). Electrodialysis of the colloidal soil material and the exchangeable bases. Journal of agricultural research 33: 553-567.

Mietz J. (1998). Electrochemical rehabilitation methods for reinforced concrete structures. A state of the art report, Publication no. 24 of the European Federation of Corrosion, The Institute of Materials, London.

Miljø-og Energiministeriet, Danmarks Miljøundersøgelser (2010). Liste over kvalitetskriterier i relation til forurenet jord og kvalitetskriterier for drikkevand. [Online] Available: http://www.mst.dk/NR/rdonlyres/0AB0AF23-4BD6-4901-BCD9-

43F6F6FD6FC1/124958/Kvalitetskriterierjord_og_drikkevandfinaljuniogjul.pdf. Date: 2013-12-01, (Danish Environmental Protection Agency).

Ottosen LM, Hansen HK and Hansen CS (2000). Water splitting at ion-exchange membranes and potential differences in soil during electrodialytic soil remediation. Journal of Applied Electrochemistry 30: 1199-1207.

Ottosen LM, Villumsen A, Hansen HK, Ribeiro AB, Jensen PE, Pedersen AJ (2001). Electrochemical soil remediation – accelerated soil weathering? In: Proceedings from the 3rd Symposium and Status Report on Electrokinetic Remediation, 18-20 April, 2001, Karlsruhe, pp. 5.1-5.14.

Ottosen LM, Kristensen IV, Pedersen AJ, Hansen HK, Villumsen A, Ribeiro AB (2003). Electrodialytic removal of heavy metals from different solid waste products. Separation science and technology 38(6): 1269-1289.

Ottosen LM, Lepkova K, Kubal M (2006). Comparison of electrodialytic removal of Cu from spiked kaolinite, spiked soil and industrially polluted soil. Hazardous Materials B137: 113-120.

Ottosen LM, Rörig-Dalgaard (2007). Electrokinetic removal of Ca(NO3)2 from bricks to avoid salt-induced decay. Construction and Building Materials 27: 390–397.

Ottosen LM, Rörig-Dalgaard I (2009). Desalination of a brick by application of an electric DC field. Materials and Structures 42: 961-971.

Ottosen LM, Ferreira CMD, Christensen I (2010a). Electrokinetic desalination of glazed ceramic tiles. Journal of Applied Electrochemistry 40: 1161-1171.

Ottosen LM, Block T, Nymark M, Christensen IV (2010b). Electrochemical in situ impregnation of wood using a copper nail as source for copper, Wood Sci Technol 45: 289-302.

Ottosen LM, Christensen IV (2012). Electrokinetic desalination of sandstones for NaCl removal - test of clay poultices at the electrodes. Electrochimica Acta 86: 192– 202.

Paz-Garcia JM, Johannesson B, Ottosen LM, Ribeiro AB, Rodriguez-Maroto JM (2011). Influence of the chemical interactions on the removal rate of different salts in electrokinetic desalination processes, In: Proceedings from the international conference on salt weathering on building and stone sculptures, Limassol, Cyprus 19-22 October 2011, pp. 373-380.

Pel L, Sawsy A, Voronina V (2010). Physical principles and efficiency of salt extraction by poulticing. Cultural Heritage 11: 59-67.

Petersen G, Ottosen LM and Jensen PE (2010) The possibility of using electrokinetics for desalination of sandstone with low porosity, In: Proceedings from the 8th fib international PhD Symposium in Civil Engineering, DTU, Denmark June 20-23 2010, pp. 455-460.

Probstein RF, Hicks RE (1993). Removal of contaminated soils by electric fields. Science 260: 498-503.

Radeka M, Kiurski J, Markov S, Marinković-Nedučin R (2007). Microbial deterioration of clay roofing tiles. In: Structural Studies, Repairs and Maintenance of Heritage Archicture X, Edited by Brebbia CA. WIT press, Southampton, Boston.

Rodriguez-Navarro C, Doehne E (1999). Salt weathering: Influence of evaporation rate, supersaturation and crystallization pattern. Earth Surf. Process. Landforms 24: 191-209.

Roy R (1949). Decomposition and resynthesis of the micas. Journal of the American ceramic society 32: 202-209.

Ruedrich J, Siegesmund S (2007). Salt and ice crystallization in porous sandstones. Environ Geol 52: 225-249

Steiger M (2005). Crystal growth in porous materials – I: The crystallization pressure of large crystals. Journal of crystal growth 282: 455-469.

Suenson E (1942). Byggematerialer, 3 bind: Natursten, 3[ed] edition. Jul. Gjellerups forlag, København, pp 117-139.

Sun TR, Geiker MR, Ottosen LM (2012). The effect of pulse current on energy saving during electrochemical chloride extraction (ECE) in concrete, Balkema in ICCRRR, Published by Taylor and Francis.

Toumi A, Francois R, Alvardo O (2007). Experimental and numerical study of electrochemical chloride removal from brick and concrete specimens. Cement and Concrete Research 37: 54-62.

Vengris T, Binkiene R, Sveikauskaité A (2001). Electrokinetic remediation of lead-, zinc and cadmium-contaminated soil. Chem Technol Biotechnol 76: 1165-1170.

West LJ, Steward DI, Binley AM and Shaw B (1999). Resistivity imaging of soil during electrokinetic transport. Engineering Geology 53: 205-215.

Winkler EM (1987). Weathering and weathering rates of natural stone. Environ Geol Water Sci 9: 85-92.

Appendix A

Long-Term electrodialytic soil remediation – Soil weathering

Gry Skibsted[1], Lisbeth Ottosen[1], Pernille E. Jensen[1] and Maria Elektorowicz[2]

[1]Department of Civil Engieering, Technical University of Denmark, Building 118, 2800 Kgs. Lyngby, Denmark.

[2]Department of Building, Civil and Environmental Engineering, Concordia University, Montreal, Quebec, Canada.

Long-term electrodialytic soil remediation – soil weathering

Gry Skibsted[1,*], Lisbeth M. Ottosen[1], Pernille E. Jensen[1] and Maria Elektorowicz[2]

[1]Department of Civil Engineering, Technical University of Denmark, Building 118, 2800 Kgs. Lyngby, Denmark.

[2]Department of Building, Civil and Environmental Engineering, Concordia University, Montreal, Quebec, Canada.

*Corresponding Author: gryp@byg.dtu.dk

Key words: Mineral dissolution, Soil weathering, Matrix changes, Si solubility, Al dissolution, Fe dissolution, Electrokinetics, Long-term treatment

Abstract Electrodialytic soil remediation (EDR) was used to evaluate the weathering risk of soil minerals during electrochemical treatment. Long-term EDR experiments were conducted with two different soils; an unpolluted soil (Soil 1) and a Pb polluted soil (Soil 2). A constant current of 5 mA was applied for 842 days and samples from the electrolytes were collected and analyzed 22 times during the treatment. The long treatment illustrates worst case concerning soil weathering. In the Pb polluted soil a white hard layer developed at the boundary facing the cation exchange membrane. SEM analysis showed that this was composed solely by (wt %) 58 % (O), 25.4 % (Si), 11.7 % (Al) and 4.9 % (Fe) and was suggested to be a combination of natural soil constituent such as quartz, kaolinite and Fe-oxides. The analytic results clearly showed that soil weathering occurs during the electrochemical treatment. Dissolution and removal of Al, Fe, Si and Ca from the soil during the EDR was the evidence of mineral dissolution; and the amounts of these elements mobilized and removed exceeds the fraction which can be extracted by digestion in 7 M HNO_3 (Danish Standard DS 259). However, the dissolved Si only constituted 0.2% and 0.3 % of the total content in total. The dissolved Al (3.5 % and 1.1 % from soils 1 and 2, respectively) migrated towards the cathode compartments and thus out of the soil matrix where it precipitated in the white layer at the membrane or passed into the catholyte, thus toxicity caused by Al-dissolution seems not to be an obstacle to electrokinetic treatment. A reduction in the dry matter was observed (4.5 % and 13.5 %), and mainly due to dissolution of $CaCO_3$ and organic matter but also a minor dissolution of soil minerals. The overall qualitative mineral composition was unaffected by EDR, except for calcite removal, which was complete; thus the observed weathering is probably related to a range of different minerals.
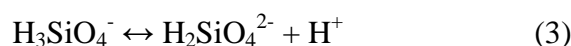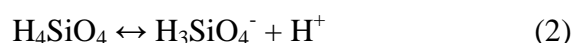
1. Introduction

This paper focuses on the release and removal of Ca, Al, Fe and Si during long-term electrodialytic soil remediation (EDR) with the aim to evaluate the weathering of the soil minerals during electrochemical soil remediation in worst case. In the paper (Skibsted et al. 2013), the long-term effect of electrodialytic soil remediation (EDR) of Pb was evaluated and both papers are products of the same electrodialytic remediation experiments, but scopes of the papers differ.

When a soil is treated electrochemically, changes in pH are arise from oxidation of water at the anode generating acid, and at the cathode the main product from the reverse reaction is hydroxyl. For the removal of heavy metals, the soil acidification causes desorption and thus mobilization of the pollutants for electromigration, thus the acidification aids the remediation. Hydroxyl ions, on the other hand, cause immobilization of the heavy metals and hamper the remediation. In EDR (Figure 1) ion-exchange membranes separate the soil from the electrolytes in the electrode compartments to prevent penetration of ions produced at the electrode reactions into the soil (Jensen et al. 1994). The use of the cation-exchange membrane hinders an alkaline front from passing into the soil from the cathode. Due to the net-negative surface of soil particles and thus less free anions than cations in the pore solution, the limiting current of the anion exchange membrane is lower than for the cation exchange membrane. During EDR the limiting current for the anion exchange membrane is exceeded, thus an acid-front is generated due to water-splitting, and this front will move through the soil towards the cathode (Ottosen et al. 2000). The pH decrease is essential for mobilization of heavy metals, but it can also affect the original soil matrix. Decrease in pH to 2.5-3 during EDR for 27 days at clay fraction < 2 μm resulted in dissolution of Al- and Fe-oxides and Si minerals (Kliem and Koch, 2000). West et al. (1999) observed a breakdown of the clay lattice in the acidified area near the anode and thus an increase in the aqueous Al and Si levels.

In the first half of the 20th century, matrix changes caused by electrokinetic treatment was investigated in works, which had removal of cations (Caldwell and Marshall 1942, Cameron and Bell 1905, Mattson 1926), to produce of hydrogen clay (Amorim et al. 2003), as the primary tasks. Caldwell and Marshall (1942) tested the possibility of using electrodialysis for converting three different clay minerals; Nontronite, Attapulgite, and Saponite, to their hydrogen clay form. For the first two clay minerals the electrodialytic treatment was successful with only a minor Si extraction, but Saponite decomposed rapidly (15.6 % Si extraction). Caldwell and Marshall (1942) suggested that it probably was a fragmental part of the clay lattice which decomposed. In the 1940's researchers used electrochemical treatment to investigate rock and soil weathering, and Roy (1949) observed that electrochemical treatment lead to decomposition of soil particles, as Muscovite released a small quantity of iron and alkali. From these early works it is obvious that electrochemical treatment can impact the soil matrix.

1.1 Dissolution of Si

Natural weathering causes dissolution of quartz and feldspar in all soils (Sokolova, 2012). Silica and silicates are the most abundant constituents in soils (Krauskopf and Bird 1995) and can also undergo natural weathering. The key step in natural weathering of silicates is repeated hydrolysis of the Si-O-Si structural unit at the surface of silicates creating a silicon bond to four OH groups. The silicon then leaves the surface as hydrated silica (H_4SiO_4) (Lasaga and Gibbs 1990). The equilibrium between α-quartz (a polymorphs crystalline form) and a silica solution (pH < 9) can be presented by equation (1). This implies that $SiO_2(aq)$ in the solution exists mainly as an uncharged monomeric species combined with two H_2O dipoles. H_4SiO_4 is a weak acid and it stepwise dissociated as given in (2) and (3). The equilibrium constants at 25 °C and 1 bar for (2) and (3) are $10^{-9.9}$ and $10^{-11.7}$ (Krauskopf and Bird 1995). The charged dissociation products of hydrated silica will be mobile in an applied electric field.

$$SiO_2 + 2H_2O \leftrightarrow H_4SiO_4 \qquad (1)$$

$$H_4SiO_4 \leftrightarrow H_3SiO_4^- + H^+ \qquad (2)$$

$$H_3SiO_4^- \leftrightarrow H_2SiO_4^{2-} + H^+ \qquad (3)$$

The intensity of Si dissolution depends on pH (Sokolova 2012). An applied electric field may act as an accelerated weathering process due to the fast acidification and continuous removal of the charged dissociation products. Previously, an indication of dissolution of Si minerals was observed in an acidified soil during EDR (Kliem and Koch 2000). Diluted acid appears to serve as cation acceptor, releasing the silica to dissolve as hydrated silica (Nutting 1937). A high solubility of silica requires sufficient acid to take the cations and sufficient water to hydrate the silica (Nutting 1945), however, an increasing acid concentration is not proportional to increasing amount of dissolved silica, as the dissolved silica will hydrate less as the acid concentration is increased. Nutting (1943) explains this with a developed competition for the water between the acid and silica in stronger acid solutions (6-20 % HCl) resulting in less dissolved silica.

Organic matter in soils apparently lowers the solubility of silica at low acid concentrations (Nutting 1943). The soil organic matter (humus) is divided into humic acids, fulvic acids, and the insoluble fraction; humins (Stevenson, 1994). The humic acids and the fulvic acids affect the dissolution rates of soil minerals differently. Fulvic acids accelerate the dissolution rates of both kaolinite and feldspar through complexation of Al at the surface of the mineral, but the rate depends on the type of ligands (Chin and Mills 1991, Drever and Stillings 1997). The fulvic acids dissolve framework cations (Si, Al, Fe and Mg) of minerals more readily than water, but the dissolution behavior depends on the complexing property of the acids present (Huang and Keller 1972). On the contrary, humic acids do not promote the dissolution of kaolinite (Chin and Mills 1991) and neither appear to increase the feldspar dissolution rates significantly at pH 4-7 (Drever and Stillings 1997).

Not only pH and content of organic acids affect the dissolution of silica; the presence of salts is important too. The solubility of amorphous silica in single salt solutions of either KCl, KNO_3, NaCl, $NaNO_3$, LiCl, $LiNO_3$, $MgCl_2$, $CaCl_2$, $MgSO_4$, $NaHCO_3$, or Na_2SO_4 decreases with increasing salt concentration. In addition, the hydration number of the present cation is important: the solubility of amorphous silica decreases with increasing hydration number, as the cations with the highest hydration number bind more water from the solvent (Marshall and Warakomski 1980). All together the ions in the soil solution both of organic acids or salts influence the solubility of silica, meaning that the release of silica from soils is highly complex. Re-precipitation of released silica may also occur, and precipitation products are for instance silicates from the Na-silicates being insolubilized by acids or the removal of H and OH from the silica-micellae, which causes them to flocculate and precipitate (Nutting 1943). When silica dissolves and dissociates, the Si-containing ions will be available for electromigration, and the present paper compares dissolution and electromigration of Si in two different soils during long term electrodialytic treatment (2½ years) in order to evaluate the risk and rate of weathering. To evaluate any adverse effects of electrokinetic soil remediation on the soil matrix, the present paper investigates the changes in soil matrix during prolonged electrodialytic remediation. Extraction of elements Ca, Al, Fe, K, Mg and Si from two different soils is evaluated in comparison with nitric acid extraction and in relation to the total contents.

2. Materials and methods

2.1 Materials

Two soils were used for the electrodialytic treatment; an unpolluted soil (Soil 1) and an industrially Pb contaminated soil (Soil 2), which was collected from an excavated pile at KMC (Kalvebod Miljøcenter); a disposal site for polluted soil in Denmark. The unpolluted soil was taken below 10 cm depth from a garden, located in the north of Zealand in Denmark. The soils were sieved through a 2.0 mm sieve, and only the fraction below 2 mm was used.

2.2 Characterization of the soil

After drying, the soil lumps formed were loosened by hand in a porcelain mortar before characterization. Soil pH was measured potentiometric in a suspension of 5 g soil and 12.5 mL 1 M KCl after 1 h of agitation. Danish standard (DS 259) was used to extract acid soluble metals from the soil; 1 g of soil added 20 mL 7M HNO_3 was autoclaved (120 °C, 200 kPa) for 30 min. After cooling, the samples were filtered through a 0.45 µm filter and cations in the extract were analyzed by ion coupled plasma – optical emission spectroscopy (ICP-OES, Varian 720-ES). The target elements were; Al, Ca, Cu, Fe, K, Mg, Pb and Si. The total content was measured after digestion of the soil in HF: 6 mL 65 % HNO_3, 2 mL 37 % HCl, and 2 mL 40 % HF were added to 0.25 g soil and treated in the microwave (Anton Paar) 1400 W, 28.7 bar. Following 12 mL 10 % H_3BO_3 was added (to complex free fluorides) and

the samples treated in the microwave again (900 W, 10.3 bar). The total concentrations were analyzed by ICP-OES (Varian Expert, model MPX). Extraction in 1 M HNO_3 for one week, was done by adding 50 mL 1 M HNO_3 to 10 g soil and after 1 week of agitation the sample was filtered through a 0.45 µm filter and cations in the extract analyzed by ICP-OES (Varian 720-ES).

The organic content was found as weight loss at 550 °C. The $CaCO_3$ content was measured volumetric after reaction with 10 % HCl, by use of a Scheibler instrument. The amount was calculated assumed that all carbonate was present as calcium-carbonate.

2.3 Experimental setup

The electrodialytic remediation (EDR) experiments were done in cylindrical Plexiglas cells with three compartments and an internal diameter at 8 cm (Figure 1). The soil sample was placed in the center compartment and separated from the two electrode compartments by Ionics(R) ion exchange membranes (AR204SZRA and CR67 HVY HMR427); an anion-exchange membrane separated the anode and the soil sample, and a cation-exchange membrane separated the cathode from the soil sample. Platinum coated rod electrodes were used. The center compartment with soil was 10 cm long and the two electrode compartments were 5 cm. Anolytes and catholytes were each 1 L of 0.01 M NaOH adjusted to pH 2 with HNO_3, continuously circulated between the electrode compartment and a glass flask. A constant current of 5 mA (corresponding to 0.1 mA/cm^2) was applied during both EDR experiments and the voltage was monitored. During EDR, the pH of the anolyte and catholyte was adjusted with 1 M HNO_3 or 5 M NaOH, respectively, to maintain pH about 2. The duration of the EDR experiments was 842 days. The initial water content of the soils was 26.8 % (Soil 1) and 16.2 % (Soil 2), obtained by adding distilled water to the soil.
The soil volume visually decreased in the experiment with soil (1) and to maintain good contact at the electrodes the cell was beaten gently against the table at day 163, 432, 457 and 519 to restore the contact.

2.4 Sampling and soil analysis

During the experiments the anolytes and catholytes were changed and samples were taken 22 times. Simultaneously, the electrodes were changed and cleaned by storage in 5 M HNO_3 overnight to dissolve the electro-precipitated mass and analyze the content. Before analysis the catholyte samples from EDR with Soil (2) was preserved according to the Danish Standard (DS 259) because it was observed that the Pb analysis were imprecise without preceding conservation: 16 mL sample added 4 mL concentrated HNO_3 was autoclaved (200 kPa, 120 °C) in 30 min. Concentrations of target elements were measured by ICP. Post EDR-treatment, the membranes were cleaned by storage for approximately 12 hours in 1 M HNO_3, and the element concentration was analyzed by ICP-OES (Varian 720-ES). The soil was divided into 10 slices perpendicular to the length of the compartment (numbered from the

anode). In each slice, the water content was measured as weight loss after drying at 105 °C for 24 h. The dry slices were crushed in a porcelain mortar and soil pH was measured as double determination in the slices and the concentrations of target elements were measured after DS 259. A hard, white precipitate had formed between the soil and the cation-exchange membrane for Soil 2 (Figure 2). The elemental composition of this precipitate was analyzed by scanning electron microscopy (SEM-EDX).

The mineral composition was determined qualitatively by X-ray powder diffraction (XRD, PANalytical X'Pert PRO diffractometer) using Cu K_α radiation and operating at 40 mA and 45 kV, and the program X'Pert High Score Plus for identification of minerals. Quality changes of the mineral matrix were analyzed by comparing XRD-graphs for the original soil samples and Slice 1 and Slice 10 after EDR.

3. Results and discussions

3.1 Initial characterization and extraction method

The concentrations of target elements in the two soils measured by the three different extractions methods; total digestion (HF), DS 259 and extraction in 1 M HNO_3 are shown in Table 1, whereas pH and concentrations of $CaCO_3$ and organic matter are shown in Table 2. The largest part of Al, Fe and Si was linked to the mineral matrix, and only minor fractions were acid soluble after DS 259. The total digestion showed that the Si content was higher than 300 g/kg, and that the Al content was approximately 35 g/kg for both soils. The concentration of Fe in Soil 2 was more than three times the concentration in Soil 1, which was due to different origin or natural weathering status of the soils: The $CaCO_3$ content was also substantially higher for Soil 2 (9.1 %) than Soil 1 (0.2 %), which was a surface soil, whereas Soil 2 was sampled from an excavated pile and may originate from deeper layers. The differences in origin and carbonate content indicate that the natural weathering status of Soil 1 had progressed further than that of soil 2, which may affect the sensitivity to electro-enhanced weathering, e.g. due to different buffer capacity against acidification.

For both soils the soluble fraction of Si in 1 M HNO_3 (0.1 %) was higher than the fraction dissolved by DS 259 (< 0.03 %). Thus, the 7 M HNO_3 solution used for the extraction of the acid soluble cations (DS 259) is too strong an acid compared to a 1 M HNO_3 solution for the dissolution of Si. This is due to less hydrated silica as the acid concentration is increased (Nutting 1945), and is in accordance with earlier observations of silica dissolution from the clay mineral montmorillonite by Nutting (1943). The dissolution of the other elements shown in Table 1 (Al, Fe, Ca, K, Mg and Pb) was as expected: higher dissolution by treatment with stronger acid.

3.2 Electromigration direction

More than 97 % of the mobilized Al migrated towards the cathode for both soils and for Soil 1 more than 99 % of the mobilized Fe also migrated as cations. In Soil 2, about 4 % of the removed Fe was transported towards the anode. Fe can form stable negatively charged complexes with organic acids like e.g. citrate (Pazos et al. 2008), and Fe may have formed negatively charged complexes with natural organic acids in the soil, and these complexes are following transported towards the anode. In general, the electromigration direction for Ca, K and Mg were towards the cathode, with more than 93 % of the extracted amounts collected in the cathode compartment and the remaining few percentages in the anode compartment. The migration direction for Si differed between the two EDR experiments (Figure 3): the part of the mobilized Si migrating towards the anode was 41 % for Soil 1 and 74 % for Soil 2. During the first 99 days of the EDR for Soil 1, the Si migrated towards both electrodes, but migration towards the anode was dominating. Afterwards, the far majority was migrating towards the cathode. For Soil 2 the Si migrated in both directions during the whole experiment, but the migration towards the anode was dominating. Silica was apparently transported in both anionic and cationic forms. Caldwell and Marshall (1942) reported from electrokinetic treatment of clay materials that Si was found at the cathode and suggested Si migrated as complexes created from fragmental parts of the clay lattice. Kliem and Koch (2000) observed Si in the anode compartment after electrodialytic remediation of soil, which can be explained by equations (2) and (3). Nutting (1943) reported that hydrated silica ($HSiO_3H$) apparently ionizes as $HSiO_3^- + H^+$ and $HSiO_2^+ + OH^-$ which together resulted in transport with and against the current during treatment of montmorillonite. Presence of NaCl also promoted the transport of Si as cations, $AlCl_3$ caused silica to migrate as anions and acids resulted in silica migrated almost equally in both directions (Nutting 1943). In a solution of Na-silicate the transport of silica towards both electrodes will be equal, too (Nutting 1943). These different observations for the migration directions of silica underline the complexity of the system. Major determining factors are pH and the composition of the soil solution.

3.3 Weathering of soil minerals

The long-term EDR of 842 days was extreme compared to what is realistic for electrokinetic soil remediation. The experiments are considered worst case in relation to soil weathering during the treatment. The pH was reduced throughout both soil specimens due to the electrodialytic treatment: from 5.9 to 2-2.5 in Soil 1 and from 7.8 to 2.5-3.5 in Soil 2 (Figure 4). At this pH it can be assumed that no $CaCO_3$ remains in the soils ($pKa_{,1}(H_2CO_3 \leftrightarrow HCO^{3-})$ = 6.35), which is confirmed by the XRD analysis (Figure 5). The removed amount of Ca (measured in the electrolytes) was 34 % higher for Soil 1 than the concentration measured after digestion in 7M HNO_3 (DS 259) (Table 3), thus the long-term EDR resulted in weathering of more Ca-minerals than the digestion.

The most common cations presented between the unit layers in clay minerals are Ca, K, and Mg, thus a part of the mobilized Ca may come from this source; however as the removed K and Mg were both below the acid soluble fractions it is not possible to determine whether part of these were extracted from acid tolerable clay minerals. The dissolution of different soil minerals differs under given conditions and this can explain the minor removal of K and Mg compared to Ca. For instance, silicates of the montmorillonite-beidellite group are much easier attacked by dilute acids than those of the kaolin, mica, talc or pyrophyllite groups (Nutting 1943). In addition, K is generally more stable, or more firmly fixed, in the interlayer space in some clay minerals than other alkaline cations (Moore and Reynolds 1997), which could explain the minor amount of K removed. In Figure 6 the accumulated amount of removed Ca during EDR for 842 days are presented. For Soil 2 the removed amount of Ca became constant at day 464 and indicates that the buffer capacity from $CaCO_3$ was eliminated. For Soil 1 the removed amount of Ca already exceeded the concentration measured by digestion in 7M HNO_3 (DS 259) at day 37 showing that the buffer capacity from $CaCO_3$ was eliminated before this day.

In Figure 7 the accumulated amounts of removed Al, Fe and Si in the electrolytes for both soils are shown. The acidification of the soil affected dissolution of Al- and Fe-oxides from the soil minerals. Al and Fe were detected in the electrolytes at day 37 for Soil 1 and at day 464 for Soil 2, simultaneously with a complete dissolution of $CaCO_3$. Removal of dissolved Al and Fe continued throughout the EDR treatment, and the limit for weathering of soil particles containing these two elements was not reached, meaning that the weathering most likely would have continued with even longer treatment. The generation of dissolved Al may be a critical factor for the EDR of polluted soil due to the toxicity of dissolved Al. The Al content was reduced by 3.5 % and 1.1 %, which corresponds to removal of 801 mg from Soil 1 and 310 mg from Soil 2, respectively. The difference is likely linked to the different buffer capacities of the soils. After the electrodialytic treatment, the HNO_3 soluble Al (DS 259) in the treated soil was 4390 ± 134 mg/kg for Soil 1 and 4610 ± 581 for Soil 2. For Soil 1 this was 10.1 % lower than the initial value, while for Soil 2 it was 6.9 % higher. From the profile of the HNO_3 soluble Al (DS 259) in the soils (Figure 8), it can be seen that the Al concentration is below the initial value (by 24.5 %) for Slice 1-5 in Soil 2. The profile with a lower concentration in slices nearest the anode and higher in the slices nearest the cathode is in accordance with the migration direction of Al towards the cathode. The reduced Al concentration in slices nearest the anode (with the lowest pH) compared to the initial value indicates that soluble Al migrates out of the soil by electrodialytic treatment and the soil toxicity is, thus, not increased. The EDR method is thus evaluated to be powerful enough to remove extra dissolved Al due to the acidification.

Migration of Si was observed from the beginning of the EDR experiments, and the pattern for removal of Si differs from those of Al and Fe in not being affected by the soils buffer capacity (Figure 7). Thus in contrast to Al and Fe removal, which may be partly avoided by ending electrokinetic treatment soon after carbonate dissolution has emerged, Si dissolution is inevitable during electrokinetic treatment. During the 842 days of treatment, the total amount of dissolved Si exceeded the available nitric acid soluble fraction (DS 259). From Soil 1; 383

mg Si was removed, but only 60 mg was nitric acid available. For Soil 2 the pattern was the same, as there 755 mg was removed, and only 109 mg was extracted by DS259. The immediate release of Si indicates that weathering of soil minerals is unavoidable. However, the total reduction of Si (based on total content and removed amount) was only 0.2 % and 0.3 % respectively for the two soils during the long-term EDR and corresponds to $< 3 \cdot 10^{-6}$ % of the current was carried by Si. Furthermore, as Si is non-toxic, the Si dissolution during electrodialytic treatment may be neglected, and mobilized Si is not a limitation for electrochemical treatment of soil.

3.4 Visual changes of the soil

When removing the cation-exchange membrane after the EDR experiment with Soil 2; a white (slightly yellow), hard layer with a thickness of app. 2 mm was found on the soil (Figure 2). This layer is a visual sign of changes in the soil composition during EDR. A sample was collected from this layer for SEM-EDX investigation. No crystals were visible and the material appeared more as a cemented matrix. SEM-EDX analysis showed that the material was composed of 58 % (O), 25.4 % (Si), 11.7 % (Al) and 4.9 % (Fe) (weight percent). There were twice as many Si atoms as Al atoms and only a minor percentage of Fe atoms. Based on this information and the color, the material could be a combination of quarts (SiO_2), kaolinite ($Al_2Si_2O_5(OH)_4$) and probably some Fe-oxides (e.g. the hydrated form of Goethite which is a yellow weathering product) (Krauskopf and Bird 1995). The sample size was too small for XRD analysis and thus exact mineral identification was impossible.

3.5 Physical changes

The solid matter was reduced with 4.5 % for Soil 1 and 13.5 % for Soil 2 during the long-term EDR. Even though the reduction was higher for Soil 2 than Soil 1, the reduction was only visible during the experiment with Soil 1, as an empty space was developed in the top of the soil compartment during the EDR. The reason why the mass change was not visible for Soil 2 is probably due to the increased moisture content (from 16.2 % to an average of 22.3 %) during the treatment, while for Soil 1, the moisture content was unaffected.

The different fractions of the solid matter reduction are shown in Figure 9. Apart from the complete removal of $CaCO_3$, the organic matter content was reduced by 32 % and 20 %, respectively, for the two soils (see Table 2). In accordance with a previous investigation (Jensen et al. 2007), the carbonate removal was a dominating factor for the solid matter reduction for the carbonate rich Soil 2. The remaining solid matter reduction, must be, a result of removed elements including dissolution of soil minerals, which is mentioned as residual weight-loss in Figure 9. The weight-loss beyond removal of $CaCO_3$ is in accordance with observations from Jensen et al. (2012) for carbonate deficient soils. The weight of the mineral matrix was reduced by 2.4 % for Soil 1 and 4.3 % for Soil 2 during the treatment. According

to the XRD-analysis (Figure 5) the overall qualitative mineral composition after EDR was, however, unaffected by EDR, as no new crystalline mineral phases were developed or phases were missing, except for calcite removal, so the weathering can be seen (Figure 9) as related to a range of different minerals.

4. Conclusion

The result of this investigation showed that soil weathering occurs during electrochemical treatment. Main chemical changes during long-term treatment are reduction in pH, total dissolution of calcite, and partial dissolution of organic matter and minerals. Dissolution and removal of Al, Fe, Si and Ca from the soil during the electrodialytic treatment is the evidence of mineral changes. The fraction of these elements mobilized and removed exceeded the fraction which could be extracted by digestion in HNO_3 (DS 259). However, the amount of dissolved Si was only 0.2 % - 0.3 % after long-term EDR treatment. Dissolution of Si is inevitable, as it starts immediately as the electric field is applied and proceeds during the entire treatment. The acidification also causes complete dissolution of carbonate and thus most of the Ca-minerals. In contrast, Al- and Fe-oxides, are not dissolved until after carbonate removal, and may thus be partly avoided by appropriate control of the remediation process. Toxicity of the electrodialytic treated soil is not increased by the Al dissolution, as dissolved Al migrates out of the soil matrix immediately upon dissolution, when external electrode compartments are used.
Re-precipitation of a minor fraction of the released Si, Al and Fe occurs next to the cation exchange membrane, but apart from that the overall qualitative mineral composition remained unchanged after 842 days of electrodialytic treatment.

References

Amorim LV, Gomes CM, Silva FLH, Franca KB, Lira HL, Ferreira HC (2003) Use of electrodialysis to Bentonitics clays dispersions. Mat. Res. Soc. Symp. Proc. 752:199-204.

Caldwell OG, Marshall CE (1942) A study of some chemical and physical properties of the caly minerals Nontronite, Attapulgite and Saponite. University of Missouri, Research Bulletin 354, pp. 15-20.

Cameron FK, Bell JM (1905) The mineral constituents of the soil solution. U.S. Dept. Agr. Bureau of Soils Bul. 30.

Chin PF, Mills GL (1991) Kinetics and mechanisms of kaolinite dissolution: effects of organic ligands. Chemical Geology 90:307-317

CRC Handbook of Chemistry and Physics (2013). 94th ed. Editor in chief: Haynes WM. Accessible by DTU digital library. (http://www.hbcpnetbase.com.globalproxy.cvt.dk)

Drever JI, Stillings LL (1997) The role of organic acids in mineral weathering. Colloids Surfaces A: Physicochem. Eng. Aspects 120:167-181

Huang WH, Keller WD (1972) Organic acids as agents of chemical weathering of silicate minerals. Nature Physical Science 239:149-151

Jensen, J.B., Kubes, V. and Kubal, M. (1994). Electrokinetic Remediation of Soils Polluted with Heavy Metals. Removal of Zink and Copper Using a New Concept. Environmental Technology, Vol. 15, pp. 1077-1082.

Jensen PE, Ottosen LM, Ferreira C, Villumsen A (2006) Kinetics of electrodialytic extraction of Pb and soil cations from a slurry of contaminated soil fines.

Jensen PE, Ottosen LM, Allard B (2012) Electrodialytic versus acid extraction of heavy metals from soil washing residue. Electrochimica Acta 86:115-123.

Kliem BK, Koch CB (2000) Electrodialytic remediation of soil material polluted by chemicals used for wood impregnation, In: Bonding of heavy metals in soil, pH.D. thesis by BK Kliem, Department of Geology and Geotechnical Engineering and Department of Chemistry, Technical University of Denmark.

Krauskopf KB, Bird DK (1995) Introduction to geochemistry, third edition. McGraw-Hill international editions, Singapore, Chapter 4.

Hansen HK, Ottosen LM, Kliem BK, Villumsen A (1997) Electrodialytic remediation of soils polluted with Cu, Cr, Hg, Pb and Zn. Chem. Tech. Biotechnol 70:67-73.

Marshall WL, Warakomski JM (1980) Amorphous silica solubilities – II. Effect of aqueous salt solutions at 25 °C. Geochimica et Cosmochimica Acta, 44:915-924.

Mattson S (1926) Electrodialysis of the colloidal soil material and the exchangeable bases. Journal of agricultural research, 33:553-567.

Moore DM, Reynolds RC (1997) X-ray diffraction and the identification and analysis of clay minerals. 2 ed, Oxford University Press inc., New York, chapter 4.

Nutting PG (1937) A study of bleach clay solubility, Franklin Inst. Jour., 224:339-362.

Nutting PG (1943) The action of some aqueous solutions on clays of the montmorillonite group. U.S. Geol. Survey Prof. paper 197-F, pp. 219-235.

Nutting (1945) The solution of soil minerals in diluted acids. Science 101:619-621.

Ottosen, L.M., Hansen, H.K. and Hansen, C.S. (2000). Water splitting at ion-exchange membranes and potential differences in soil during electrodialytic soil remediation. Journal of Applied Electrochemistry, Vol. 30, pp. 1199-1207.

Pazos M, Gouveia S, Sanromán MA, Cameselle C (2008) Electromigration of Mn, Fe, Cu and Zn with citric acid in contaminated clay. Environmental science and health part A 43:823-831.

Roy R (1949) Decomposition and resynthesis of the micas. Journal of the American ceramic society, 32:202-209.

Skibsted G, Ottosen LM, Jensen PE, Elektorowicz M. Long-Term electrodialytic soil remediation – effect of removal efficiency of lead. (Appendix B in PhD-thesis)

Sokolova TA (2013) The Destruction of Quartz, Amorphous Silica Minerals, and Feldspar in Model Experiments and in Soils: Possible Mechanisms, Rates, and Diagnostics (the analysis of Literature). Eurasion Soil Science, 46:91-105.

Stevenson FJ (1994) Humus chemistry: Genesis, composition, reactions. 2nd edition, Wiley & Sons, Inc., New York.

West LJ, Steward DI, Binley AM, Shaw B (1999) Resistivity imaging of soil during electrokinetic transport. Engineering Geology 53:205-215.

Tables and Figures

Table 1: Concentrations of the target elements in (mg/kg dry matter) for the two soils, measured by total digestion, DS 259 and by 1 M HNO3 extraction, including the fraction of total content for DS 259 and extraction in 1 M HNO_3.

Soil	Element	Total digestion	DS 259 (7 M HNO_3)	Fraction	1 M HNO_3	Fraction
		mg/kg	mg/kg	%	mg/kg	%
Soil 1	Al	36,200	4,890	13.5	869	2.40
	Fe	13,000	7,440	57.5	1,710	13.2
	Si	333,000	60	0.02	414	0.12
	Ca	7,530	3,390	45.0	1,340	17.8
	K	17,000	1,350	7.94	198	1.16
	Mg	2,380	1,240	52.1	349	14.7
	Pb	22	12	54.5	10	43.0
Soil 2	Al	34,000	4,310	12.7	1,290	3.79
	Fe	39,300	13,100	33.6	2,990	7.67
	Si	315,000	109	0.03	420	0.13
	Ca	45,400	40,900	90.1	21,500	47.4
	K	15,600	1,190	7.6	188	1.21
	Mg	2,970	1,620	54.5	450	15.2
	Pb	529	342	64.7	233	44.0

Table 2: Initial pH and content of organic matter and $CaCO_3$ in the two soils, including final pH and content of organic matter after EDR

	Soil 1		Soil 2	
	Before	After	Before	After
pH	5.9	2.4 ± 0.1	7.7	3.0 ± 0.4
Organic matter (%)	6.4	4.6 ± 0.2	3.3	3.1 ± 0.2
$CaCO_3$ (%)	0.2		9.1	

Table 3: Initial amount of Ca, K and Mg in the EDR experiments and the expected HNO_3 soluble (DS 259) amount, included the removed amounts of Ca, K and Mg measured in the electrolytes

Element		Initial	HNO_3 soluble	Removed
		mg	mg	mg
Soil 1	Ca	4750	2140	2870
	K	10700	849	295
	Mg	1500	784	376
Soil 2	Ca	37500	33800	21800
	K	12900	984	323
	Mg	2450	1340	400
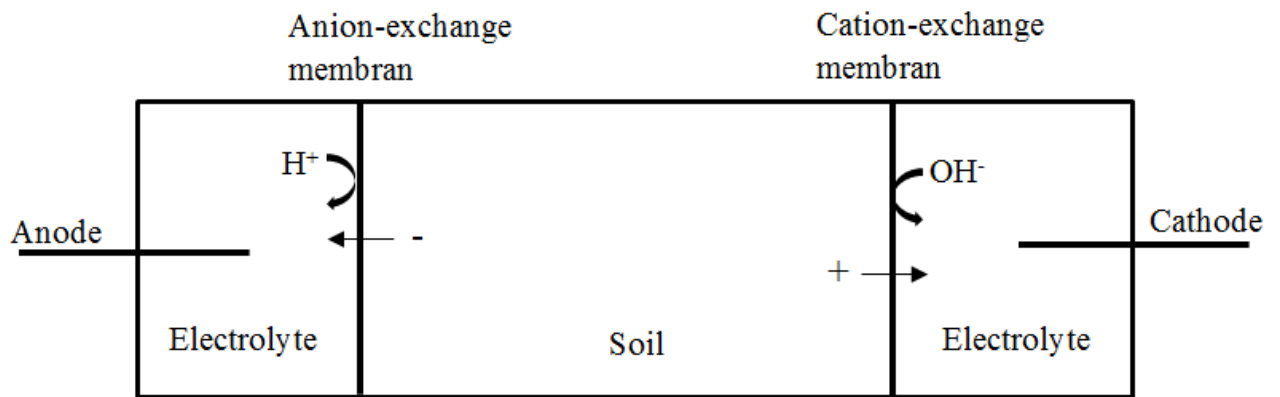
Figure 1: Schematic illustration of the electrodialytic setup.

Figure 2: Cathode end of the soil sample after EDR on Soil 2, when the cation-exchange membrane was removed.
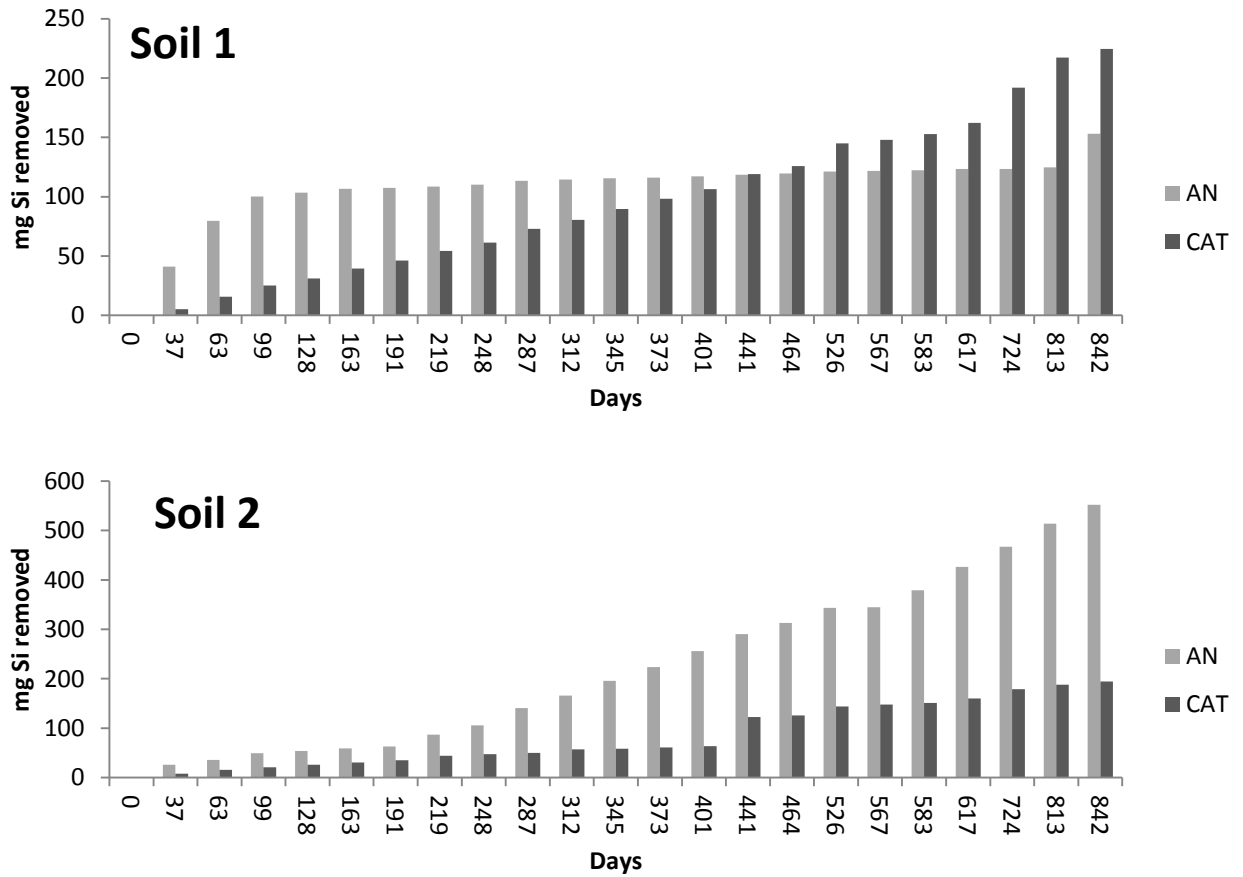
Figure 3: Accumulated amount of Si migrated towards respectively the anode and the cathode.
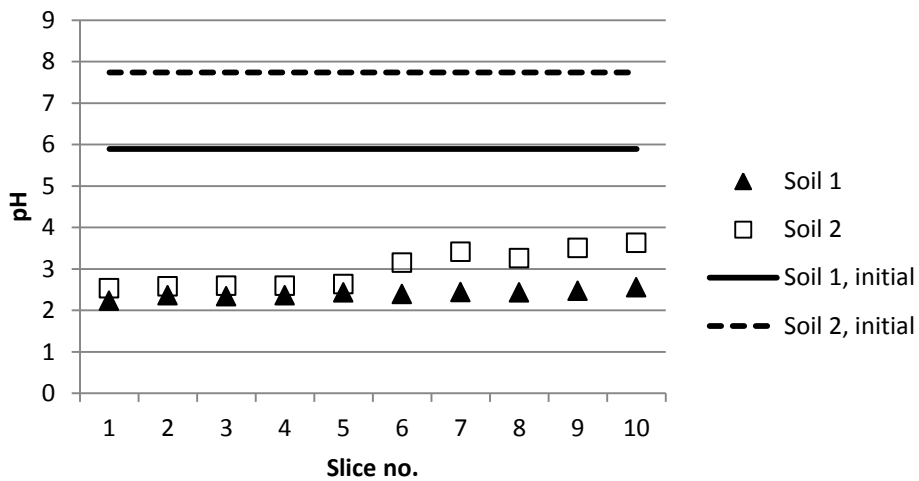
Figure 4: Profile of pH in the 10 slices after EDR, including the initial soil pH.
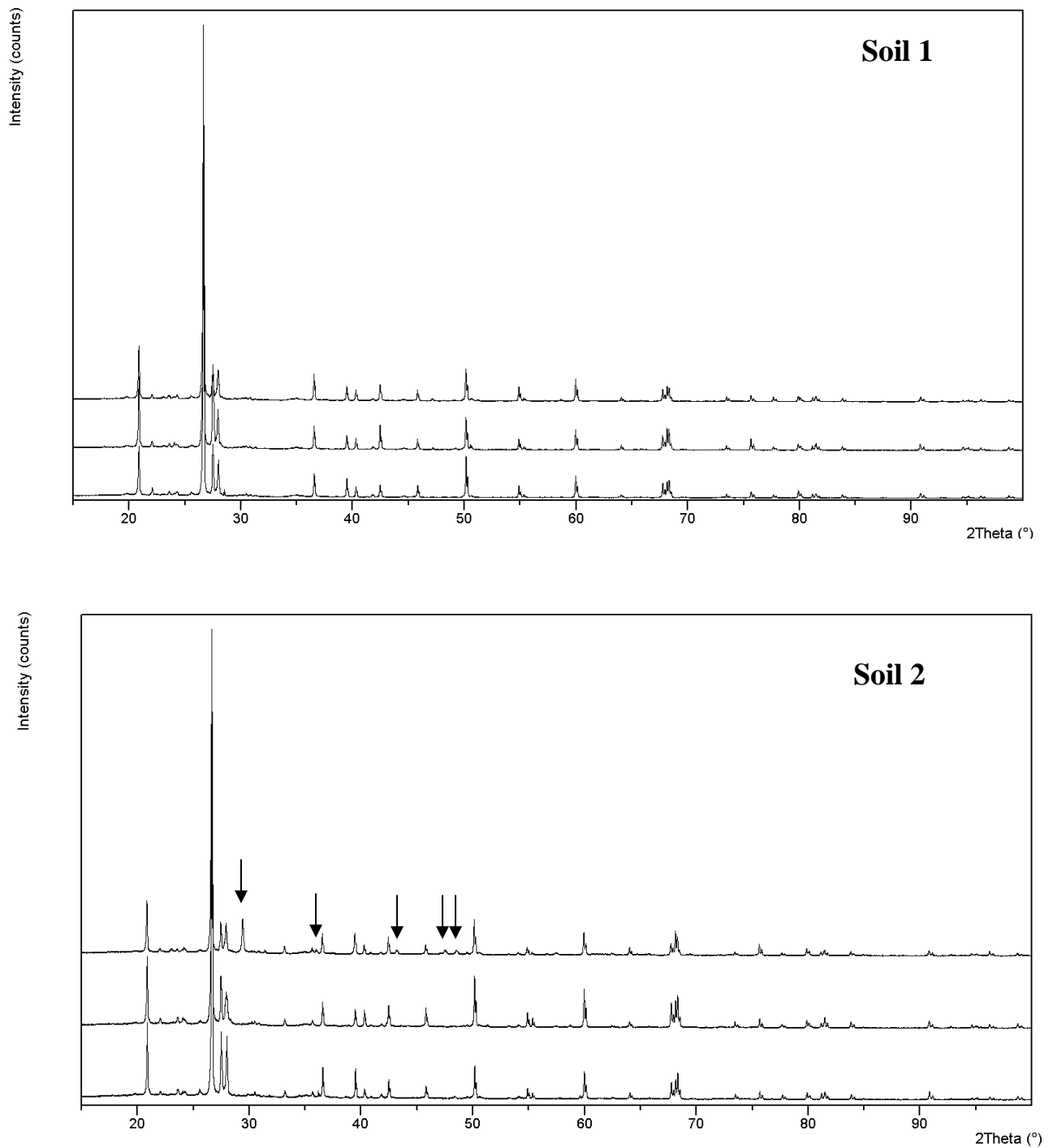
Figure 5: Qualitative XRD analysis of the soil samples. From the top in each XRD-graph the first pattern is the initial soil sample, the second is Slice 1 after EDR and the pattern in the bottom is Slice 10 after EDR. The arrows marks the peaks identified as Calcite for Soil 2. To compare the peaks in the XRD-graphs for the original soil samples and Slice 1 and Slice 10 after EDR the location of the vertical offset is changed.
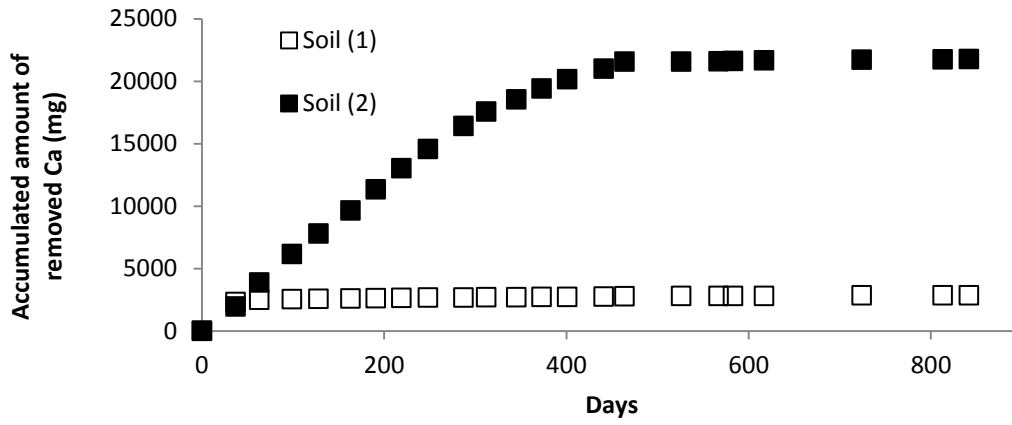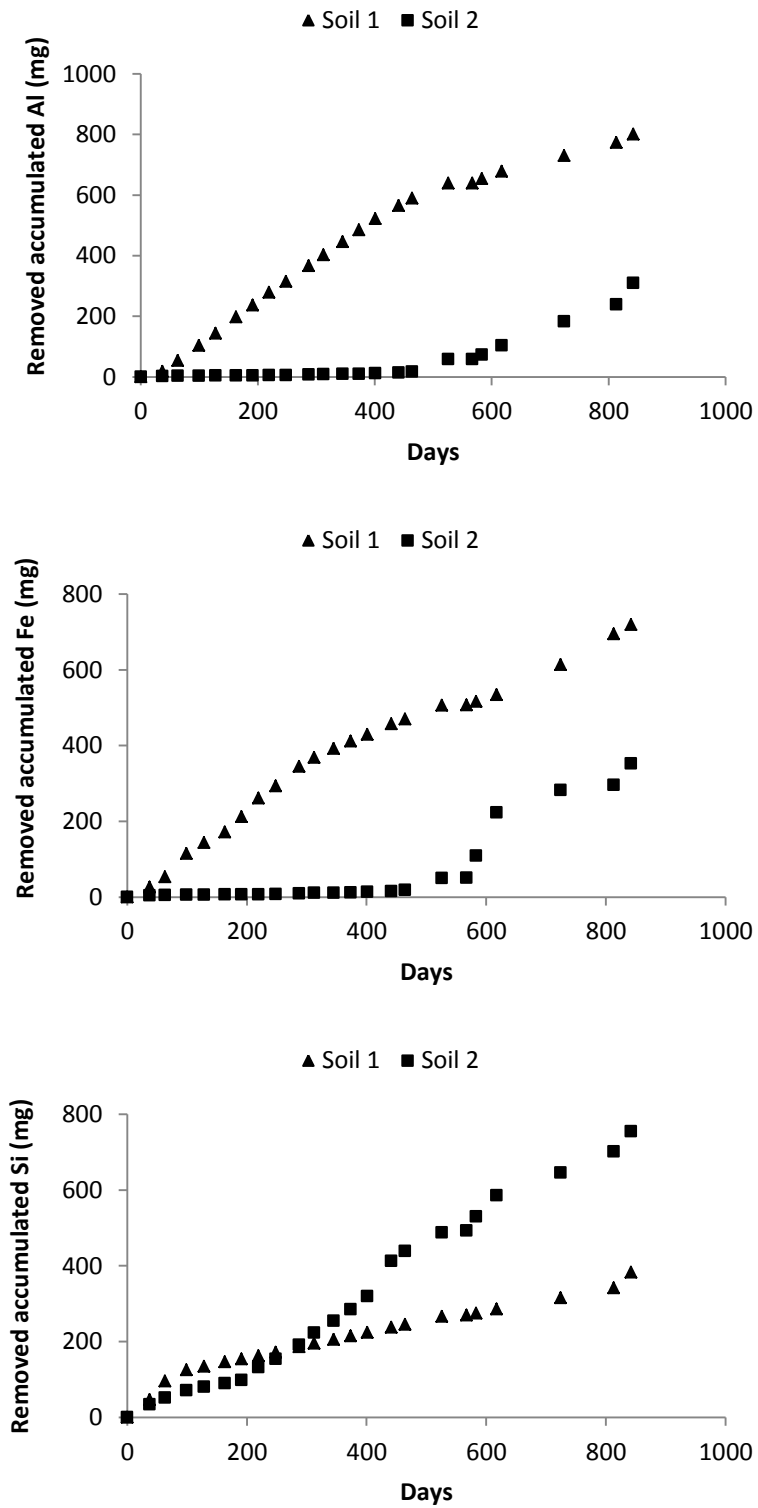
Figure 6: Removed accumulated amounts of Ca for Soil 1 and Soil 2 during EDR.

Figure 7: Removed accumulated amounts of Al, Fe and Si for Soil 1 and Soil 2 during EDR.
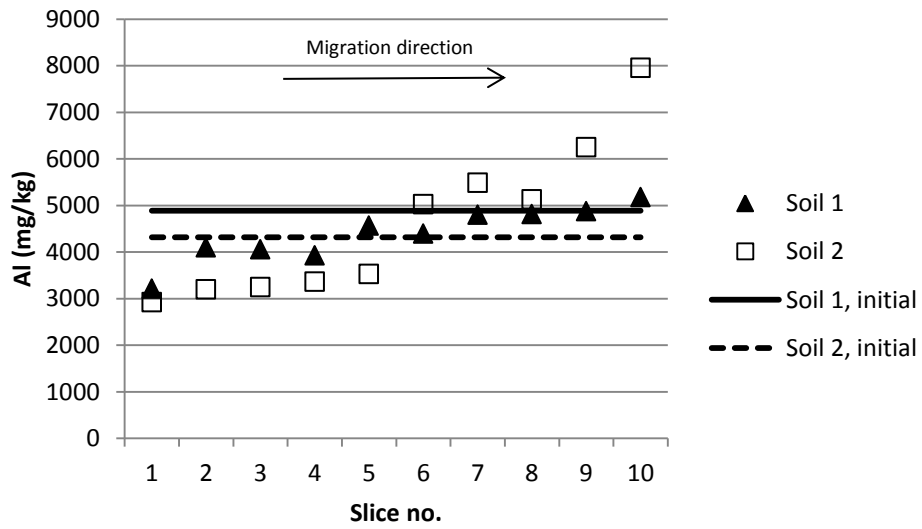
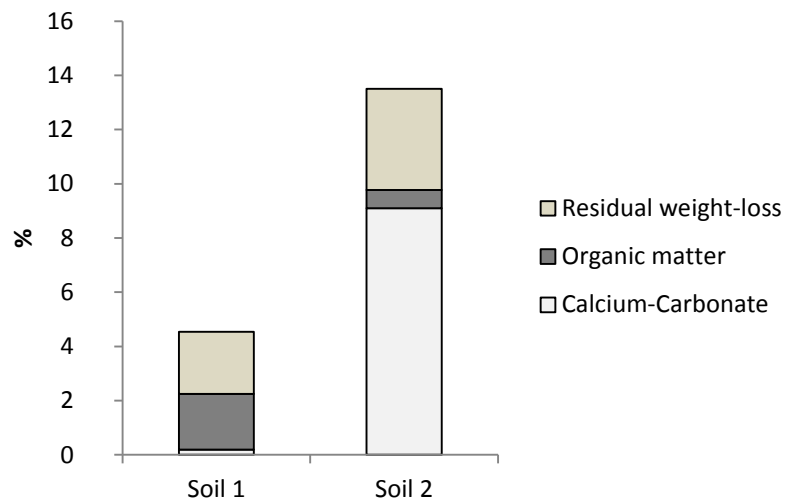Figure 8: Profile of HNO$_3$ soluble Al (DS 259) in the 10 slices before and after EDR.

Figure 9: Composition of the weight-loss for both soils.

Appendix B

Long-term electrodialytic soil remediation – Effect on removal efficiency of lead

Gry Skibsted[1], Lisbeth Ottosen[1], Pernille E. Jensen[1] and Maria Elektorowicz[2]

[1]Department of Civil Engieering, Technical University of Denmark, Building 118, 2800 Kgs. Lyngby, Denmark.

[2]Department of Building, Civil and Environmental Engineering, Concordia University, Montreal, Quebec, Canada.

Long-term electrodialytic soil remediation – effect on removal efficiency of lead

Gry Skibsted[1,*], Lisbeth M. Ottosen[1], Pernille E. Jensen[1] and Maria Elektorowicz[2]

[1]Department of Civil Engineering, Technical University of Denmark, Building 118, 2800 Kgs. Lyngby, Denmark.

[2]Department of Building, Civil and Environmental Engineering, Concordia University, Montreal, Quebec, Canada.

*Corresponding Author: gryp@byg.dtu.dk

Key words: Electrokinetic, Lead, Cadmium, Long-term effects

Abstract Electrodialytic soil remediation (EDR) experiments with very long duration were conducted to investigate the effect on the removal of Pb. The long-term experiments were conducted with two different soils; an industrially Pb and Cd contaminated soil with high carbonate content and an unpolluted soil with low carbonate content. The experiment with unpolluted soil was conducted to investigate the effect on the naturally occurring Pb. A constant current was applied for 842 days and samples from the electrolytes were collected and analyzed 22 times during the treatment. The acid soluble concentration of Pb was on average reduced by 27.8 %, while 8.1 % of the total Pb was removed from the Pb-contaminated soil. Pb was mobilized by decreasing pH; when the buffer capacity of $CaCO_3$ was eliminated, the removal rate of Pb increased considerably and during the following 260 days 82.9 % of the removed Pb was transported to the electrolytes with a remediation rate of 0.8 mg/week. The last 118 days of EDR only affected a remediation rate of Pb at 0.2 mg/week and was only amounting to 9.7 % of the removed Pb. This showed that an extremely prolonged duration of EDR not necessarily result in significantly higher remediation of Pb, as the efficiency of the applied electric field on Pb removal decreased significant with prolonged duration.

In the soil region closest to the anode more of both Pb and Cd than initially acid soluble were removed. This was seen for both soils, but the acid soluble concentration was only reduced with 69 % and 48 %, respectively. This shows that EDR result in redistribution of Pb and Cd from the acid insoluble fraction to the acid soluble fraction. Prolonged EDR on the unpolluted, low-carbonate soil showed that it was possible to reduce the Pb and Cd content even from the background level, but at the expense of an increased mobilization of Al.

1. **Introduction**

In the early 1990's the research for removal of heavy metals from polluted soils by electrokinetics was initiated (Acar and Alshawabkeh 1993, Lageman at al. 1989, Probstein and Hicks 1993). Electrokinetic remediation methods are based on application of an electric field and utilization of the transport processes obtained. When an electric field is applied to a soil, electromigration of charged species will occur towards the opposite charged electrode. Water oxidation at the anode generates acid and at the cathode hydroxyl is produced by reduction of water. Penetration of the ions produced at the electrodes into the soil can be prevented by using electrodialytic soil remediation (EDR), a method where ion-exchange membranes separates the soil from the electrolytes (Jensen et al. 1994), see Figure 1. The cation-exchange membrane between the soil and the cathode compartment hinder an alkaline front from passing into the soil from the cathode. Because of the net-negative surface of soil particles (Alloway 1995) and overall electroneutrality a lack of negatively charged species available for migration in the soil can arise. To compensate; water-splitting at the anion-exchange membrane occurs and generates an acid-front, which moves towards the cathode (Ottosen et al. 2000). For most trace elements the soil has its maximum bonding capacity at neutral pH and this capacity will often be reduced in acidified or alkaline environments but in general the mobility of the cations increases upon acidification (Alloway 1995). Pb mobilization is linked to the acidification and Jensen et al. (2006[a]) illustrated a prompt release of Pb from the soil when the soils buffer capacity was eliminated and a sudden acidification occurred.

The pH is not the only controlling factor for the mobility of Pb in soils. Jensen et al. (2007) evaluated the importance of speciation and the soil composition such as organic matter, for the feasibility of EDR, and observed that Pb speciation is of primary importance. Specifically, organic matter and stable compounds like $PbCrO_4$ can impede and possibly even preclude soil remediation (Jensen et al. 2007). The speciation of Pb in industrially polluted soils depends on the stability of the original speciation of Pb at the time of the pollution and the contamination level, while the soil characteristics are of secondary importance (Jensen et al. 2006[b]). Ottosen et al. (2006) showed that aging is important for the adsorption strength of Cu in spiked soils and that Cu was adsorbed stronger in industrially polluted soil than in spiked soils even though the soil types were very similar. This is in accordance with observations by Darmawan and Wada (1999), who showed through experiments with six different soils spiked with $Pb(NO_3)_2$ that the amount of Pb in the exchangeable fraction decreased with longer incubation time. In Table 1 results of electrochemical removal of Pb from different particulate matrices are collected. In general the removal efficiency of electrochemical treatment is much higher for spiked matrices than from industrially polluted.

The aim of this paper is to evaluate if extremely prolonged electrodialytic treatment can increase the fraction of removed Pb. For this purpose two soils are used. An industrially Pb contaminated soil and an unpolluted $CaCO_3$ deficiency soil. The objective by using an unpolluted soil to is to evaluate how the heavy metals from the natural soil minerals are

affected when treated electrochemically. The weathering of the soil minerals due to the long-term applied electric field is evaluated in (Skibsted et al. 2013).

2. Materials and methods

2.1 Materials

Two soils were used for the electrodialytic remediation experiments. An industrially Pb contaminated soil (Soil A) which was collected from an excavated pile at KMC (Kalvebod Miljøcenter); a disposal site for polluted soil in Denmark, and an unpolluted soil (Soil B) from a garden located in the north of Zealand in Denmark. Soil (B) was taken below 10 cm depth. The soils were sieved through a 2.0 mm sieve and only the fraction below 2 mm was used.

2.2 Characterization of the soils

After drying, the soil lumps formed were loosened by hand in a porcelain mortar before characterization. Soil pH was measured potentiometric in a suspension of 5 g soil and 12.5 mL 1 M KCl after 1 h of agitation. The conductivity was measured with a conductivity electrode in a suspension of 5 g soil and 12.5 mL distilled water after ½ h of agitation. Danish standard (DS 259) was used to extract acid soluble metals from the soil; 1 g of soil and 20 mL 7 M HNO_3 was autoclaved (200 kPa, 120 °C) in 30 min. After cooling the samples were filtered through a 0.45 µm filter and cations in the extract were analyzed by ion coupled plasma – optical emission spectroscopy (ICP-OES, Varian 720-ES). The total metal content was measured after digestion of the soil in HF; 6 mL HNO_3 65 %, 2 mL HCl 37 %, and 2 mL HF 40 % were added to 0.25 g soil and treated in the microwave (Anton Paar) 1400 W, 28.7 bar. Following 12 mL H_3BO_3 10 % was added (to complex free fluorides) and the samples treated in the microwave again (900 W, 10.3 bar). The total concentration was analyzed by ICP-OES (Varian Expert, model MPX).

The organic content was found as weight loss at 550 °C. The carbonate content was measured volumetric after reaction with 10 % HCl, by use of a Scheibler instrument. The amount of carbonate was calculated assuming that all carbonate is present as $CaCO_3$. To evaluate the lead desorption dependency on pH, 5 g of dried, crushed soil was extracted for 7 days on an agitation table in 25 mL solution of distilled water or HNO_3 in the concentrations; 0.01 M, 0.05 M, 0.10 M, 0.40 M, 0.50 M, or 1.00 M (double determination). The samples were settled for 10 min and pH measured before filtration (0.45 µm filter), and the extract analyzed by ICP-OES (Varian 720-ES).

Speciation of Pb in the soil were analyzed by sequential extraction; 0.5 g soil was treated in four steps as follows: I) Extraction with 20 mL 0.11 M acetic acid pH 3 (adjusted by NH_3 or HNO_3) for 16 h. II) Extraction with 20 mL 0.1 M $NH_2OH \cdot HCl$ pH 2 (adjusted by 1M HNO_3) for 16 h. III) Extraction with 5 mL 8.8 M H_2O_2 for 1 h and heating at 85 °C for 1 h with lid

followed by evaporation of the liquid phase at 85 °C until volume was reduced to < 1 mL by removal of the lid. Step III) was repeated, but the sample was evaporated until almost dryness. After cooling the sample it was extracted with 25 mL 1 M NH_4OOCH_3 pH 2 (adjusted with concentrated HNO_3) for 16 h. IV) Digestion according to DS 259. Extractions were made by agitation. Between each step the samples were centrifuged at 3000 rpm for 15 min, and the extract were decanted, filtered through a 0.45 μm filter and analyzed by ICP-OES (Varian 720-ES). Before initiation of the next step, the sample was washed with 10 mL distilled water by agitation for 15 min, centrifuged at 3000 rpm for 15 min and the extract was decanted.

2.3 Experimental setup

The electrodialytic remediation (EDR) experiments were carried out in cylindrical Plexiglas cells with three compartments and an internal diameter at 8 cm (Figure 1). The soil was placed in the centre compartment and separated from the two electrode compartments by Ionics(R) ion exchange membranes (AR204SZRA and CR67 HVY HMR427); an anion-exchange membrane separated the anode and the soil sample, and a cation-exchange membrane separated the cathode from the soil sample. Platinum coated rod electrodes were used. The centre compartment with soil was 10 cm long and the two electrode compartments were 5 cm. Anolytes and catolytes were 1 L of 0.01 M NaOH adjusted to pH 2 with HNO_3, continuously circulated between the electrode compartment and a glass flask. A constant current of 5 mA (corresponding to 0.1 mA/cm^2) was applied during both EDR experiments and the voltage was monitored. The initial water content of the soils was 16.2 % (Soil A) and 26.8 % (Soil B), obtained by adding distilled water to the soil. During EDR, the pH of anolyte and catolyte was adjusted with 1 M HNO_3 or 5 M NaOH, respectively, to maintain pH about 2. The duration of the EDR experiments was 842 days.

The soil volume visually decreased in the experiment with soil (B) and to maintain good contact at the electrodes the cell was beaten gently against the table at day 163, 432, 457 and 519 to restore the contact.

2.4 Sampling and soil analysis

During the experiments the anolytes and catolytes were changed and samples were taken 22 times. Simultaneously, the electrodes were changed and the removed cleaned by storage in 5 M HNO_3 overnight, to dissolve the electro-precipitated mass and analyze the content. Before analysis, the catolyte samples were preserved according to the Danish Standard (DS 259); 16 mL sample added 4 mL concentrated HNO_3 was autoclaved (200 kPa, 120 °C) in 30 min. Concentrations of target elements were measured by ICP-OES (Varian 720-ES). When finishing the experiments, the membranes were cleaned by storage for 12 hours in 1 M HNO_3, and the concentration was analyzed by ICP-OES (Varian 720-ES). The soil was divided into 10 slices perpendicular to the length of the compartment (numbered from the anode end). In each slice, the water content was measured as weight loss after drying at 105 °C. The dry slices were crushed gently by hand in a porcelain mortar and soil pH was measured as double

determination in each slice and so was the concentrations of target elements after DS 259. In slice 1 (Soil A) the total concentration were measured after total digestion by HF.

3. Results and discussions

3.1 Soil Characterization

The concentrations of the trace elements in the two soils measured by the two different extraction methods; total digestion and DS 259, are given in Table 2. The difference between the two extractions methods is illustrated in Figure 2. DS 259 gives information of the acid soluble fraction where the total digestion includes the acid insoluble fraction of the trace elements. The acid insoluble fraction covers the elements incorporated in the mineral matrix or present as acid insoluble species. According to the Danish Limiting values, which are based on DS 259, Soil (A) was highly polluted with Pb, as the limiting concentration was exceeded more than eight times. The other analyzed trace elements meet the limiting values except for Cd which exceeds the limiting value, too, and with a factor of 2-3. The acid insoluble fraction of Pb in Soil (A) was 35 %.The acid soluble concentrations of all the tested trace elements were below the target limits for Soil (B) as expected.

Initial values of pH, conductivity, carbonate and organic matter are presented in Table 3. The buffer capacity against acid is expected to be higher for Soil (A) due to the higher $CaCO_3$ content (9.1 %) compared to Soil (B) (0.2 %). When relating the Ca concentration and the carbonate content for Soil (A) it is found that 80 % of the Ca can be present as $CaCO_3$. The initial conductivity was similar for the two soils, but pH and content of organic matter differed.

3.2 Speciation and mobilization of Pb

Sequential extraction was used to evaluate how strong Pb was bound in the soil. The sequential extraction procedure covered the amount of Pb possible to extract by DS 259 (the acid soluble fraction). The results from the sequential extraction are shown in Figure 3. The shown acid insoluble fraction is calculated by subtracting the total concentration extracted by the sequential extraction from the initial acid insoluble concentration. For Soil (A) the acid insoluble fraction of Pb was 35 % (187 mg/kg), 32 % was in the residual fraction and 33 % was extracted from the three first steps in sequential extraction; Ion exchangeable/carbonate bound, easily reducible oxides and the fraction as was organic bound. For Soil (B) the acid insoluble fraction of Pb was 47 % (10 mg/kg), 24 % was in the residual acid soluble fraction and 29 % was linked in the three first fractions.

The pH-desorption dependency of Pb in Figure 4 shows that desorption increased with decreasing pH for both soils. For Soil (A) the acid soluble fraction of Pb constituted 65 %. Less was though desorbed even at the relatively low pH values reached in Figure 4. At pH 1.8

only 34 % of the total Pb content was desorbed. Compared to mobility as revealed through sequential extraction this can almost be related to what was bound in fraction I, II and III (Ion exchangeable/ carbonate bound, easily reducible oxides and organic bound). For Soil (B) a lower fraction compared to the acid soluble fraction was desorbed as well. At pH 2.1 only 2.4 % was desorbed and at pH 1.4 it was 13 %.

3.3 Soil conditions after EDR

The average values for the 10 slices of pH, organic content, carbonate content and Pb and Cd concentrations are in

Table 4. The soil was acidified during both EDR experiments and the final average pH was below 3. The pH profiles in Figure 5 shows that slice 1 was more acidified than slice 10 in both experiments and pH varied in the soil matrix from 2.5-3.6 (Soil A) and 2.2-2.6 (Soil B), respectively.

The water content did not change markedly for Soil (B) due to the long-term EDR, but for Soil (A) it increased from 16.2 % to 22.3 %. The organic matter content was reduced for both soils; from 3.3 % to 3.1 % (Soil A) and from 6.4 % to 4.6 % (Soil B). The conductivity was reduced more for Soil (A) than Soil (B) during the electrodialytic treatment. The change in the conductivity will directly affect the voltage. In both experiments the voltage increased; Soil (A) from 4.3 V to 48.6 V and Soil (B) from 3.4 V to 19.3 V, and thus the increase in voltage was highest where the decrease in conductivity was most pronounced. The increase in voltage is probably also related to the decrease in organic content.

3.4 Electrochemical removal

After application of 5 mA for 842 days the average acid soluble Pb concentration in Soil (A) was still higher than the Danish limiting value (Figure 6). The Pb profile in Soil (A) shows that the concentration was highest in the cathode end of the soil matrix, which is in accordance to the pH profile and the electromigration direction of Pb. The primary electromigration direction for Pb was towards the cathode as also reported by West et al. (1999), Jensen et al. (2007) and Hansen et al. (1997). In Slice 1 the acid soluble Pb and Cd was reduced by 69 % and 48 %, respectively, but in slice 10 the concentration of Pb was higher than the initial value. The final average acid soluble concentration of Cd meets the Danish limiting value, but in slice 9 and 10 it was higher than the allowed 0.5 mg/kg. Soil (B) did meet the Danish limiting values for Cd and Pb both before and after the long-term EDR, but the reduction in both Pb and Cd (Figure 7) showed that it was possible to reduce the background level.

The differences between the total concentration (acid soluble + acid insoluble) of Pb and Cd in the initial soils and in slice 1 after EDR are shown in Figure 7. In both cases the removed amount of the elements was higher than the initial acid soluble fraction. This shows that Pb and Cd from the acid insoluble fraction changes status to acid soluble during EDR.

Redistribution of speciation was also reported for Cu by Ribeiro and Mexia (1997), where a passage of current induced a redistribution of Cu from less soluble to more soluble fractions in the soil.

In pace with the elimination of $CaCO_3$ and thus the buffer capacity, Ca ions were removed. From Figure 8 it can be seen that the Ca removal ends after 464 days of EDR for Soil (A). For Soil (B) it was already exceeded at day 37 (the first sampling). This is probably an indication for elimination of the buffer capacity from $CaCO_3$. Al removal from the soil increased sharply at the exact same time as the Ca removal stopped (see Figure 9). The accumulated removed amount of Al increased throughout the remaining treatment time. Wild (1989) describes the Al in soil solution among others to depend on the dissolution of gibbsite and soluble Al in equilibrium with gibbsite increases significantly at pH < 4. This can explain why removal of Al initiated after the buffering capacity from $CaCO_3$ was eliminated, as the acidification here reached a limit where Al was mobilized.

From the pH-desorption dependency (Figure 4) the mobilization of Pb first increased significantly at pH < 2 for Soil (B), while for Soil (A) the pH value for the Pb-mobilization was between 2 and 4. Until the buffering capacity from $CaCO_3$ was exceeded, the removed amount of Pb may originate from a fraction of Pb co-precipitated in the carbonates (Ottosen et al, 2001). The removal rate for Pb increased considerably after the buffer capacity from $CaCO_3$ was eliminated (Figure 9). This can be explained by the pH dependent mobilization of Pb. For Soil (A) pH is probably not lowered enough before day 464 to mobilize Pb. For calcareous soils electro-remediation has been reported slowly in previous works and it has been suggested to use enhancement solutions, which forms complexes with Pb and pH thus elimination of the $CaCO_3$ content is not obligatory to the remediation. Enhancement solutions tested are EDTA (Amrate et al. 2005) and citic acid (Ottosen et al. 2005).

Jensen et al. (2006) described the removal of Pb from soil with four phases; I) the lag-phase where Ca is removed and the soils buffer capacity eliminated, II) Pb is almost released at once from the soil, mobilized by the acidified conditions, III) low removal rate of Pb and IV) the removal ceased. In Figure 9 it is easy to identify the three first phases, but phase II) could not be characterized as a prompted release from the soil, as the phase cover the duration from day 464-724 (corresponds to 31 % of the total treatment time). The experiments were conducted with a stationary setup where the mobilization is momentary, while the four phases defined by Jensen et al. (2006) was from a setup with stirred soil solutions. The different setup might be the reason why a prompted release of Pb not was observed. In phase II) 29.4 mg Pb was removed from Soil (A) and in phase III) (day 724-842) the amount was 3.4 mg, this corresponds to 82.9 % and 9.7 %, respectively of the total Pb collected in the electrolytes during the EDR. The remediation rate in those two phases was 0.8 mg Pb/week and 0.2 mg Pb/week, respectively, and show that the efficiency of the applied electric field on the Pb removal decreases significantly with time. Because of the sampling interval, the exact duration of phase II) cannot be determined. Phase II) is until somewhere between 617 days and 724 days. Phase II) continues into phase III) in this period. The remediation rate of Pb decreases in phase III). The Pb content in the overall matrix was only reduced with 8.1 % of

the total content, but in slice 1 the total reduction of Pb was 66 %. The acid soluble concentration of Pb in the treated soil matrix was on average reduced by 27.8 %.

The EDR experiments showed that an extremely prolonged treatment time not necessarily result in a significantly higher remediation of Pb. A main effect of the long-term electrodialytic treatment is release of Al from the soil matrix, which is preferably avoided due to the toxicity of dissolved Al. Soil (B) represented a situation where the buffer capacity from calcite was quickly eliminated and the initial level of Pb was background level. Pb was removed from Soil (B) continuously during the electrodialytic treatment (Figure 9) and the overall acid soluble fraction reduced too (Figure 7), but at the expense of an increased mobilization of Al. More Pb than initially acid soluble was removed and together with the dissolution of Al this indicated that Pb was mobilized due to dissolution of minerals. In total 1.1 % (Soil A) and 3.5 % (Soil B) Al were removed during the EDR experiments.

4. Conclusion

An extremely prolonged duration of EDR does not necessarily result in a significantly higher remediation of Pb, as the efficiency of EDR decreases with prolonged duration. The acid soluble concentration of Pb was on average reduced by 27.8 %. In total the overall Pb content was reduced by 8.1 % from the industrially Pb-contaminated soil, but in the region closest to the anode compartment the reduction was 66 %. The mobilization of Pb was initiated after the buffering from $CaCO_3$ was eliminated and then 82.9 % of the Pb was transported to the electrolytes with a remediation rate of 0.8 mg/week. The last 118 days the remediation rate was reduced to 0.2 mg/week and the amount corresponds to 9.7 % of the Pb collected at the electrolytes.

In the region of the soil closest to the anode compartment (Slice 1), where the highest reduction of Pb and Cd was obtained in both experiments, more of the elements were removed than corresponding to the acid soluble fraction from the beginning. Nevertheless the acid soluble Pb concentration was only reduced with 69 % and the Cd concentration with 48 % in this part of the soil. This indicates that the EDR induce a redistribution of Pb and Cd between the acid soluble phase and the acid insoluble phase. It was possible to reduce the Pb content below the initial background level in the unpolluted $CaCO_3$ deficiency soil, but at the expense of an increased mobilization of Al. Both Al and Pb dissolution occurred continuously during EDR of the unpolluted soil.

References

Acar YB, Alshawabkeh AN (1993). Principles of electrokinetic remediation. Environ. Sci. Technol. 27:2638-2647.

Alloway, B.J. (1995). Heavy Metals in Soils, second edition. Blackie Academic & Professional, Glasgow, UK, Chapter 2.

Amrate, S.; Akretche, D.E.; Innocent, C.; Seta, P. (2005) Removal of Pb from a calcareous soil during EDTA-enhanced electrokinetic extraction. Science of the Total Environment 349, 56– 66

Altin A, Degirmenci M (2005) Lead (II) removal from natural soils by enhanced electrokinetic remediation. Sci. Total Environment 337:1-10.

Darmawan, Wade S (1999) Kinetics of speciation of copper, lead, and zinc loaded to soils that differ in cation exchanger composition at low moisture content. Commun. Soil sci. plant anal. 30:2363-2375.

Hamed J, Acar YB, Gale RJ (1991) Pb(II) removal from kaolinite by electrokinetics. Geotechnical Engineering 117:241-271.

Han SJ, Kim SS (2003) Application of enhanced electrokinetic extraction for lead spiked kaolin. Civil Engineering, 7:499-506.

Hansen HK, Ottosen LM, Kliem BK, Villumsen A (1997) Electrodialytic remediation of soils polluted with Cu, Cr, Hg, Pb and Zn. Chem. Tech. Biotechnol 70:67-73.

Jensen, J.B., Kubes, V. and Kubal, M. (1994). Electrokinetic Remediation of Soils Polluted with Heavy Metals. Removal of Zink and Copper Using a New Concept. Environmental Technology, Vol. 15, pp. 1077-1082.

Jensen PE, Ottosen LM, Ferreira C, Villumsen A (2006[a]) Kinetics of electrodialytic extraction of Pb and soil cations from a slurry of contaminated soil fines. Hazardous Materials (B138), 493-499.

Jensen PE, Ottosen LM, Pedersen AJ (2006[b]) Speciation of Pb in industrially polluted soils. Water, Air and Soil Pollution 170:359-382.

Jensen PE, Ottosen LM, Harmon TC (2007) The effect of soil type on the electrodialytic remediation of Lead-contaminated sol. Environ. Eng. 24:234-244.

Kim SO, Moon SH, Kim KW (2001) Removal of heavy metals from soils using enhanced electrokinetic soil processing. Water, air and soil pollution, 125:259-272.

Kim WS, Kim SO, Kim KW (2004) Enhanced electrokinetic extraction of heavy metals from soils assisted by ion exchange membranes. Hazardous Materials 118:93-102.

Lageman R, Pool W, Seffinga G (1989) Electro-reclamation: Theory and Practice. Chemistry and industry, pp. 585-590.

Li RS, Li LY (2000) Enhancement of electrokinetic extraction from lead-spiked soils. Environ. Eng. 126:849-857.

Ottosen, L.M., Hansen, H.K. and Hansen, C.S. (2000). Water splitting at ion-exchange membranes and potential differences in soil during electrodialytic soil remediation. Journal of Applied Electrochemistry, Vol. 30, pp. 1199-1207.

Ottosen LM, Lepkova K, Kubal M (2006) Comparison of electrodialytic removal of Cu from spiked kaolinite, spiked soil and industrially polluted soil. Hazardous Materials B137:113-120.

Ottosen, L.M.; Hansen, H.K.; Ribeiro, A.B.; Villumsen, A. (2001) Removal of Cu, Pb and Zn in an applied electric field in calcareous and non-calcareous soils. Journal of Hazardous Materials, 85/3, 291-299

Ottosen, L.M.; Pedersen, A.J.; Ribeiro, A.B.; Hansen, H.K. (2005) Case study on the strategy and application of enhancement solutions to improve remediation of soils contaminated with Cu, Pb and Zn by means of electrodialysis. Engineering Geology 77, 317-329

Probstein RF, Hicks RE (1993) Removal of contaminants from soil by electric fields. Science 260:498-503.

Ribeiro AB, Mexia JT (1997). A dynamic model for the electrokinetic removal of copper from a polluted soil. Hazardous Materials (56), 257-271.

Skibsted G, Ottosen LM, Jensen PE, Elektorowicz M. Long-term electrodialytic soil remediation – Soil weathering (Appendix A in the PhD-thesis)

Vengris T, Binkiene R, Sveikauskaité A (2001) Electrokinetic remediation of lead-, zinc and cadmium-contaminated soil. Chem Technol Biotechnol 76:1165-1170.

West LJ, Steward DI, Binley AM, Shaw B (1999) Resistivity imaging of soil during electrokinetic transport. Engineering Geology 53:205-215.

Wild A. (1989) Russel's Soil Conditions and Plant Growth, 11th edition. John Wiley & Sons, Inc. New York.

Tables and Figures

Table 1: Results for electrochemical treatment of Pb contaminated matrices.

Reference	Spiked/industrial	Removed Pb
Kim et al. (2001)	Industrially polluted soil from a mining area	50 %
Jensen et al. (2007)	Ten industrially polluted soils	0.7-39.4 %
Li and Li (2000)	spiked carbonate-rich illitic soil	80 %
Vengris et al. (2001)	Sandy soil spiked with $Pb(NO_3)$	70 %
Altin and Degirmenci (2005)	Soils spiked with $Pb(NO_3)$	70 %
Hamed et al. (1991)	Kaolinite spiked with $Pb(NO_3)$	75-95 %
Li and Li (2000)	Kaolinite spiked with Pb	60 %
Kim et al. (2001)	Kaolinite spiked with $Pb(NO_3)$	75 %
Han and Kim (2003)	Kaolinite spiked with $Pb(NO_3)$	75 %
Kim et al. (2004)	Kaolinite spiked with $Pb(NO_3)$	90-96 %
Altin and Degirmenci (2005)	Kaolinite spiked with $Pb(NO_3)$	95 %

Table 2: Concentrations of trace elements and calcium in (mg/kg dry matter) for the two soils, measured by total digestion and DS 259.The Danish limiting values is included for the trace elements.

	Soil A		Soil B		
Elements	Total digestion	DS 259	Total digestion	DS 259	Danish limiting values
As	14	3.1	5.2	0.2	20
Cd	1.9	0.7	0.9	0.2	0.5
Cr	54	8.2	63	7.2	500
Cu	432	239	8.2	5.2	500
Ni	18	8.7	9.2	4.7	30
Pb	529	342	22	12	40
Zn	513	332	32	22	500
Ca	45,400	40,900	7,530	3,390	

Table 3: Initial values of pH and conductivity (double measurements), $CaCO_3$ and Organic matter (triple measurements) for Soil B and Soil A

		Soil A	Soil B
pH		7.7	5.9
Conductivity	mS/cm	0.859	0.835
$CaCO_3$	%	9.1 ± 0.4	0.2 ± 0.0
Organic matter	%	3.3 ± 0.1	6.4 ± 0.1
Initial water content	%	16.2 ± 0.1	26.5 ± 0.3

Table 4: Final pH, conductivity, water content, organic matter and acid soluble concentrations of Cd and Pb after EDR (Average of the 10 slices)

	pH	Conductivity mS/cm	Water content %	Organic matter %	Pb mg/kg	Cd mg/kg
Soil A	3.0 ± 0.4	0.180 ± 0.043	22.3 ± 0.6	3.1 ± 0.2	273 ± 166	0.43 ± 0.11
Soil B	2.4 ± 0.1	0.560 ± 0.043	26.3 ± 0.7	4.6 ± 0.2	9.86 ± 3.79	0.05 ± 0.08
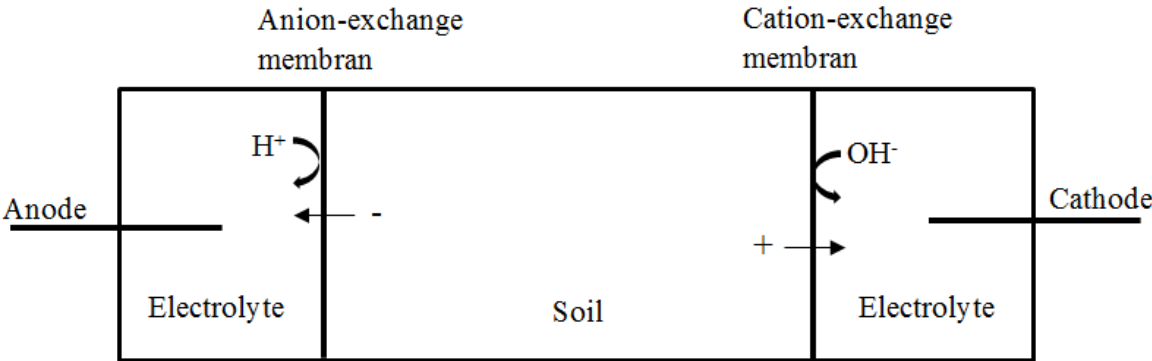
Figure 1: Schematic illustration of the electrodialytic setup
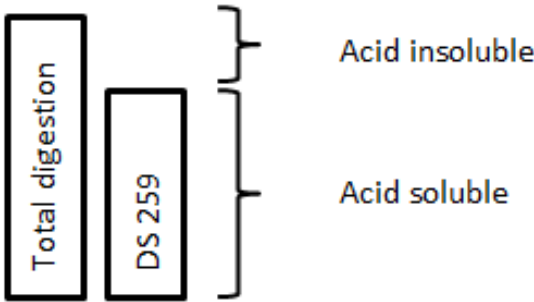
Figure 2: Illustration of the difference between the two used extractions methods.
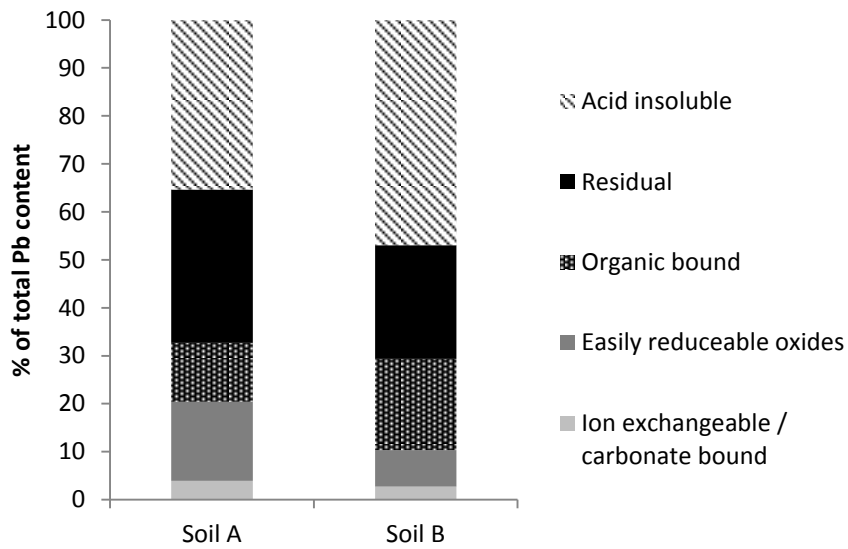
Figure 3: Sequential extraction of Pb for the two soils presented as percent of the total content measured by total digestion.
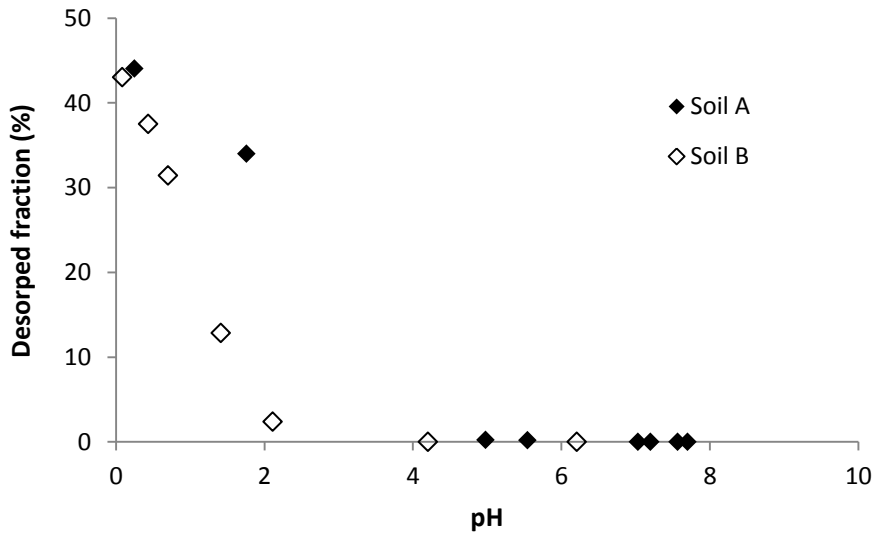
Figure 4: The pH-desorption dependency of Pb, expressed as fraction of the total lead content measured by total digestion.
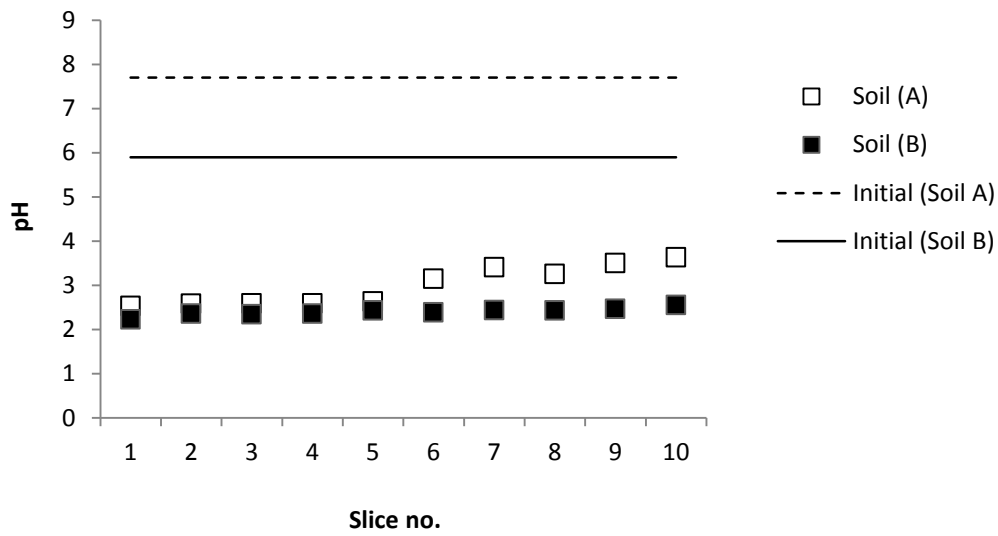
Figure 5: Profile of pH in Soil (A) and Soil (B) after EDR for 842 days.
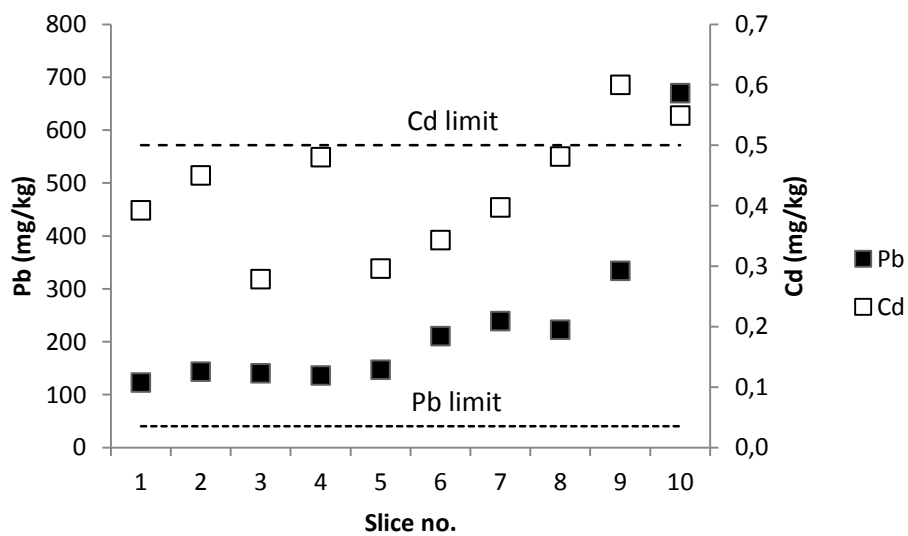

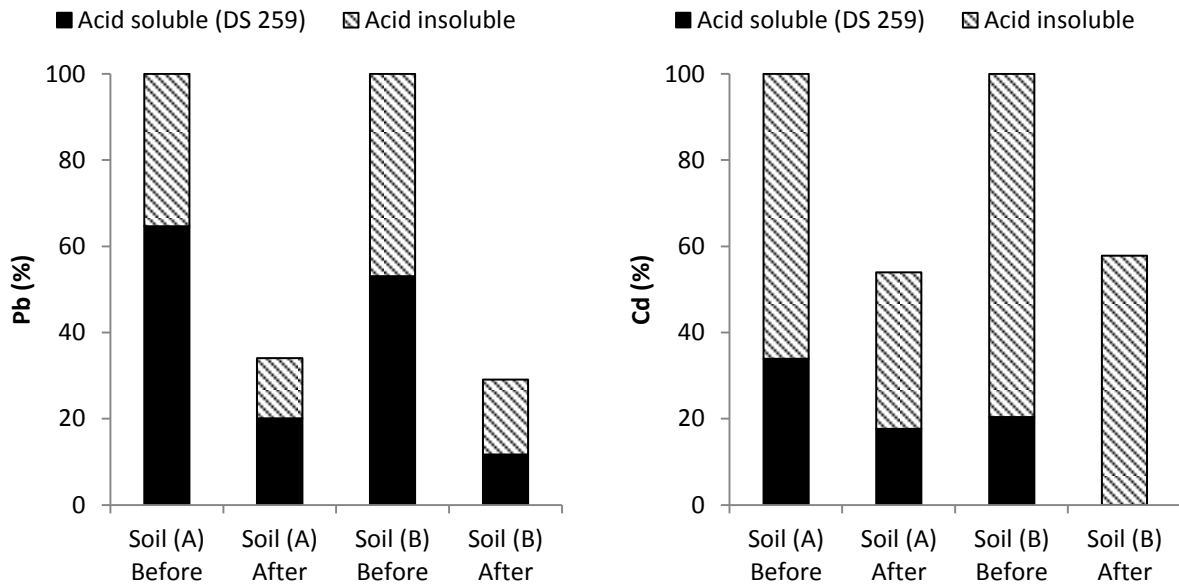Figure 6: Pb and Cd profile in Soil (A) after EDR for 842 days.

Figure 7: Distribution of the lead and cadmium content between acid soluble (DS 259) and acid insoluble fraction before and after EDR for Slice no. 1.The fractions after EDR is calculated as percentage of the total content before EDR.
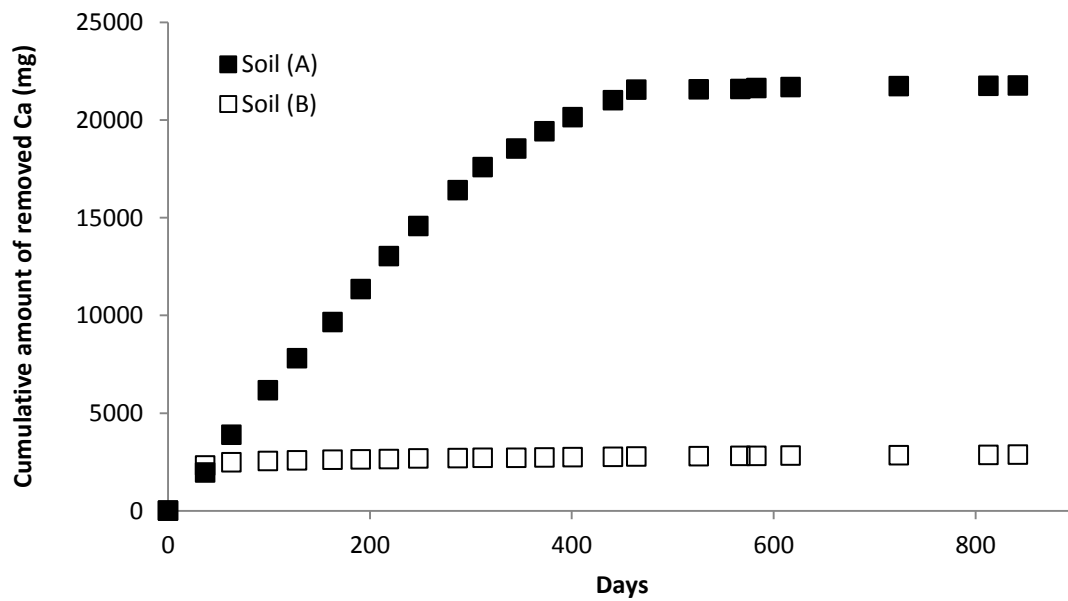

Figure 8: Cumulative amounts of removed calcium from electrolytic solutions during ED.
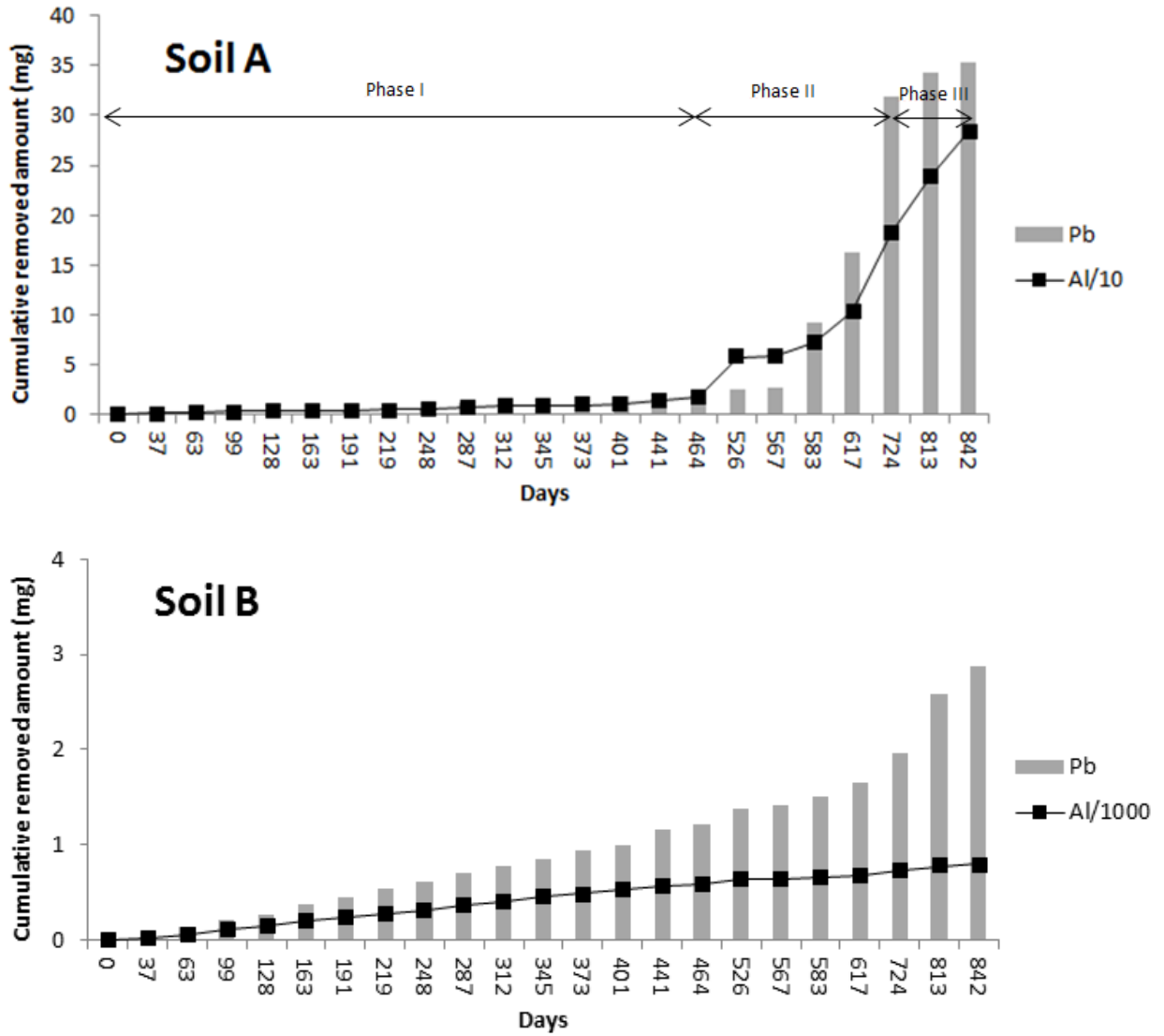
Figure 9: Cumulative removed amounts of Pb and Al. Soil (A); the amount of Al is presented as $(\cdot 10^{-1})$ and identification of phase I), II) and III). Soil (B); the amount of Al is presented as $(\cdot 10^{-3})$.

Appendix C

The possibility of using electrokinetics for desalination of sandstone with low porosity

Gry Skibsted, Lisbeth Ottosen and Pernille E. Jensen

Department of Civil Engieering, Technical University of Denmark, Building 118, 2800 Kgs. Lyngby, Denmark.

The possibility of using electrokinetics for desalination of sandstone with low porosity

GRY PETERSEN, LISBETH M. OTTOSEN AND PERNILLE E. JENSEN

BYG, Technical University of Denmark
Brovej, Building 118, Dk-2800 Kgs. Lyngby, Denmark
gryp@byg.dtu.dk

Abstract Salt-induced decay of sandstone is caused by salt crystallization within the pore structure. The salt is transported into the material with moisture. The crystallization pattern depends on several aspects, such as: Changes in moisture content, the type of salt, and the pore structure. This work provides visual observations of salt-induced decay patterns of a Danish Nexø sandstone with low porosity (8.0 %) after exposure to two different salt solutions. Suction from a NaCl solution leads to efflorescence (precipitation on the outer surface) while Na_2SO_4 resulted in loss of surface (subflorescence). Electrokinetic desalination could efficiently be used for desalination of the Nexø sandstone and reduce the risk for decay: By applying 10 mA for only 72 hours it was possible to reduce the sulphate concentration from 2209 mg/kg to 1022 mg/kg nearest the cathode.

1. Introduction

Salt-induced decay of porous sandstone is a high risk factor for cultural heritage and monuments. One of the most common reasons for the deterioration of stone is the crystallization phenomena that take place in pores and cracks at and near exposed surfaces [2]. The presence of salts in pore materials can be due to natural sources (e.g. capillarity suction from soil, sea water spray, wind) [3, 4] as well as anthropogenic (e.g. fertilizers or de-icing salt) [3]. The salt enters the porous material with moisture and the position where the salt crystallizes is determined by the dynamic balance between the rate of evaporation of water from the surface and the rate of resupply of solution to that site [2]. If the rate of resupply of solution to the surface is sufficient to compensate the rate of evaporation, the solution deposits on the surface and is named efflorescence. If the rate of transport of solution through the pores of the masonry does not bring fresh liquid to the surface as rapidly as the vapor departs, a dry zone develops beneath the surface. Crystallization of salts then occurs within the pores of the stone at the boundary between the wet and dry regions, generating spalls, flakes, or blisters [2]. This phenomenon is named subflorescence. Efflorescence is primarily a visual problem as it can be removed easily from the surface, while subflorescence is the more damaging mechanism [2, 5, 6]. Commonly, the salt crystallization mechanisms are influenced by the properties of the salt solution, the properties of the growing salts, the climatic conditions, and the properties of the substrate [3]. The salt-induced decay is caused by a crystal pressure. It is not fully understood how this pressure develops to be strong enough to create damage inside the pore structure [3, 4, 6]. It is known, however, that the salt-

induced decay is not only caused by crystallization in a single pore, but requires growth of the crystal through a region of the body comparable in size to the strength controlling flaws of the stone [7]. Not all salts are equally harmful for the porous material. E.g. Rodriguez-Navarro & Doehne [6] showed that evaporation from a saturated Na_2SO_4 solution causes more damage in limestone than evaporation from a saturated NaCl solution because it easily forms supersaturated solutions which are the mechanism for the generation of stress [8]. According to Price and Brimblecombe [9] at 20°C $Na_2SO_4 \cdot 10H_2O$ is the stable form of sodium sulfate at relative humidity (RH) between 71 % and 93 %. $Na_2SO_4 \cdot 10H_2O$ occupies 314 % more volume than the anhydrous salt [9]. This can result in an enormous volume change for the salt of sodium sulfate with changes in RH, which is likely to be a major factor involved in the development of crystal pressure.

The salt induced-decay can be avoided by reducing the salt content in the porous sandstone before the salt content increases to a destroying level. According to the Austrian ÖNORM B3355-1 "Trockenlegung von Feuchtem Mauerwerk–Bauwerksdiagnostik und Planungsgrundlagen" (Dehumidification of masonry-building diagnostics and planning principles), there is no risk for sulfate induced decay when the level of sulfate is below 0.1 % weight (1000 mg/kg). In the range between 0.1 % weight to 0.25 % weight (2500 mg/kg) individual evaluation is necessary, and above 0.25 % weight active salt removal is advised. By conservators the most commonly used method for reduction of salt content is by using a poultice. Recently an alternative method was tested by Ottosen and Rörig-dalgaard [1] who obtained a chloride removal of 99 % from a brick with a porosity of 28.2 % by electrokinetics. In this study the possibility of reducing the sulphate content in a Danish Nexø sandstone with a porosity of 8.0 % using by the electrokinetic desalination method is investigated. Furthermore, the salt-induced decay caused by Na_2SO_4 on an identical sandstone is illustrated by a suction experiment.

2. Electrokinetic desalination

In a solution, the electrical current is due to the transport of ions (electromigration) through the electrolyte. This movement is motivated by the electrode processes. There are two primary electrode processes; Oxidation of water at the anode (1) generates acid, while reduction of water at the cathode (2) generates base [10].

$$H_2O \rightarrow \tfrac{1}{2}O_2\ (g) + 2H^+ + 2e^-$$

(1)

$$2H_2O + 2e^- \rightarrow H_2\ (g) + 2OH^-$$

(2)

The electrokinetic desalination method is based on electromigration due to an applied electric field. In porous sandstones the electromigration will take place through the pore

solutions and transport process will result in movement of cations (Na^+) and (H+) towards the cathode and anions (SO_4^{2-}) and (OH-) toward the anode as illustrated in figure 1.
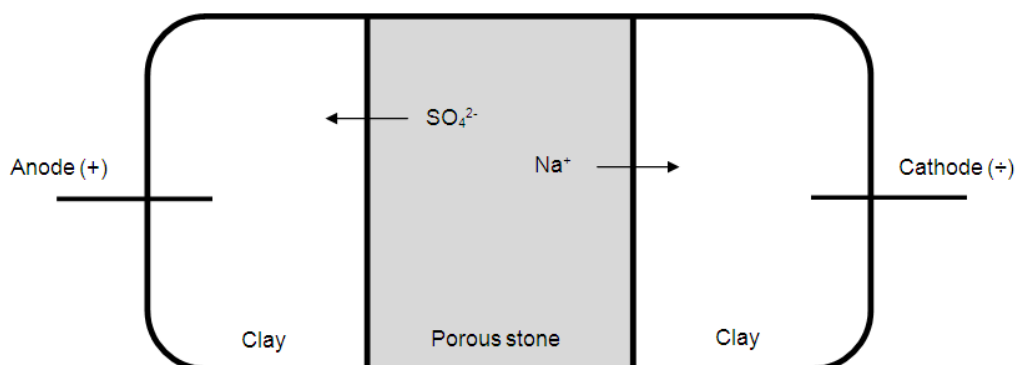

Figure 1: Principle of electrokinetic desalination.

3. Materials and methods

The stone used for the experiments was a violet/red Nexø Sandstone. The stone was removed during a minor renovation at Kronborg Castle, Helsingør, Denmark. It was visually inhomogeneous and separate layers were clear. Nexø Sandstones consist of grains of mainly quartz and feldspar, and the bonding material is silicon [11]. The stone used for the experiments was cut into smaller pieces by a mechanical saw. The porosity (pore volume fraction) of the experimental sample was measured in triplicate by vacuum saturation resulting 8.0 %.

Two samples (9.7 x 2.2 x 2.5 cm) of the stone were used in the suction experiment for visualizing salt-induced decay. A beaker with salt solution was wrapped with plastic film to hinder evaporation of water from the beaker, the stone sample was placed through a hole in the middle of the film such that approximately 4 cm of the sample was exposed to the salt solution and the rest of the sample (5-6 cm) was above both the solution and the plastic film. The setup is shown in Figure 2. The samples were placed in either a solution of 1.4 M NaCl or a solution of 1.4 M Na_2SO_4. After two weeks the samples were visually inspected.

For the desalination experiment the stone pieces were 10.5 x 10.5 x 3.5 cm. Three pieces were submerged in a solution of Na_2SO_4 (115.52 g/L) for 14 days. Two experiments were made; one with an applied current at 10 mA for 72 hours and one without any applied current (diffusion experiment). The third stone were wrapped in plastic and used as a reference. The diffusion experiment was made to identify the desalination pattern from simple diffusion. For the experiment with current and diffusion, the experimental set-up was inspired by Ottosen and Rörig-Dalgaard [1] as shown in the Figure 3: The electrokinetic desalination was performed transverse to the separate layers in the stone matrix. The electrode compartments were filled with clay (mixture of kaolinite and $CaCO_3$) and placed on each side of the stone. The two holes in the electrode compartments were closed with rubber corks and an inert electrode (platinum coated) was placed through the cork furthest away from the stone. During

the experiment the stone was wrapped in plastic to avoid evaporation of moisture. After the electrokinetic treatment, the stone was segmented with a hammer and chisel into three slices; anode end, cathode end, and middle section. The dried samples were crushed and 10 g powder was suspended in 25 ml distilled water and placed on a shaking table for at least 24 h. The samples were settled for 10 min and pH and conductivity were measured. Then the samples were filtered through a 0.45 μm filter and the extract was used for further analysis. The sodium concentration was analyzed with AAS after adding 0.025 ml 10 % $LaCl_3$ to 5 ml sample and the sulfate concentration was measured with ion chromatograph.

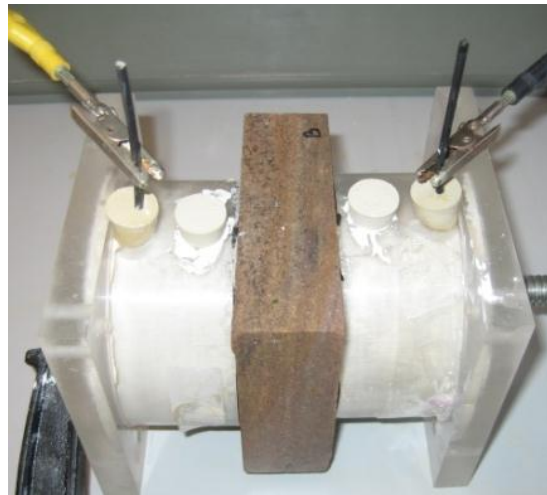Figure 2: Suction set-up

Figure 3: The electrokinetic desalination set-up.

4. Results and discussion

Figure 4 and 5 illustrate clearly that the type of salt plays an important role for the salt decay pattern in the sandstone. Figure 4 shows the result of exposure to suction in NaCl solution. The result was efflorescence, since the salt precipitated on the outer surface. Figure 5 shows the result after exposure to suction from the Na_2SO_4 solution. The surface was blistering in pieces with a thickness of approximately 1 mm. This loss of surface was a clear example of subflorescence. There were no visual signs of precipitation on the outer original surface, only where the stone was damaged due to loss of surface. From this simple suction experiment it was observed that salt can have a damaging effect and result in decay on this sandstone, and in accordance with literature [5, 6] it was evident that Na_2SO_4 is the more damaging of the two tested salts.

Figure 4: Efflorescence. Nexø sandstone exposed to NaCl solution.

Figure 5: Subflorescence. Nexø sandstone exposed to Na_2SO_4 solution

During the electrokinetic desalination experiment, sodium was transported towards the cathode and sulfate ions towards the anode. This is the reason why the lowest sulfate concentration and the highest sodium concentration was observed in the section nearest to the cathode in the stone sample as shown in Figure 6. The initial sulfate concentration was 2209 mg/kg and the final concentration in the cathode end (third part closed to cathode) after the electrokinetic treatment was 1022 mg/kg. This corresponds to a reduction of 53.7 % in that part of the stone. According to the Austrian ÖNORM 3355-1, this level is very close to the limit for no risk (<1000 mg/kg). 481 mg sulfate was removed from the stone during the electrokinetic desalination experiment (based on measurements in the clay from the anode), and the final average concentration was 1240 mg/kg, which corresponds to a total reduction of 44 %. The conductivity was high in all three parts of the stone after the electrokinetic treatment, thus it would probably be possible to continue the desalination process to reach a lower and more homogeneous level of sulfate in the stone. Although the carbonated clay acted as a buffer substance during the electrochemical treatment, a pH variation was seen through the stone as a consequence of the electrode processes (Figure 6). This is a side effect which must be coped with, if the method is implemented.

In the diffusion experiment, pH did not change during the different parts of the stone, but as expected, pure diffusion was not as effective a desalination method as the electrokinetic treatment. From Figure 6 it can be seen that only in the parts nearest to the clay compartments, the sulfate and sodium concentrations were reduced.
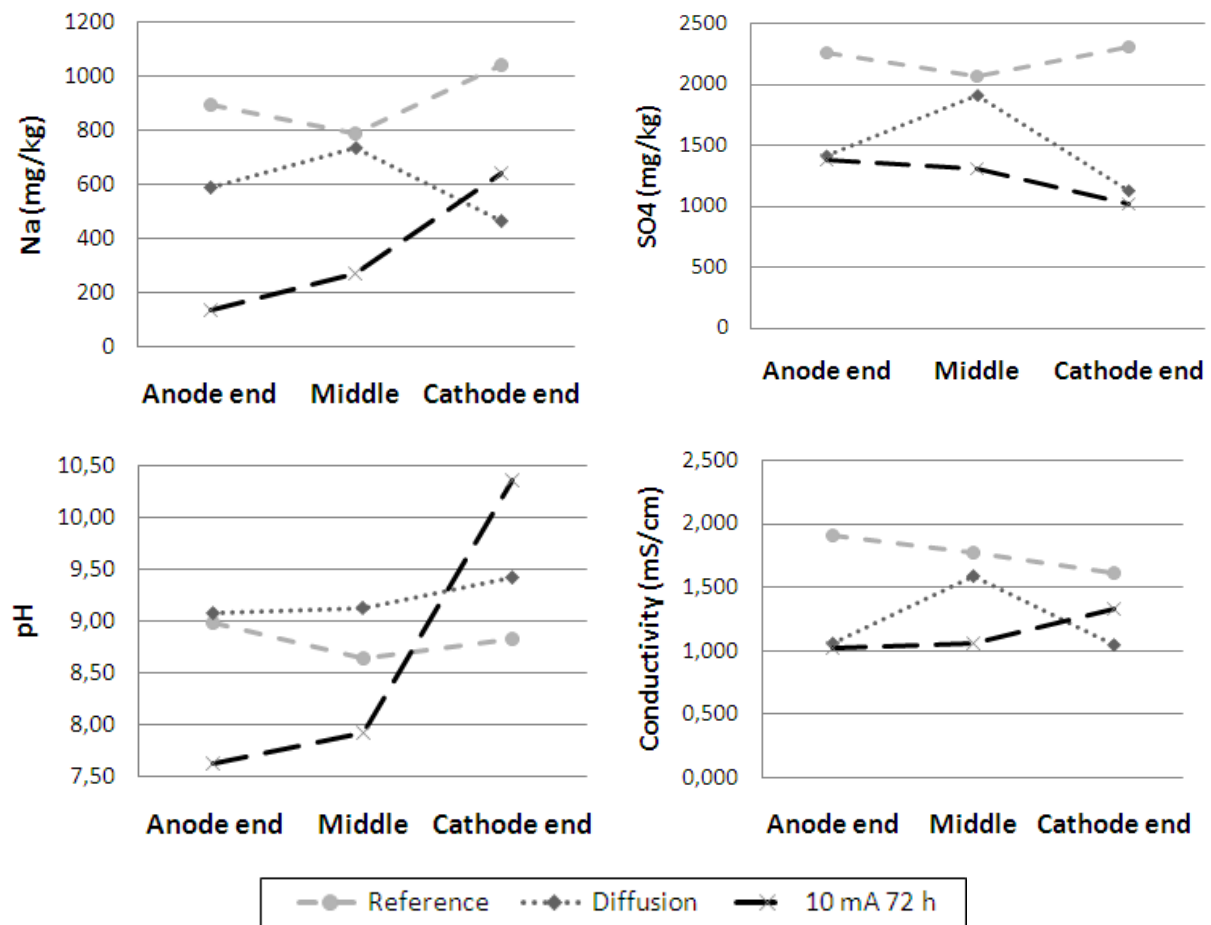
Figure 6: The meassured sodium and sulfate concentration, the pH and the conductivity in the three parts of the stone.

5. Conclusions

It was observed that capillary suction of a salt solution may have a harmful effect on the Nexø sandstone. The response on suction from a NaCl solution is efflorescence of a white powder on the surface. The decay pattern from suction in a Na_2SO_4 solution has a more damaging character as subflorescence, where a loss of surface is the result. From the electrokinetic desalination experiment it was visualized that the method is a more rapid method than diffusion for sulfate removal from sandstone with low porosity (8.0 %).

6. Future work

Additional parameters need to be investigated before the method is recommended to be used on heritage buildings and monuments. It should be investigated to which extent the applied current produces changes in the original matrix of sandstone due to the developed pH profile, and how low a level of salt can be reached by the electrochemical desalination method

without developing too much resistance. Furthermore it would be of interest to identify the desalination pattern and coupled flow from the desalination of mixed types of salts.

7. References

[1] L.M. Ottosen and I. Rörig-dalgaard, "Desalination of a brick by application of an electric DC field," *Materials and structures* vol. 42, pp. 961-971, 2009

[2] S.Z. Lewin, "The mechanism of masonry decay through crystallization," Conservation of Historic Stone Buildings and Monuments, Washington, D.c.: National Academy of Sciences, pp. 120-144, 1982

[3] J. Ruedrich and S. Siegesmund, "Salt and ice crystallization in porous sandstones," *Environ Geol* vol. 52, pp. 225-249, 2007

[4] E.M. Winkler, "Weathering and Weathering Rates of Natural Stone," *Environ Geol Water Sci* vol. 9, no. 2, pp. 85-92, 1987

[5] D. Benavente, M.A. García del Cura, J. García-Guinea, S. Sánchez-Moral and S. Ordóñez, "Role of pore structure in salt crystallisation in unsaturated porous stone," *Journal of Crystal Growth* vol. 260, pp. 532-544, 2004

[6] C. Rodriguez-Navarro and E. Doehne, "Salt weathering: Influence of evaporation rate, supersaturation and crystallization pattern, " *Earth Surf. Process. Landforms* vol. 24, pp. 191-209, 1999.

[7] G.W. Scherer, "Crystallization in pores," *Cement and Concrete Research* vol. 29, pp. 1347-1358, 1999

[8] M. Steiger and S. Asmussen, "Crystallization of sodium sulfate phases in porous materials: The phase diagram Na_2SO_4-H_2O and the generation of stress," *Geochimica et Cosmochimica Acte* vol. 27, pp. 4291-4306, 2008

[9] C. Price and P. Brimblecombe, "Preventing salt damage in porous materials," In Eds A. Roy and P. Smith, "Preventive conservation: Practice, theory and research" Ottawa Congres, 12-16 Sep. pp. 90-93, 1994

[10] Y.B. Acar and A.N. Alshabkeh, "Principles of Electrokinetic Remediation," *Environ. Sci. Technol*. vol. 27, no. 13, pp. 2638-2647, 1993.

[11] E. Suenson, "Bygningsmaterialer, 3. Bind: Natursten," Jul. Gjellerups Forlag, pp. 117-139, 1942.

Appendix D

Electrochemical desalination of bricks – removal of Cl^-, NO_3^- and SO_4^{2-}

Gry Skibsted, Lisbeth Ottosen and Pernille E. Jensen

Department of Civil Engieering, Technical University of Denmark, Building 118, 2800 Kgs. Lyngby, Denmark.

Submitted

Electrochemical desalination of bricks – removal of Cl⁻, NO₃⁻ and SO₄²⁻

Electrochemical desalination of bricks – removal of Cl^-, NO_3^- and SO_4^{2-}

Gry Skibsted*, Lisbeth M. Ottosen and Pernille E. Jensen

Department of Civil Engineering,
Technical University of Denmark, Building 118,
*2800 Kgs. Lyngby, Denmark*
*Corresponding author: gryp@byg.dtu.dk

Keywords: Electrokinetics, Desalination rates, Salt decay, Sulfate, Electrode processes

Abstract Soluble salts can play an important role in deterioration of porous stone materials of buildings and monuments. Electrochemical desalination (ED) was suggested for reducing the salt content in such materials to stop deterioration. An electric DC field is applied to the porous, moist stone material and the ions of the problematic salts are transported into poultices placed externally. During the process acid is produced at the anode and hydroxyl at the cathode from electrolysis. To eliminate the risk for damaging of the stone due to these pH changes a $CaCO_3$ rich poultice is used as buffering material between the electrodes and the stone. When buffering the produced acid the poultice acts as source for free Ca-ions, which may affects the removal of sulfates, due to precipitation of $CaSO_4$. The aim of the present work is to evaluate the influence of Ca^{2+} on the removal of SO_4^{2-} in comparison to removal of Cl^- and NO_3^-, where no precipitation with Ca^{2+} is expected in the moist pores. A red brick contaminated with Na single salts was used and 15 ED experiments were carried out with varying durations of 1, 2, 5 and 8 days. The results showed high removals: 99% (Cl^-), 100 % (NO_3^-), and 89 % (SO_4^{2-}) in less than 8 days. The removal per valence for SO_4^{2-} was only 75 % of the ED removal for Cl^- and NO_3^- which were almost similar. Calcium penetration from the anode clay into the brick caused decreased ED removal rate of SO_4^{2-} compared to Cl^- and NO_3^-, but did not hinder desalination.

1. Introduction

Salt-induced decay has high impact on deteriorations of porous bricks and stone materials. The salts enter the porous material with moisture and due to continuous evaporation and supply of salt solution, the solution inside the porous material can be supersaturated over time and the salts crystallize (Lewin 1982). The crystals can generate a pressure on the pore walls, which can result in cracking and blistering of the materials surface (Winkler 1987; Rodriguez-Navarro and Doehne 1999; Ruedrich and Siegesmund 2007). Among the most common salts in building materials are NaCl, $NaNO_3$, Na_2SO_4 and $MgSO_4$ (Steiger 2005). Electrochemical treatment is an effective method to reduce the Cl^- content in porous materials; first Electrochemical Chloride Extraction (ECE) from concrete and lately Electrochemical Desalination (ED) of bricks has been studied. Earlier obtained results with ECE are; 30-75 % chloride reduction from concrete in 90 days after applying 1 A/m^2 (Fajardo et al. 2006), 40 % chloride reduction in 50 days after application of 1 A/m^2 (Orellan et al. 2004) and 85 % chloride reduction by applying 28.6 A/m^2 to the exposed steel surface (Ihekwaba et al. 1996). ED was used to reduce the Cl^- content in single bricks, and Ottosen and Rörig-Dalgaard (2009) obtained 99 % removal of Cl^-. The concept of ED is illustrated in Figure 1. When applying an electric DC field to a porous, moist material the ions in the pore solution will transport the current (electromigration) between the electrodes; anions in the direction of the anode and cations the opposite way. When the electrodes are placed in external compartments, as in Figure 1, the electrode compartments are storage location for the ions removed from the stone. Electromigration is not dependent on the pore size of the material and thus is applicable even for small pore sizes (Probstein & Hicks 1993). Furthermore the applied electric field affects the whole matrix as opposed to the poulticing methods, which are used in conservation today. Poulticing is working from the surface of the object and the transport mechanisms utilized are diffusion and advection (Sawdy *et al.* 2008). Poulticing is also highly dependent on the pore size distribution of stone and poultice (Sawdy et al. 2008). Electrolysis of water at the electrodes are the primary electrode processes in ED, i.e. oxidation of water at the anode (1) and reduction of water at the cathode (2).

$$H_2O \rightarrow 2H^+ + \tfrac{1}{2}O_2(g) + 2e^- \tag{1}$$

$$2H_2O + 2e^- \rightarrow 2OH^- + 2H_2(g) \tag{2}$$
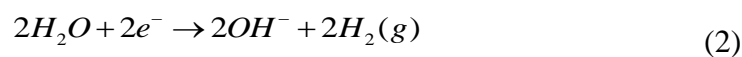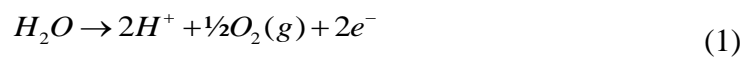
To avoid extreme pH changes in the stone, the electrodes are placed in $CaCO_3$ rich poultice. The poultice play several important roles (a) buffering of the acid produced at the anode and to some extent hydroxides from the cathode, (b) forms good electrical contact between the stone and the metallic electrodes, and (c) act as storage matrix for the removed ions (Ottosen & Rörig-Dalgaard 2009). A side effect is though that the $CaCO_3$ in the poultice acts as source for Ca^{2+} and CO_3^{2-} ions when buffering the acid (3). In the poultice at the anode the reaction between the acid and the carbonate leads to bicarbonate and carbonic acid formation resulting

in release of Ca^{2+}. In the poultice around the cathode precipitation of calcium hydroxide decrease the amount of OH^- entering the stone (Paz-García et al. 2012).

$$CaCO_3 \leftrightarrow Ca^{2+} + CO_3^{2-} \qquad (3)$$
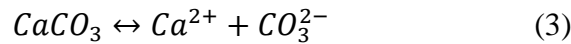
Electrochemical desalination experiments conducted without buffering at the electrodes have underlined that the buffering poultice is vital to the method. Visible damage of limestone due to the acid generated at the anode has been reported (Herinckx et al. 2011). In addition it was shown that electromigration of target ions was inhibited due to an extremely high potential drop created by collision of the alkaline and acidic fronts in the stone, as this zone was depleted for ions (Kamran et al. 2012).

Previously it was found in pilot scale experiments with ED with buffer poultice that SO_4^{2-} was not removed as effectively as Cl^- and NO_3^- (Ottosen et al. 2008). Based on numerical modelling of ED of single bricks with $CaCO_3$ rich poultice at the electrodes, Paz-García et al. (2011) considered Ca^{2+} to be responsible for the slower SO_4^{2-} removal, because calcium electromigrated into the stone and precipitated with free SO_4^{2-} in the pores forming $CaSO_4$. The present work is an experimental study of ED with the aim to evaluate the influence of Ca^{2+} electromigration from the anode poultice on the removal of Cl^-, NO_3^- and SO_4^{2-} in single bricks.

2. Experimental

2.1 Brick samples

Typical Danish red, baked clay bricks with the porosity 31.5 % were used in the experiments. To have homogeneous samples the outer first cm from all surfaces was removed by wet cutting. The remaining parts of the stones were cut further into 15 samples of the size: 3 cm x 3 cm x 10 cm. The samples were dried at 105°C for 24 h before submerged in one of three sodium salt solutions (five samples in each solution); 15.00 g/L NaCl, 18.23 g/L Na_2SO_4, or 21.81 g/L $NaNO_3$. The brick samples were contaminated with Na salts in a concentration so the initial Na concentration was the same. Due to the valence the initial molar concentration of SO_4^{2-} was only half the concentration of Cl^- and NO_3^-. The bricks were submerged for 7 days.

2.2 Experimental setup

Electrode compartments with the size 3 x 3 x 3 cm^3 were placed at each end of the brick (Figure 2). The frame of the electrode compartments were folded in thin plastic and jointed with tape to fit the ends of the stones. The frames were filled with poultice; a mixture of kaolinite and $CaCO_3$ (patent by Rörig-Dalgaard and Ottosen 2011). Inert electrode mesh was placed at the end of each electrode compartments (away from the brick). The brick sample and electrode compartments were wrapped in plastic film to hinder evaporation of moisture

during ED. A constant current of 2 mA was applied and the voltage was monitored. The durations of the ED experiments were 1, 2, 5 or 8 days. Reference samples without applied current were made for each salt. The experimental characteristics (dry weight, initial water content, current, voltage range and duration) are given in Table 1.

2.3 Analytical

After ED the brick samples were segmented with hammer and chisel into five segments; numbered from the anode end (Figure 2). The reference bricks (experiment 1, 6 and 11) were segmented after 7 days submersion. The water content in the five brick segments was measured and calculated as weight loss after drying at 105°C per dry weight. The dried segments were grinded in a mechanical mortar. Following 10 g powder was suspended in 25 ml distilled water and agitated for 24 h. The samples settled for 10 min and pH and conductivity were measured by electrodes. The samples were filtered through 0.45 μm filter. Na and Ca concentrations were analyzed by atomic adsorption spectrometry (AAS, GBC 932AA). Cl^-, SO_4^{2-}, and NO_3^- were analyzed by ion chromatography (IC, Dionex DX-120).

3. Results and discussions

Average pH, conductivity, water content and salt concentrations in the brick samples at the end of the desalination experiments are shown in Table 2. The pH in the brick samples increased from initially 9.5 to above 10. This pH increase indicates that hydroxide ions electromigrated into the brick samples from the cathode compartment, where the poultice thus did not fully neutralize the hydroxide ions.

The conductivity decreased from 1.4 mS/cm to $\leq$ 0.3 mS/cm in all three cases due to the decreased salt concentrations. The water content remained constant in the bricks during the first 2 days of ED, but was reduced by prolonged treatment. After 8 days the water content was reduced to 6 % (experiment 5, 10 and 15). The deviations in moisture content between the 5 segments of each sample is relatively low (<0.8 %), thus the moisture reduction was not an evident indication of electroosmotic transport; which implies lower water content in the vicinity of the anode than in the cathode end of the sample as seen in Ottosen and Rörig-Dalgaard (2009). The decrease in water content in the bricks after 5 and 8 days shows rather that evaporation of moisture from the samples was not eliminated by wrapping the sample and electrode compartments in plastic.

3.1 Desalination

The remediation profiles for the three target anions are showed in Figure 3. After 1 day of treatment a minor reduction of anion concentration in segments at the anode is observed, but the major reduction is in segment 5. As the anions electromigrate towards the anode, segment no. 5 (closest to the cathode) was desalinated first followed by segment no. 4 and so forth.

The anion concentrations were evaluated in accordance to the Austrian ÖNORM B 3355-1 "Trockenlegung von Feuchtem Mauerwerk-Bauwerksdiagnistik und planungsgrundlagen". The norm is for pure salt solutions, and does not take the porosity and the specific matrix into account, but it is the only norm of its kind at present. The Austrian ÖNORM operates with two threshold values; a critical limit and a limit of no risk. At concentrations above the critical limit active salt removal is advised and in between the two limits an individual evaluation is necessary. For the three chosen anions the limits are (critical limit/limit for no risk):

- Cl^- (1000 mg/kg / 300 mg/kg)
- NO_3^- (1500 mg/kg / 500 mg/kg)
- SO_4^{2-} (2500 mg/kg / 1000 mg/kg)

For experiments with Cl^- and NO_3^- the initial anion concentration (See Table 2) is above the critical limit meaning that action is needed. The initial SO_4^{2-} concentration is below the critical limit but above the limit for no risk. In the case of Cl^- and NO_3^- the average concentration after 1 day of ED were already below the critical limit, but seen in more details, the concentrations in the middle of the samples are still too high in both cases, see Figure 3. For the sample with NaCl it was only segment no. 3 and for the sample with $NaNO_3$ it was segment no. 2, 3 and 4. After 2 days of ED the concentration in the entire samples for both Cl^- and NO_3^- were reduced to below the critical limit. After 5 days of ED the concentrations were below the limit for no risk for all three anions.

The present study thus shows that ED is applicable for removal of the three anions; Cl^-, NO_3^- and SO_4^{2-}. During 8 days of ED at 2 mA the anion content in the bricks are reduced by: 99 % (Cl^-), 100 % (NO_3^-), and 89 % (SO_4^{2-}). For Cl^- and NO_3^- the reduction is already obtained after 5 days.

3.2 Transport number

The transport number (t), also termed electromigration number, is the fraction of current carried by each ion present in the solution (Laidler and Meiser, 1999).The transport number for an anion is expressed by (4), where the total amount of coulomb consumed (Q_{total}) at a specific current strength (I) and duration time (t) is given by (5). The amount of coulomb used for migration of a specific ion is given by (6) where Δn is the reduced molar amount of the ion. F is Faradays constant (96,485 $C \cdot mol^{-1}$) and z the valence of the ion.

$$t_{ion} = \frac{Q_{ion}}{Q_{total}} \qquad (4)$$

$$Q_{total} = I \cdot t \qquad (5)$$

$$Q_{ion} = \Delta n \cdot F \cdot z \qquad (6)$$

The transport numbers for Cl^-, NO_3^-, SO_4^{2-} and Na are shown in Table 3. The transport numbers based on ED for 8 days were almost identical; 0.34 (Cl^-), 0.33 (NO_3^-) and 0.30 (SO_4^{2-}). The transport numbers decreased with longer duration and was the lowest for the longest experiments (8 days). This shows that fraction of current carried by other ions than the target anions increased with time. In the case of Cl^- and NO_3^- the transport numbers were almost nil between the 5th and 8th day of ED because neither Cl^- nor NO_3^- was left in the bricks to be removed after 5 days. The current might instead have been carried by e.g. H^+, Ca^{2+} and OH^-.

During the first day of ED the transport numbers were 0.63 (Cl^-), 0.76 (NO_3^-) and 0.42 (SO_4^{2-}). The ion mobility pr. valence for Cl^- and NO_3^- are higher than the mobility pr. valence for SO_4^{2-} (Atkins and Paula, 2001) and thus it was expected that the transport numbers for both Cl^- and NO_3^- was higher than the transport number for SO_4^{2-}, but a transport number above 0.5 might indicate that diffusion was significant. The transport numbers were calculated without consideration of diffusion which might be a reason for the unrealistic high calculated transport numbers for chloride and nitrate. For the same samples the transport numbers for Na were 0.20 (Cl^-), 0.56 (NO_3^-) and 0.40 (SO_4^{2-}). For $NaNO_3$ the fraction of current carried by both Na and NO_3^- is above 1 which is not possible without supplemented by diffusion. Diffusion of ions from the brick to the poultice must be expected, especially as the used brick has a higher porosity than the Nexø sandstone used by Petersen et al. (2010) where diffusion was observed. The diffusion was probably also the reason for the drop in the anion concentration in segments near the anode (in all three cases) after 1 day of ED, see Figure 3.

3.3 ED removal rates

The ED removal rate for the anions per valence were based on the trend lines from 0-5 days of ED in Figure 4, where the desalination is progressing. The desalination was concluded after 5 days and the ED removal rates pr. valence were in mmol/kg/day respectively; 5.69 (Cl^-), 5.96 (NO_3^-) and 4.23 (SO_4^{2-}). The ED removal rate for Cl^- was little slower than for NO_3^-, which is opposite to the ion mobility of the two ions. The ion mobility thus not the determining factor for the removal rate and cannot be used for prediction. The ED removal rate per negative charge of SO_4^{2-} was only approximately 75 % of the ED removal rates for Cl^- and NO_3^-, The reason for the slower ED removal rate for SO_4^{2-}, can in addition to the lower ion mobility per valence than Cl^- and NO_3^- also be due to precipitation of gypsum ($CaSO_4$) as Paz-García et al. (2011) reports based on chemical-numerical modelling of a similar system.

3.4 Gypsum formation

The Ca^{2+} produced when $CaCO_3$ buffers the acid generated by electrolysis at the anode electromigrated or diffuse into the bricks during ED. This is seen by the increase in average Ca concentrations (Table 2) for all experiments from 0-2 days of ED. At day 5 the content decreased again in samples with Cl^- and NO_3^-, which was opposite to the sample with SO_4^{2-}, where the Ca content increased until day 5 and the reduction first was obtained at day 8. This shows that the Ca content reduces again with prolonged ED, but the reduction is slower for

samples with SO_4^{2-}. Gypsum formation can be the cause for the lower SO_4^{2-} ED removal rate compared to Cl^- and NO_3^-. The Ca profile for the ED experiment with bricks contaminated with SO_4^{2-} (Figure 5) shows that the major fraction of Ca was found in the first two segments. The theoretically pore solution concentrations of Ca and SO_4^{2-} (mmol/L) in segment 1 and 2 were calculated based on information on the initial weight of the sample and the moisture content. The values of both Ca and SO_4^{2-} concentrations presented in the pore solutions (Table 4) were more than three orders of magnitude higher than the solubility of gypsum; 0.15 mmol/L (CRC 2010). Precipitation of gypsum is not considered deleterious to the desalination as the average concentrations of both Ca and SO_4^{2-} were reduced by prolonging ED from 5 to 8 days in the present case.

Continued dissolution of gypsum occurs as long as Ca^{2+} and SO_4^{2-} are removed from the pore solution by the applied electric field. When using poultice containing $CaCO_3$ as a buffer against acidification, it is not possible to avoid the electromigration of released Ca^{2+}. On the other hand, the buffering effect of the poultice is necessary. Without a buffering system, the brick (and mortar in the case of masonry) could be damaged by acidification, as it was seen for limestone by Herinckx et al. (2011). The desalination process can also stop (Kamran et al. 2012) as the current after some time is carried by protons and hydroxyl ions with high ionic mobility, which causes a narrow zone with very high electrical resistance, where the two ions meet and forms water molecules. The system with a buffering poultice overcomes the challenges Herinckx et al. (2011) and Kamran et al. (2012) experienced, as full desalination without lowering of brick pH was obtained in the present work.

4. Conclusion

The ED method was effective for reducing the content of Cl^-, NO_3^-, and SO_4^{2-} in bricks to concentrations which are considered harmless. In experiments with salt present as pure, single Na salts, 99 % (Cl^-), 100 % (NO_3^-), and 89 % (SO_4^{2-}) was removed in less than 8 days. The order of the ED removal rates for the specific anions were; $NO_3^- > Cl^- >> SO_4^{2-}$, and the ion mobility thus not the determining factor for the removal rate as the order here is $Cl^- > NO_3^- > SO_4^{2-}$. The ED removal rate per valence for SO_4^{2-} was only 75 % of the ED removal rates for Cl^- and NO_3^- (which were almost similar). A combination of lower ionic mobility of SO_4^{2-} and electromigration of Ca from the poultice at the anode into the brick and subsequently precipitation of $CaSO_4$ is probably responsible for the slower ED removal of SO_4^{2-}. The concentrations of Ca and SO_4^{2-} in the pore solution decreased after 5 days of ED and precipitation of gypsum is thus not considered as a permanent problem. Poultice with $CaCO_3$ as acid buffer substance is thus suitable also when SO_4^{2-} is the target anion.

References

Atkins P, de Paula J (2010) Physical Chemistry, Vol. 1: Thermodynamics & Kinetics, 9 ed. WH Freeman and Company, New York, p 939

CRC Handbook of Chemistry and Physics (2010). 90th ed. Accessible by DTU digital library.

Fajardo G, Escadeillas G, Argiguie G (2006) Electrochemical chloride extraction (ECE) from steel-reinforced concrete specimens contaminated by "artificial" sea-water. Corros Sci 48:110-125.

Herinckx S, Vanhellemont Y, Hendrickx R, Roels S, De Clercq H (2011) Salt removal from stone building materials using an electric field. In: Proceedings from the international conference on salt weathering on building and stone sculptures, Limassol, Cyprus 19-22 October 2011, pp 357-364

Kamran K, Van Soestbergen M, Huinink HP, Pel L (2012) Inhibition of electrokinetic ion transport in porous materials due to potential drops induced by electrolysis. Electrochem Acta 78:229-235

Ihekwaba NM, Hope BB, Hansson CM (1996) Pull-out and bond degradation of steel rebars in ECE concrete. Cement Concr Res 26(2):267-282.

Laidler KJ, Meiser JH (1999) Physical chemistry, 3rd ed. Houhton Mifflin Company, Boston, pp. 264-297.

Lewin SZ (1982) The mechanism of masonry decay through crystallization. Conservation of Historic Stone Buildings and Monuments, Washington, D.C.: National Academy of Science, 120-144

Orellan JC, Escadeillas G, Arliguie G (2004) Electrochemical chloride extraction: efficiency and side effects. Cement and Concrete Research 34:227–234

Ottosen LM, Rörig-Dalgaard I, Villumsen A (2008) Electrochemical removal of salts from masonry – Experiences from pilot scale. In: Proceedings from the international conference on salt weathering on building and stone sculptures, Copenhagen, Denmark October 22-24 2008, pp 341-350

Ottosen LM, Rörig-Dalgaard I (2009) Desalination of a brick by application of an electric DC field. Materials and structures 42:961-971

Paz-García JM, Johannesson B, Ottosen LM, Ribeiro AB, Rodríguez-Maroto JM (2011) Influence of the chemical interactions on the removal rate of different salts in electrokinetic desalination process. In: Proceedings from the international conference on salt weathering on building and stone sculptures, Limassol, Cyprus 19-22 October 2011, pp 373-380

Paz-García JM, Johannesson B, Ottosen LM, Alshawabkeh AN, Ribeiro AB, Rodríguez-Maroto JM (2012) Modeling of electrokinetic desalination of bricks. Electrochem. Acta (2012), doi:10.1016/j.electacta.2012.05.132

Petersen G, Ottosen LM and Jensen PE (2010) The possibility of using electrokinetics for desalination of sandstone with low porosity, In: Proceedings from the 8th fib international PhD Symposium in Civil Engineering, DTU, Denmark June 20-23 2010, pp 455-460

Probstein RF, Hicks E (1993) Removal of contaminants from soils by electric fields. Science 260:498-503

Rodriguez-Navarro C, Doehne E (1999) Salt weathering: Influence of evaporation rate, supersaturation and crystallization pattern. Earth Surf. Process. Landforms 24:191-209

Rörig-Dalgaard, Ottosen LM (2011) Desalination of porous materials by use of buffer electrode units. EPO patent 2276716.

Ruedrich J, Siegesmund S (2007) Salt and ice crystallization in porous sandstones. Environ Geol 52:225-249

Sawdy A, Heritage A, Pel L (2008) A review of salt transport in porous media, assessment methods and salt reduction treatments. In: Proceedings from the international conference on salt weathering on building and stone sculptures, Copenhagen, Denmark October 22-24 2008, pp 1-27

Steiger M (2005) Crystal growth in porous materials – I: The crystallization pressure of large crystals. Journal of crystal growth 282:455-469

Winkler EM (1987) Weathering and weathering rates of natural stone. Environ Geol Water Sci 9:85-92

Tables and Figures

Table 1: Conducted experiments.

Experiment No.	Anion	Dry weight (g)	Initial water content (%)	Current (mA)	Voltage (V)	Duration (Days)
1	Cl⁻	163.5	11.7	0	0	0
2		162.6	12.0	2.0	4.5-5.9	1
3		154.4	12.3	2.0	4.3-6.0	2
4		158.8	11.8	2.0	4.6-24.08	5
5		163.3	12.1	2.0	5.2-129.4	8
6	NO$_3^-$	149.7	12.4	0	0	0
7		151.4	11.9	2.0	4.8-6.1	1
8		150.8	11.8	2.0	5.0-6.3	2
9*		150.5	12.2	2.0	4.4-50.2	5
10		148.0	12.1	2.0	4.3-134.6	8
11	SO$_4^{2-}$	150.7	11.7	0	0	0
12		159.2	12.0	2.0	5.3-7.0	1
13		162.2	12.2	2.0	5.0-6.2	2
14**		159.9	12.2	2.0	6.0-28.1 (83,0)	5
15		161.7	12.6	2.0	5.2-135.8	8

At day 4: The anode clay was dry. 0.5 mL water was added to the anode clay.
**At day 2: The anode clay was dry. 1.0 mL water was added to the anode clay. At day 4: The anode clay was dry and the voltage was raised to 83.0 V. 1.5 mL water was added to anode clay, to lower voltage (result: 26.8 V).*

Table 2: Average pH, conductivity, final water content and salt concentrations in the brick samples at the end of the desalination experiments.

Experiment no.	pH	Conductivity (mS/cm)	Water content (%)	Na (mmol/kg)	Ca (mmol/kg)	Anion (mmol/kg)
1	9.6 ± 0.3	1.4 ± 0.0	11.4 ± 0.3	21.0 ± 0.3	0.1 ± 0.1	29.1 ± 1.0
2	9.5 ± 0.4	1.2 ± 0.2	11.5 ± 0.3	18.8 ± 7.0	0.3 ± 0.4	22.2 ± 7.3
3	9.8 ± 0.7	1.0 ± 0.3	11.7 ± 0.3	16.0 ± 9.1	0.5 ± 0.8	14.7 ± 10.6
4	10.5 ± 0.1	0.4 ± 0.2	9.1 ± 0.5	7.2 ± 7.0	0.1 ± 0.1	0.2 ± 0.0
5	10.2 ± 0.3	0.2 ± 0.0	6.9 ± 0.4	1.0 ± 0.5	0.3 ± 0.1	0.2 ± 0.0
6	9.4 ± 0.0	1.4 ± 0.0	12.1 ± 0.2	23.7 ± 1.4	0.1 ± 0.0	30.8 ± 0.8
7	9.5 ± 0.3	1.1 ± 0.2	11.7 ± 0.3	17.1 ± 8.3	0.4 ± 0.5	21.7 ± 7.8
8	9.8 ± 0.5	0.9 ± 0.2	10.5 ± 0.4	15.1 ± 10.1	0.7 ± 0.9	13.1 ± 10.0
9	10.2 ± 0.0	0.4 ± 0.3	7.6 ± 0.0	7.0 ± 0.0	0.1 ± 0.0	0.0 ± 0.0
10	10.0 ± 0.1	0.1 ± 0.0	6.1 ± 0.8	0.5 ± 0.0	0.2 ± 0.0	0.0 ± 0.0
11	9.4 ± 0.2	1.3 ± 0.0	11.3 ± 0.3	23.9 ± 0.4	0.1 ± 0.1	14.2 ± 1.7
12	9.5 ± 0.4	1.1 ± 0.2	11.6 ± 0.3	19.3 ± 8.8	0.5 ± 0.9	11.7 ± 3.4
13	9.8 ± 0.7	0.9 ± 0.3	11.1 ± 0.4	16.9 ± 10.0	0.5 ± 0.9	7.8 ± 5.8
14	10.1 ± 0.4	0.5 ± 0.3	9.3 ± 0.3	5.9 ± 9.8	1.0 ± 1.2	3.5 ± 4.4
15	10.4 ± 0.1	0.3 ± 0.2	6.0 ± 0.8	1.9 ± 3.0	0.6 ± 0.7	1.6 ± 3.0

Table 3: Calculated transport numbers

Experiment	Duration (Days)	Anion	Na
2	0-1	0.63	0.20
3	0-2	0.60	0.21
4	0-5	0.50	0.24
5	0-8	0.35	0.23
7	0-1	0.76	0.56
8	0-2	0.72	0.35
9	0-5	0.51	0.28
10	0-8	0.33	0.25
12	0-1	0.42	0.40
13	0-2	0.55	0.31
14	0-5	0.39	0.33
15	0-8	0.30	0.26

Table 4: Calculated concentration of Ca and SO_4^{2-} represented in the pore solution in segment 1 and 2 after ED at respectively 5 and 8 days.

	Ca (mmol/L)		SO_4^{2-} (mmol/L)	
Segments:	1	2	1	2
Experiment 14	528	341	378	453
Experiment 15	569	60	485	136
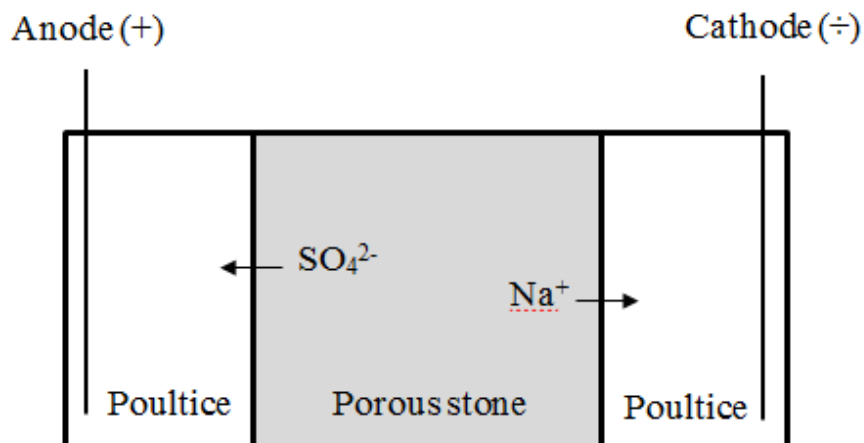
Figure 1: Principle of the electrochemical desalination method with separate compartments for electrodes.
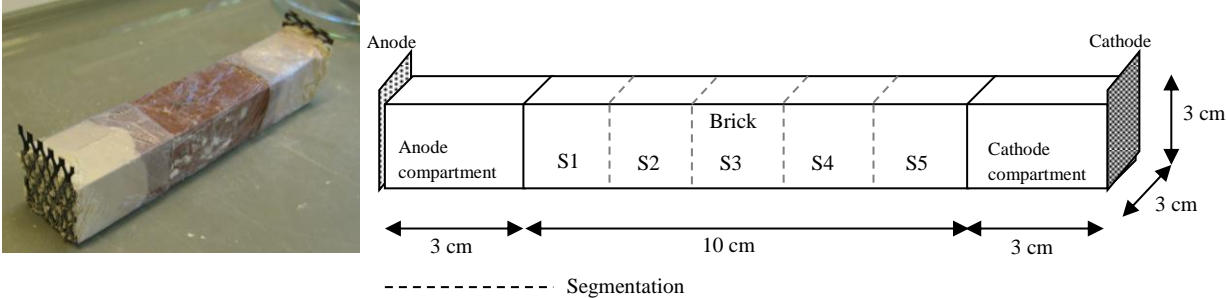
Figure 2: Picture of the experimental setup and a schematic illustration included the segmentation after the electrochemical treatment.
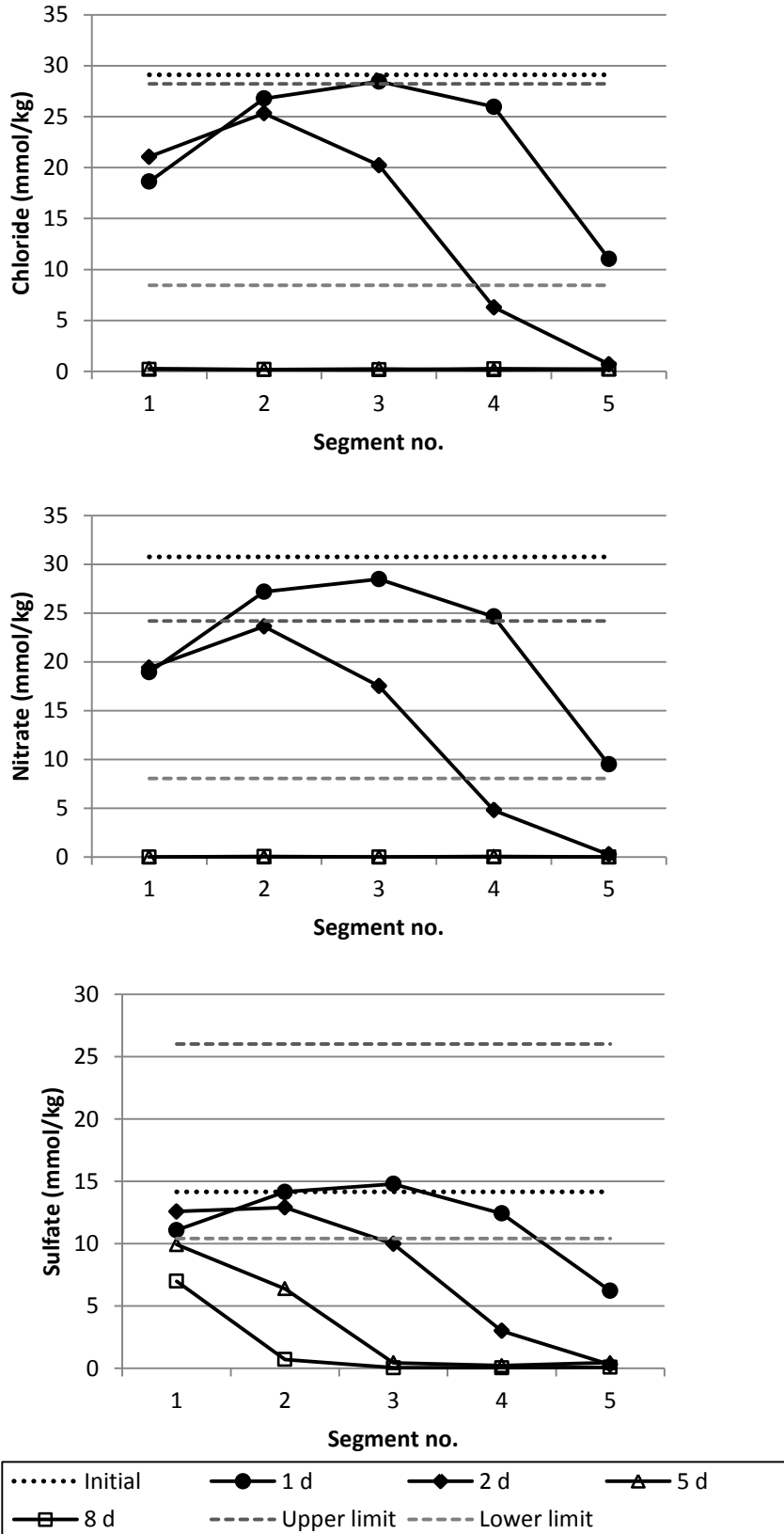
Figure 3: Profile of Cl$^-$, NO$_3^-$ and SO$_4^{2-}$ during the electrochemical desalination.
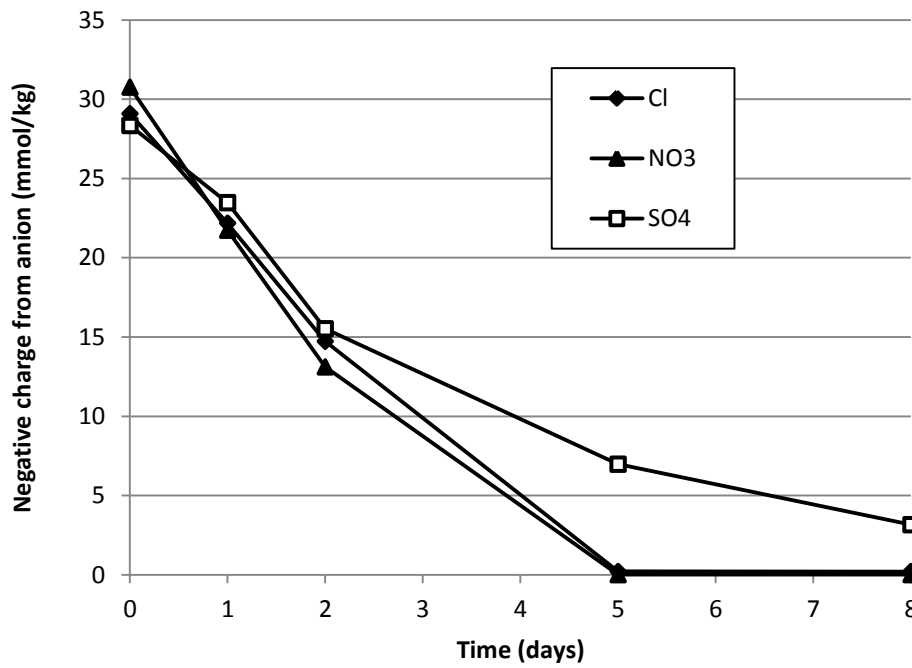
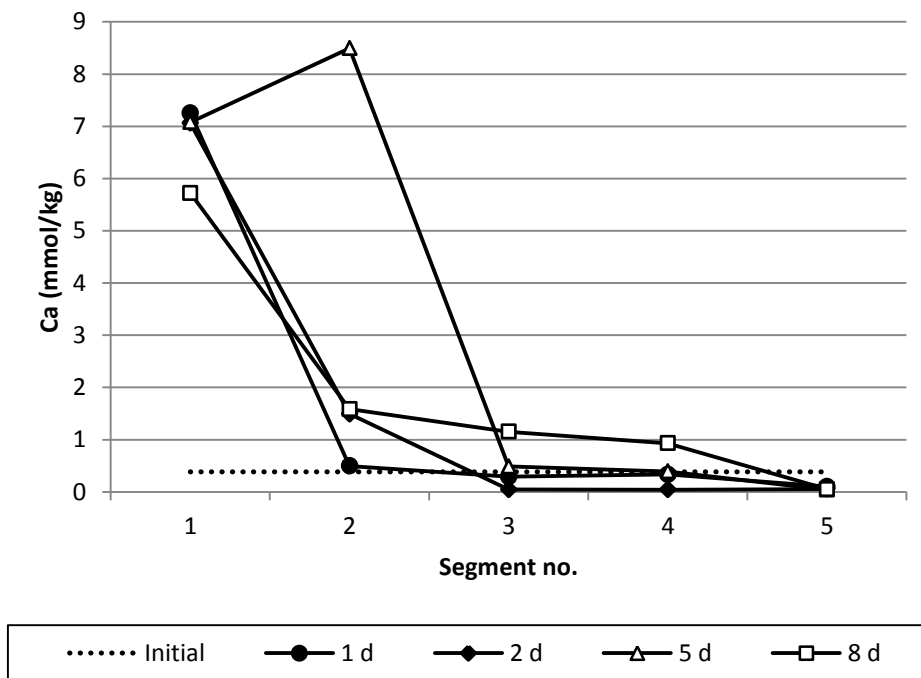Figure 4: Remaining concentration of negative charge from Cl^-, NO_3^-, and SO_4^{2-} versus experimental time.

Figure 5: Profile of Ca during electrochemical desalination in the segments for bricks contaminated with SO_4^{2-}.

Appendix E

Electrochemical desalination of limestone contaminated with Na_2SO_4 – the importance of buffering anode produced acid

Gry Skibsted, Lisbeth Ottosen and Pernille E. Jensen

Department of Civil Engieering, Technical University of Denmark, Building 118, 2800 Kgs. Lyngby, Denmark.

Electrochemical desalination of limestone spiked with Na_2SO_4 –importance of buffering anode produced acid

Gry Skibsted*, Lisbeth M. Ottosen, Pernille E. Jensen

Department of Civil engineering, Technical University of Denmark,
Building 118, 2800 Kgs. Lyngby, Denmark
*Corresponding Author: gryp@byg.dtu.dk

Key words: Electrochemical desalination, Electrokinetic, Gypsum, Porosity, Salt decay, Electrode processes, Buffering
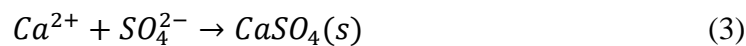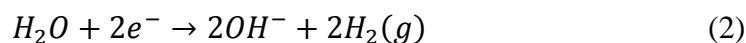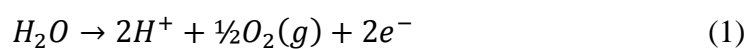
Abstract: The presence of soluble salt can cause decay of porous stone materials. Electrochemical Desalination (ED) is a technology under development to reduce the content of soluble salts to prevent deterioration. ED was carried out with samples of Gotland sandstone spiked with Na_2SO_4. Two different setups were compared: with and without carbonate containing poultice for buffering of the acid produced at the anode. The ED experiments were made in duplicates. In one of the experiments, the content of SO_4^{2-}, Ca^{2+} and Na^+ in the treated samples were analyzed chemically and changes in mineral composition were detected by XRD. In the other experiment, the porosity was evaluated in thin sections from the region closest to the anode. The reduction of SO_4^{2-} obtained by ED with poultice in the electrode compartments was 72 %, while only 62 % when no poultice was used. There were indications of gypsum formations in the region closest to the anode both with and without the use of poultice, but a higher degree of gypsum was seen in the setup without poultice. Buffering of the acid produced at the anode was shown important to avoid decomposition of the stone seen as increased porosity close to the anode due to dissolution of calcite in case no buffering system was used. No changes in the mineral composition were detected by XRD in the region closest to the anode.

1. Introduction

Salt induced decay is an important contributor in the weathering process of porous stone materials. Dissolved salts can enter the porous matrix with moisture, and due to repeated cycles of supply of salt solution and drying, the salt precipitates inside the stone; consequently spalls, flakes or blistering are generated (Lewin 1982). The impact of salt depends on the kinds of salts present, the size and shape of the capillary system, the moisture gradient, and the exposure to solar radiation (Winkler 1987). Most methods for treating salt damaged

materials aim at reducing the salt content of the affected object, and for desalination of larger objects in situ, one of the most common approaches is to use a poultice (Pel et al. 2010). During poultizing soluble salts are extracted through the application of a moistened absorbing material (poultice/plaster) on the surface of the object. Water penetrates from the poultice into the porous space of the object and dissolves the soluble salts. The concentration difference between the salt solution within the object and the water contained in the poultice generates an outward ion movement (diffusion). The evaporation of water from the poultice to the surrounding air and the capillary transport from the substrate connected with this evaporation is another factor of salt removal (Vergés-Belmin and Siedel 2005) and the transport mechanism for the dissolved salt is here advection. Salt transport and accumulation is determined by drying behavior of the plaster/substrate system and, therefore, by the pore size of both the plaster and the substrate (Petković et al. 2007).

An alternative method to poultizing is electrochemical desalination (ED): An applied electric DC field promotes the movement of salt ions in the pore solution of a porous, moist material (Ottosen and Rörig-Dalgaard 2009) by electromigration, i.e. the movement of ions in an applied DC electric field. When the electrodes are placed at the surface of the stone in poultice, as in Figure 1, the electrode compartments become storage locations for ions removed from the stone. In electrolysis the primary electrode process is oxidation of water at the anode generating acid (1) and at the cathode hydroxyl is produced (2) due to reduction of water. To avoid penetration of the acid produced at the anode into the stone, carbonate-rich poultice can be used for buffering in the electrode compartment (Ottosen and Rörig-Dalgaard 2009). The poultice furthermore maintains good contact between stone and the metallic electrode. ED is effective for reduction of Cl^-, NO_3^- and SO_4^{2-}, the last mentioned, however at a slower remediation rate, when soluble Ca-ions are available (Skibsted et al. 2013) due to precipitation of gypsum (3). When the poultice contains $CaCO_3$ the poultice acts as source for Ca^{2+}.

$$H_2O \rightarrow 2H^+ + \tfrac{1}{2}O_2(g) + 2e^- \qquad\qquad (1)$$

$$H_2O + 2e^- \rightarrow 2OH^- + 2H_2(g) \qquad\qquad (2)$$

$$Ca^{2+} + SO_4^{2-} \rightarrow CaSO_4(s) \qquad\qquad (3)$$

The limestone; Gotland sandstone, is a soft, gray stone with approximately 20 % porosity and a fairly high degree of homogeneity, which makes it suitable for sculptures. The relatively high porosity and the $CaCO_3$ bonding cause Gotland Sandstone to be sensitive to outdoor conditions. Calcite can chemically be transformed to gypsum when exposed to acid-rain (Suneson 1942). Nord and Tronner (1995) observed based on samplings from two monuments built of Gotland sandstone, that rain dissolve calcite and decrease the Ca concentration; but a hard, thin gypsum crust can be formed at the surface, resulting in increased Ca surface concentrations compared to fresh stone samples.

In ED treatments with calcite-based materials where the electrodes are placed directly at the stone surface, the acidic environment around the anode can cause damage to the solid matrix, as observed by Herinckx et al. (2011). From a combination of numerical and chemical modeling it was shown that the calcite dissolves due to the progress of the electrochemical reaction leading to porosity changes in that region (Paz-García el al. 2012). This paper aims at investigating this effect experimentally and evaluate whether the poultice used for buffering the acidic environment around the anode is sufficient to avoid porosity changes of the matrix during ED. Thin sections from stone samples before and after the treatment, impregnated with (yellow) fluorescent epoxy, can have their macro- and microporosity clearly delineated under a fluorescent microscope and subsequently quantified by image analysis or easily photographed (Yanguas and Dravis, 1985). The fluorescence method illuminates the porosity against an almost totally black background and helps to focus attention on the porous network (Gies 1987). The hypothesis is that if the acid produced at the anode during ED is not buffered, the calcite in the matrix of the stone will dissolve and a higher porosity arises. In addition to the investigation of porosity changes, we evaluate whether the location of the source of Ca^{2+} (from the poultice or from the stone itself) influences the reduction in SO_4^{2-} content during ED.

2. Materials and methods

Three pieces of the limestone; Gotland sandstone supplied from Kronborg Castle in Elsinore were used. The stones had not been used as building stones. The first was used to evaluate the homogeneity of Gotland sandstone, the second was used to test its buffering capacity against acid, and the third was used for electrochemical desalination experiments, see Table 1. The buffering capacity against acid was also found for the poultice used in the electrode compartments during ED.

2.1 Analytical methods

The water content was calculated as weight loss after drying at 105 °C. The pH and conductivity were measured by suspending 10 g of powdered sample in 25 mL distilled water, agitated for 24 h and after settling for 10 min, pH and conductivity were measured by electrodes. The suspension was then filtrated through 0.45 μm filter and Na and Ca concentrations were analyzed by atomic adsorption spectrometry (AAS, GBC 932AA) and SO_4^{2-} was analyzed by ion chromatography (IC, Dionex DX-120). The carbonate content was measured volumetric after reaction with 10 % HCl, by use of a Scheibler instrument. The amount of carbonate was calculated assumed that all carbonates were present as $CaCO_3$.

2.2 Homogeneity test

The homogeneity of a piece of Gotland sandstone was investigated through the parameters capillary suction in two directions and measurements of pH, conductivity and carbonate content. One sandstone piece was cut into 5 samples (5 x 5 x 10 cm^3). The samples were dried at 105 °C for 24 h. The dry samples were weighed and placed in a plastic tray on a pair of metal spikes, with the height 5 mm. Placement of samples on the spikes allowed water to be sucked into the stone by capillary forces. The tray contained distilled water with the height 5 mm above the spikes. The water level was kept constant manually. The sandstones were weighed after 1, 2, 4, 6, 8, 16, 30, 60, 120, 180, 240 and 360 min. Capillary suction was conducted with the same samples in two directions, with suction areas of respectively 5 x 5 cm^2 (Direction 1) and 5 x 10 cm^2 (Direction 2). After the capillary suction tests, the samples were dried at 105 °C before drilling samples were made, by use of a 10 mm bit and for the powder pH, conductivity and carbonate content were analyzed in duplicate.

2.3 Buffer capacity against acid

The poultice and stone samples were dried at 105 °C for 24 h and crushed in a mechanical mortar (Vibrating Cup Mill PULVERISETTE 9) for 30 seconds. Powder samples (5.0 g) were suspended in 25 mL distilled water or HNO_3 (0.01 M, 0.02 M, 0.05 M, 0.10 M, 0.20 M, 0.40 M, 0.60 M, 0.80 M and 1.00 M) for 24 h before measuring pH. Each extraction was made in duplicate.

2.4 Electrochemical desalination

The third Gotland sandstone was cut into 6 samples (3 x 3 x 10 cm^3). As the analytical methods were destructive, the ED experiments were made in duplicates: One for chemical analysis and the other for determination of porosity changes through thin sections by light microscopy. The samples were first dried at 105 °C for 24 h, before sample A1, B1, B2, C1 and C2 were submerged in a solution of 32.00 g/L Na_2SO_4 for 24 days. Sample A2 was used for a fluorescent epoxy saturated thin section of the original stone (described later).
The ED experimental setup used in experiments B1 and B2 (Figure 2) was identical to the setup used in Skibsted et al. (2013). Towards the metallic electrode mesh an electrode compartment with the size 3 x 3 x 3 cm^3 was placed. The frame of the electrode compartments were folded in thin plastic and jointed with tape to fit the ends of the stones. The frames were filled with poultice; a mixture of kaolinite and $CaCO_3$ (Rörig-Dalgaard and Ottosen 2011) with an initial water content of 30 %. The stone sample and electrode compartments were wrapped in plastic film to hinder evaporation of moisture during ED. In ED experiments C1 and C2 the inert electrode mesh was placed directly at each end of the stone, only fixed with a thin layer of pure kaolinite, to maintain electrical contact between electrode and sandstone. In all four experiments a constant current of 2 mA was applied for 8 days. See Table 2 for experimental conditions.

After ED the stone samples from experiments B1 and C1 were segmented with hammer and chisel into five segments; numbered from the anode end. Sample A1 was segmented after submersion in the Na_2SO_4 solution for 24 days. The water content was analyzed before the dried segments were crushed in a mechanical mortar and the powder analyzed for pH, Na, Ca and SO_4^{2-}.

2.5 XRD

The quality of the mineral composition and identification of $CaSO_4$ was determined by X-ray diffraction analysis (PANalytical X'Pert PRO diffractometer) using Cu K_α radiation and operating at 40 mA and 45 kV, and the program X'Pert High Score Plus for identification of gypsum and anhydrite. Mineral changes in the matrix were analyzed by comparing XRD-graphs for A1, B1 and C1 (only segment no. 1).

2.6 Thin sections and evaluation of porosity

Samples A2, B2 and C2 were vacuum saturated with (yellow) fluorescent epoxy resin and thin sections (thickness of 0.03 mm) over the cross-section were made on an automatic thin section machine by 'Pelcon Materials and Testing ApS'. One thin section from A2 and two thin sections from both B2 and C2 were made with the distance 0.5 mm and 3 mm from the anode compartment (See Figure 2 for location of the thin sections in sample B2 and C2). The area of each thin section was 3 x 3 cm^2. The thin sections were examined by light microscopy using a blue excitation filter and a yellow emission filter (Leitz Wetzlar Germany K510). The images were converted into quantifiable data by the Imaging software NIS-elements, version 4.10 where a histogram were obtained for each thin section based on pixel intensity of the RGB-image (Red/Green/Blue image). The light intensities were quantized to integers between 0 and 255 (x-axis) and the y-axis was the frequency as pixels with a specific intensity were represented in the image. Microscope settings were kept constant and were identical for all five thin sections examined.

3. Results and discussions

3.1 Homogeneity and sensitivity

Even though the Gotland sandstone has a fairly high degree of homogeneity (Suneson 1942) it is important to assess the variances in the matrix before evaluating changes caused by ED. Uniform capillary suction may be regarded as a good evidence of homogeneity in the direction of penetration (Gummerson et al. 1980). In this case sorptivity (the capacity to absorb liquid by capillarity) was used to evaluate if the Gotland sandstone matrix was appropriate for evaluation of changes in pore volume due to ED. The sorptivity in the two

directions were 0.235 kg/m^2/s$^{1/2}$ and 0.306 kg/m^2/s$^{1/2}$, respectively (Table 3). Sorptivity should be independent of the direction, and the two different values for sorptivity indicated that it was a layered matrix. In Table 4 the pH, conductivity and CaCO$_3$ content are listed and the relative low standard deviations showed that the matrix was homogeneous in relation to those parameters even though it was anisotropy in relation to the sorptivity. To avoid the influence of the anisotropy parameter it was necessary to apply the electric field in the same directions for all samples in the ED experiment.

The Gotland sandstone (Stone 2) was sensitive to acid and had an excellent buffer capacity against acid at concentrations below 0.2 M, see Figure 3. Actually the buffer capacity of the Gotland sandstone at acid concentrations < 0.2 M was as good as the one for the used poultice. The carbonate content for the Gotland sandstone and poultice were 6.0 % and 69.2 %, respectively and was the reason for the higher buffer capacity of the poultice compared to the Gotland sandstone at suspension in acid concentrations at 0.4-1.0 M. The buffer capacity of the Gotland sandstone against acid is related to the composition of the stone; as it compensates the attack of acid by dissolution of the bonding material calcite. Calculation of the buffer capacity against acid for the matrix shows that a carbonate content of 6 % is sufficient to buffer the acid in concentrations up to 0.1 M and in suspension with 0.2 M the pH should be 1. This indicates a secondary buffer system in the matrix beyond calcite.

3.2 Electrochemical desalination

3.2.1 Changes in pH

The pH of the Gotland Sandstone (Stone 3) after submersion in Na$_2$SO$_4$ was 10.9 as average of the 5 segments (Table 5). At the end of ED experiment C1 without buffering poultice, the pH was decreased to an average of 9.7. The buffering poultice in ED experiment B1 resulted in a smaller pH reduction and pH was 10.5 as average at the end of this experiment (Table 5). The pH profile in the sandstone from anode to cathode (Figure 4) underlines the importance of preventing acid in penetration into the stone. In the experiment without buffering poultice (C1) pH was reduced from 10.9 to 7.3 in the segment closest to the anode whereas with buffering poultice (B1) pH was only reduced to 10.3 in the same segment. In neither of the two experiments pH was changed in the segment closest to the cathode during ED. The initial pH of the poultice used in B1 was 8.7 and after the ED experiment pH was reduced to 7.7 in the anode compartment and increased to 11.1 in the cathode compartment. From pH in the poultice and in segment no. 1 after ED experiment B1, it can be seen that the poultice fulfill its purpose as buffer material.

3.2.2 Water content

The water content was reduced during ED from 8.7 % to 3.7 % (B1) and 4.5 % (C1), respectively. There was no evident indication of electroosmotic flow in the stone matrix, which commonly implies a profile with lower water content in the vicinity of the anode than in the cathode end of the sample, and the water reduction was rather a result of evaporation.

For B1 the water content in the poultice was reduced too, during ED (C1 was without poultice). The initial value was 30 % and at the end the water content in the cathode end (27 %) was higher than in the anode end (25 %), revealing electroosmotic water transport and in accordance with observations by Ottosen and Christensen (2012).

3.2.3 Desalination and gypsum formation

The SO_4^{2-} reduction during ED was 72 % when the buffering poultice was used in the setup (B1) and only 62 % without poultice (C1). For Ca and Na the same tendency of higher reduction in experiment B1 than C1 was seen (Table 5).

Calcite is soluble in diluted acid, where carbonate act as buffer for the acid and thus the concentration of Ca increases. The profiles of water soluble Ca and SO_4^{2-} after ED are presented in Figure 5. In both experiments the content of soluble Ca and SO_4^{2-} were reduced in segments 2-5, but increased in segment 1. The same pattern was observed for ED with buffering poultice for sulfate removal from Red Bricks in Skibsted et al. (2013). In the applied electric field SO_4^{2-} is transported towards the anode, but accumulates to some extent in the stone segment closest to the anode. Free Ca-ions from the anode end (originating either from the poultice or the Gotland Sandstone buffering the acid at the anode) are transported towards the sandstone to the cathode, but the concentration of Ca is not lowered in segment 1 as in the other segments. The reason why the Ca and SO_4^{2-} concentrations are not decreased in segment 1 is probably precipitation of gypsum (Skibsted et al. 2013). When gypsum is formed, the ions are no longer mobile in the applied electric field. Gypsum formation is in accordance to (Nord and Tronner 1995) who found an increase in the Ca surface concentration when gypsum was formed at the surface of at Gotland sandstone matrix from calcite dissolved by acid-rain and re-precipitated by the SO_4^{2-} from the rainwater. The Ca concentration in segment 1 increased 51 % without poultice (C1), but only 3 % with poultice (B1). In the same segment SO_4 increased with 66 % (C1) and 28 % (B1). The gypsum formation is thus larger in experiment C1 compared to B1, and the poorer overall SO_4^{2-} reduction for C1 is related to this formation of gypsum as the sulfate content is almost equally low in the rest of the segments for the two experiments (Figure 5). In B1, calcite was dissolved from the poultice in the anode compartment, and Ca-ions migrate towards the cathode, but the first distance was in the poultice between the anode and the sandstone before entering in the sandstone. At the same time SO_4^{2-} migrated towards the anode and a part of the calcium ions was probably hindered in entering the sandstone due to gypsum formation in the poultice. This is on the contrary to experiment C1 where the calcite dissolution occurred from the surface of the sandstone where SO_4^{2-} already were presented from the beginning of the ED. The theory about gypsum formation in the region where the Ca^+ front and the SO_4^{2-} front collide is in accordance with modelling by Paz-Garcia et al. (2011) of SO_4^{2-} desalination from bricks with $CaCO_3$-rich poultice.

3.2.4 Risk for inhibition of desalination

Earlier Kamran et al. (2012) showed that electromigration of target ions was inhibited due to an extremely high potential drop created by collision of the alkaline and acidic fronts in the

stone in an inert fired-clay brick, as this zone was depleted for ions (Kamran et al. 2012). This phenomenon will not occur during the ED from a matrix where a sacrificing matrix for neutralizing the acid produced at the anode is used or alternatively if the sacrificing matrix is the porous material itself as the Gotland Sandstone used in this work. Several reactions are involved and the electromigration of protons and hydroxyl-ions are not equal and the collision of the alkaline and acidic front will thus not result in a full depletion of ions in a narrow zone.

3.3 Mineralogy

The XRD-analysis of segment no. 1 for A1, B1 and C1 are presented in Figure 6. By comparing the three XRD-patterns for the samples of Gotland sandstone before and after ED there is no qualitative difference in the mineralogy, as the peaks in the three cases are located at the exact same positions. This shows that the ED treatment does not result in loss of major mineral phases or formation of major new phases in the sandstone. In Figure 7 segment no. 1 from C1 (the sample where the $CaSO_4$-formation is expected most pronounced) is compared with the simulated pattern from the scan of pure gypsum (reference code in X'Pert High Score Plus are 01-071-2701, Boeyens and Ichharam 2002) and anhydrite (Reference code in X'Pert High Score Plus are 01-072-0916, Kirfel and Will 1980) to identify $CaSO_4$-formation. There are no correlations between the peak locations for C1 and gypsum or the anhydrite, thus $CaSO_4$-formation cannot be verified by the XRD analysis. This however does not mean that there is no gypsum formation. A specific mineral crystal with a content < 1 % is difficult to identify by XRD (the peaks will eclipse by the background scatter) and the content of calcium and sulfate in segment no. 1 for C1 was far below 1 %. In segment no. 1 for C1 it was 0.2 % (Ca) and 0.4 % (SO_4).

3.4 Porosity changes

Possible changes in the sandstone porosity due to ED with and without poultice were evaluated indirectly by comparing thin sections analyzed in a light microscope. The histogram for the reference (thin section from sample A2) is presented in Figure 8 and is the average of five images of same thin section. In practice the thin section was moved between each of the 5 images without changing microscope settings. The frequency of the "peak" was most dominating at color intensity 80-95 with an average for the five images of 13.2 % of total pixels in the image. In this interval the deviation in the intensity was 9.9 %. The initial porosity was not completely homogeneous and changes can only be evaluated if the change deviate more than 9.9 % compared to the reference image.

In Figure 9 is the histograms for the thin sections from (B2) and (C2) including the average of the reference with standard deviation for the color intensity 80-95 presented. The variation in the frequency for I, II and IV compared to the reference is within the calculated deviation of the reference, thus there are no observable changes in the porosity for those thin sections by this method. This is in consistency with the expected for thin section I and II (B2), as the acid produced at the anode was buffered by the poultice. In the distance 0.5 mm from the anode

end in (C2) (thin section III) the frequency for the color intensity 80-95 was increased with 12 % from the reference meaning a higher porosity as the value is above the calculated standard deviation. This increase in porosity was expected as no buffering poultice was used, so dissolution of calcite from the stone matrix was a consequence of the acid attack. Thin section (IV) showed no significant porosity change compared to the reference even though this section was closer to the anode than thin section (III). As mentioned in previous chapter, pH decreased from 10.5 to 7.3 in the segment closest to the anode and the water soluble Ca content increased with 51 %. As the calcite in the stone matrix was the only source of Ca-ions, an increase in pore volume should be expected. However, in the same region of the sample precipitation of gypsum occurred, which causes a decrease in porosity. The molar volume will increase with a factor of 2, when calcite is chemically transformed to gypsum (Nord and Tronner 1995). The decrease in porosity closest to the surface is thus expected to be an indication of a larger volume of gypsum formed than calcite dissolved.

The gypsum formation is expected to be very surface near, as it is from here the calcite dissolution occurs and during the ED (before the desalination is finished) the SO_4^{2-} continuously pass here, available for precipitation with the newly formed Ca^{2+}. The increase in porosity in thin slice (III) may have developed after the SO_4^{2-} was removed. Increased porosity of the sandstone was thus seen in a thin section from an ED experiment without use of buffering poultice. This indicates dissolution of a solid phase from the sandstone. It was however also shown, that a finding of no change in porosity cannot lead to the conclusion that no dissolution has happened as the porosity is a balance between dissolved volume and volume of new solid phases developed by precipitation. The reduction in pH is a condition for the dissolution of calcite, thus the buffering of the acid generated at the anode is a precaution for eliminating the risk of porosity changes.

4. Conclusion

Buffering the acid generated at the anode is important, otherwise pH will decrease in the stone from the anode and in calcite bound sandstones the consequence is increased porosity due to dissolution of calcite.

Increased porosity of the sandstone was seen in a thin section from an ED experiment without use of buffering poultice indicating dissolution of a solid phase from the sandstone. It was however also shown, that a finding of no change in porosity cannot lead to the conclusion that no dissolution has happened if pH is reduced, as the porosity is a balance between dissolved volume and volume of new solid phase by precipitation (e.g. gypsum).

Gypsum formation cannot be avoided in the region closest to the anode during electrochemical desalination of sulfate contaminated stone samples, when calcium is dissolved due to acidification either from the stone matrix or in the poultice used for buffering

the acid at the anode. The calcium source affects the degree of gypsum formation within the stone; without poultice more gypsum was formed in the stone matrix than with poultice.

Changes in the qualitative composition of the major minerals (presence > 1 %) of the sandstone during ED were not detected by XRD.

The reduction of SO_4^{2-} obtained was 72 % for electrochemical desalination with poultice in the electrode compartments against 62 % if no poultice was used. The major difference was caused by the formation of gypsum in the sandstone closest to the anode.

References

Boeyens, J.C.A., Ichharam, V.V.H., Z. Kristallogr.-New Cryst. Struct., 217, 9, (2002)

Castellote M, Andrade C, Alonso MC (1999). Changes in concrete pore size distribution due to electrochemical chloride migration trials. ACI Materials Journal (96), 314-319.

Gies RM (1987) An improved method for viewing micropore systems in rocks with the polarizing microscope. SPE Formation Evaluation 2:209-214.

Gummerson RJ, Hall C, Hoff WD (1980) Water Movement in Porous Building Materials – II. Hydraulic Suction and Sorptivity of Brick and Other Masonry Materials. Building and Environment, 15:101-108.

Herinckx S, Vanhellemont Y, Hendrickx R, Roels S, De Clercq H (2011) Salt removal from stone building materials using an electric field. In: Proceedings from the international conference on salt weathering on building and stone sculptures, Limassol, Cyprus 19-22 October 2011, pp 357-364

Kamran K, Van Soestbergen M, Huinink HP, Pel L (2012) Inhibition of electrokinetic ion transport in porous materials due to potential drops induced by electrolysis. Electrochem Acta 78:229-235

Kirfel, A., Will, G., Acta Crystallogr., Sec. B: Struct. Crystallogr. Cryst. Chem., 36, 2881, (1980)

Lewin SZ (1982) The mechanism of masonry decay through crystallization. Conservation of Historic Stone Buildings and Monuments, Washington, D.c.: National Academy of Sciences, pp. 120-144, 1982

Nord AG, Tronner K (1995) Effect of acid rain on sandstone: The Royal palace and the Riddarholm church, Stockholm. Water, Air and Soil Pollution 85:2719-2724.

Ottosen LM, Rörig-Dalgaard I (2009) Desalination of a brick by application of an electric DC field. Materials and structures 42:961-971

Ottosen LM, Christensen IV (2012) Electrokinetic desalination of sandstones for NaCl removal – Test of different clay poultices at the electrodes. Electrochimica Acta (86), 192-202.

Paz-García JM, Johanesson B, Ottosen LM, Alshawabkeh AN, Ribeiro AB, Rodríguez-Maroto JM (2012) Modeling of electrokinetic desalination of bricks. Electrochemical Acta 86:213-222.

Paz-García JM, Johanesson B, Ottosen LM, Ribeiro AB, Rodríguez-Maroto JM (2011) Influence of the Chemical Interactions on the removal rate of Different Salts in Electrokinetic Desalination Processes. In: Proceedings from the international conference on salt weathering on building and stone sculptures, Limassol, Cyprus 19-22 October 2011.

Pel L, Sawsy A, Voronina V (2010) Physical principles and efficiency of salt extraction by poulticing. Cultural Heritage 11:59-67.

Petković J, Huinink HP, Pel L, Kopinga K, van Hees RPJ (2007) Salt transport in plaster/substrate layers. Materials and structures 40:475-490.

Radeka M, Kiurski J, Markov S, Marinković-Nedučin R (2007). Microbial deterioration of clay roofing tiles. In: Structural Studies, Repairs and Maintenance of Heritage Archicture X, Edited by Brebbia CA. WIT press, Southampton, Boston.

Skibsted G, Ottosen LM, Jensen PE. Electrochemical desalination of bricks – removal of Cl^-, NO_3^- and SO_2^{2-}. (Submitted – Appendix D in the PhD-Thesis).

Suenson E (1942) Bygningsmaterialer, 3. Bind: Natursten. Jul. Gjellerups Forlag, pp. 117-139, 1942

Vergés-Belmin V, Siedel H (2005) Desalination of Masonries and Monumental Sculptures by Poulticing: A Review. Restoration of buildings and monuments 11: 391-408.

Winkler EM (1987) Weathering and weathering rates of natural stone. Environ Geol Water Sci 9:85-92

Yanguas JE, Dravis JJ (1985) Blue fluorescent dye technique for recognition of microporosity in sedimentary rocks. Journal of Sedimentary Petrology 55:600-602.

Tables and Figures

Table 1: The experimental purpose for the three Gotland sandstones

Stone	Number samples	Sample size (cm^3)	Purpose	
1	5		Test of homogeneity:	
		5 x 5 x 10	Capillary adsorption, pH, conductivity and $CaCO_3$	
2	Powdered sample		Test of buffer capacity against acid	
3	6	3 x 3 x 10	A1:	Reference sample for ED experiments
			A2:	Thin section of original material matrix
			B1:	With buffering poultice at electrodes: Chemical analysis
			B2:	With buffering poultice at electrodes: Thin section
			C1:	Without buffering poultice at electrodes: Chemical analysis
			C2:	Without buffering poultice at electrodes: Thin section

Table 2: Experimental conditions

	Submerged	Electrode clay	Current mA	Voltage V	Duration Days
A1	Yes		0.0	0.0	0
A2	No		0.0	0.0	0
B1	Yes	Poultice	2.0	4.9-35.6	8
B2	Yes	Poultice	2.0	5.4-86.2	8
C1	Yes	Kaolin	2.0	2.6-91.3	8
C2	Yes	Kaolin	2.0	2.9-119.9	8

Table 3: Determined sorptivity S ($kg/m^2/s^{1/2}$) in two directions with the suction area A (m^2).

Direction	Suction area (m^2)	Sorptivity ($kg/m^2/s^{1/2}$)
1	0.0026	0.235 ± 0.043
2	0.0052	0.306 ± 0.004

Table 4: $CaCO_3$, pH and conductivity: average value and deviations for the 5 samples from stone no. 1 (homogeneity test).

Analysis	Average value
pH	8.66 ± 0.04
Conductivity (mS/cm)	0.41 ± 0.02
$CaCO_3$ (%)	5.0 ± 0.2

Table 5: Experimental results (A1, B1 and C1)

Sample	pH	Water content %	Ca mg/kg	Na mg/kg	SO_4^{2-} mg/kg	Reduction Ca (%)	Na (%)	SO_4^{2-} (%)
A	10.9 ± 0.6	8.7 ± 0.1	1225 ± 138	1057 ± 164	2499 ± 221			
B	10.5 ± 0.2	3.7 ± 0.6	318 ± 534	213 ± 262	700 ± 1397	74,0	79,8	72,0
C	9.7 ± 1.4	4.5 ± 0.6	400 ± 809	396 ± 551	959 ± 1788	67,4	62,5	61,6
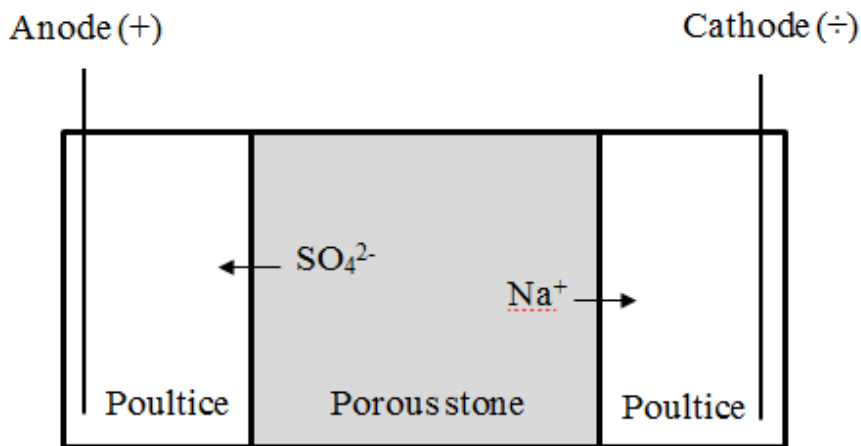
Figure 1: Principle of the electrochemical desalination method with separate compartments for electrodes
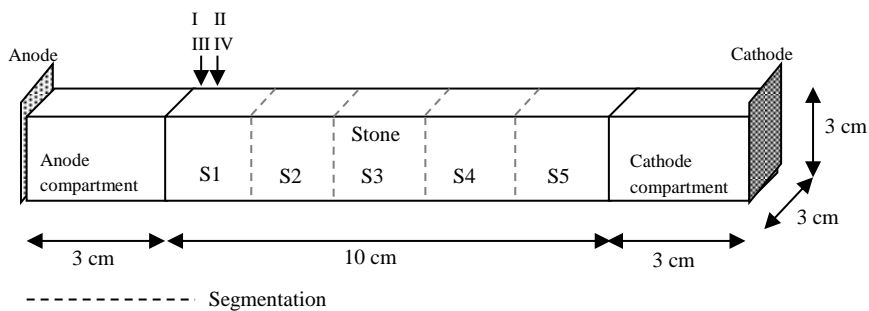
Figure 2: Illustration of the electrochemical desalination setup with poultice in the electrode compartments. The arrows indicate the locations for the thin sections; I and II from sample B2 (ED with poultice) and III and IV from sample C2 (ED without poultice).
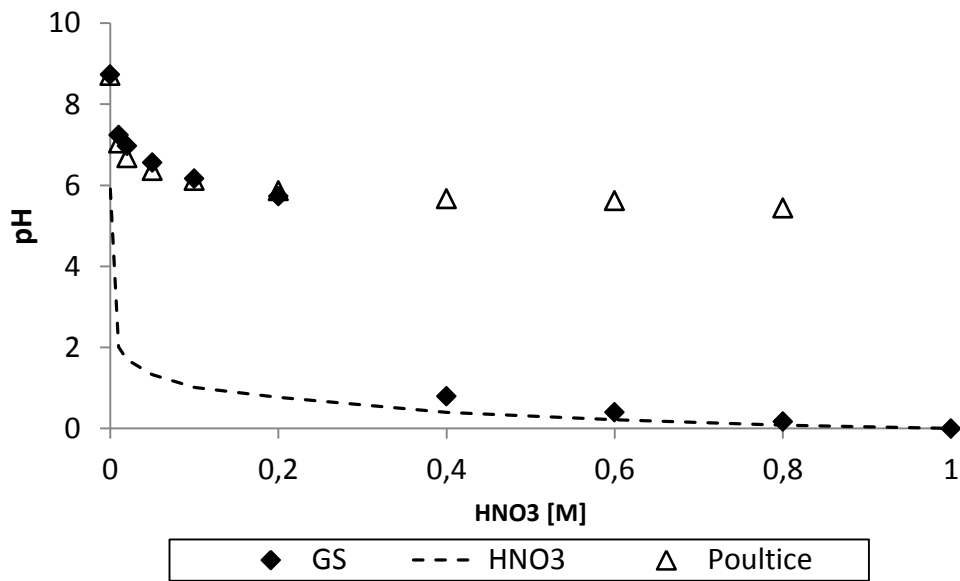
Figure 3: Buffer capacity against acid at 24 h for the Gotland sandstone (GS) and the used poultice, incl. pH for the pure HNO_3 solution at the same concentrations.
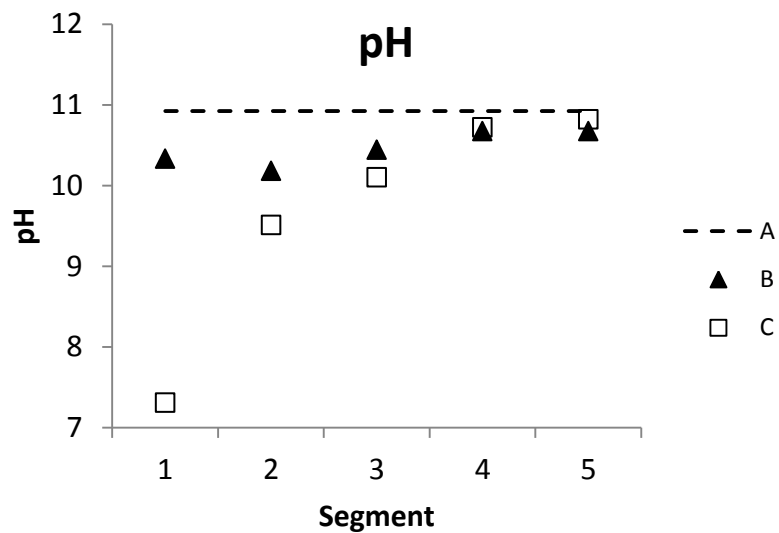
Figure 4: Profile of pH before (A1) and after ED; with poultice (B1) and without poultice (C1).
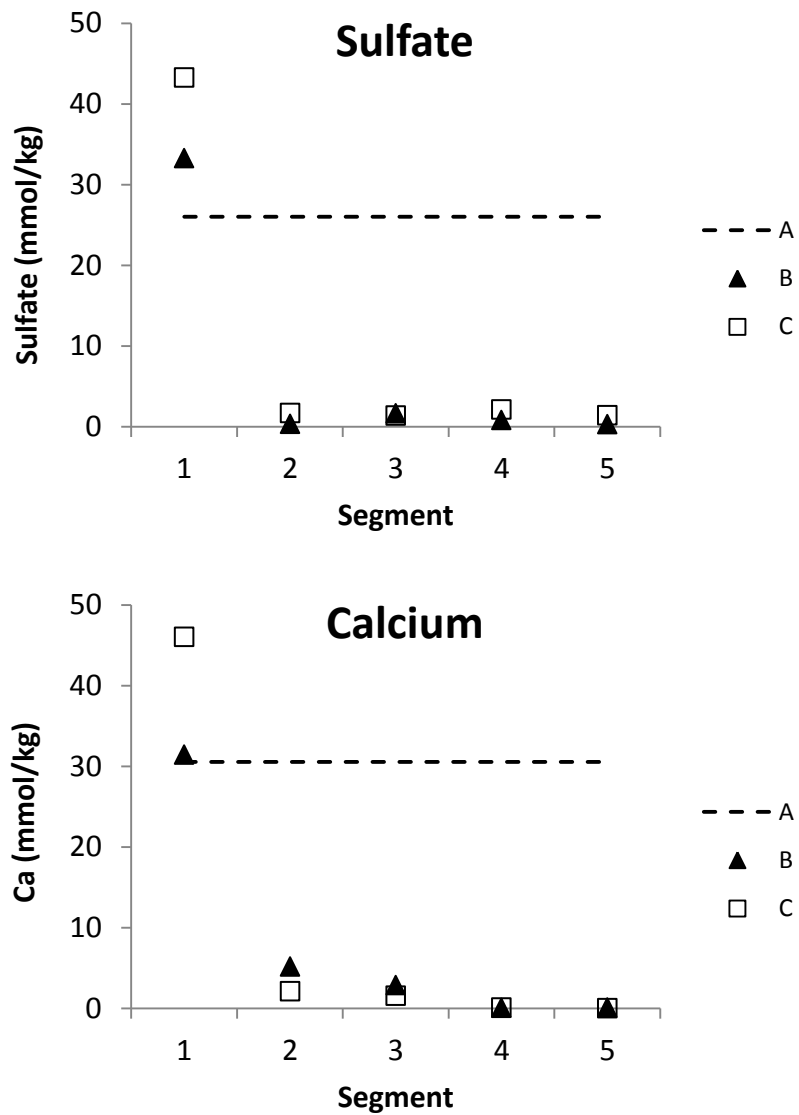
Figure 5: Profile of sulfate and calcium before (A1) and after ED; with poultice (B1) and without poultice (C1).
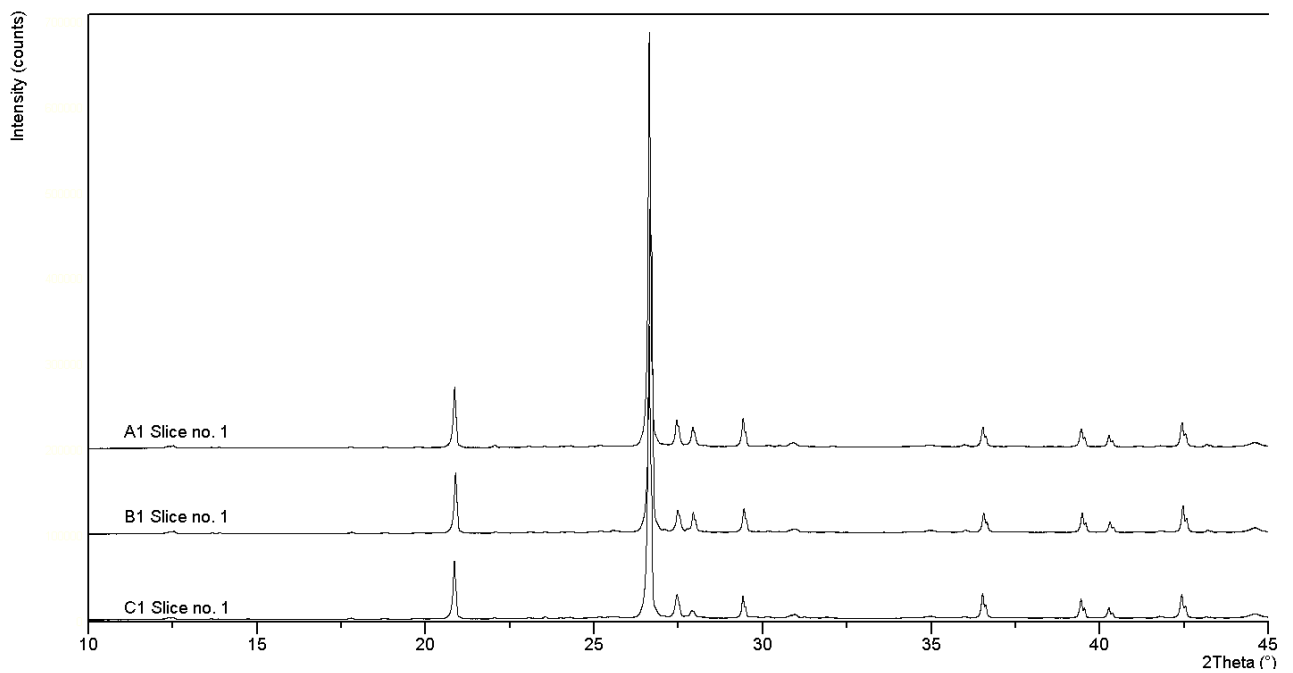
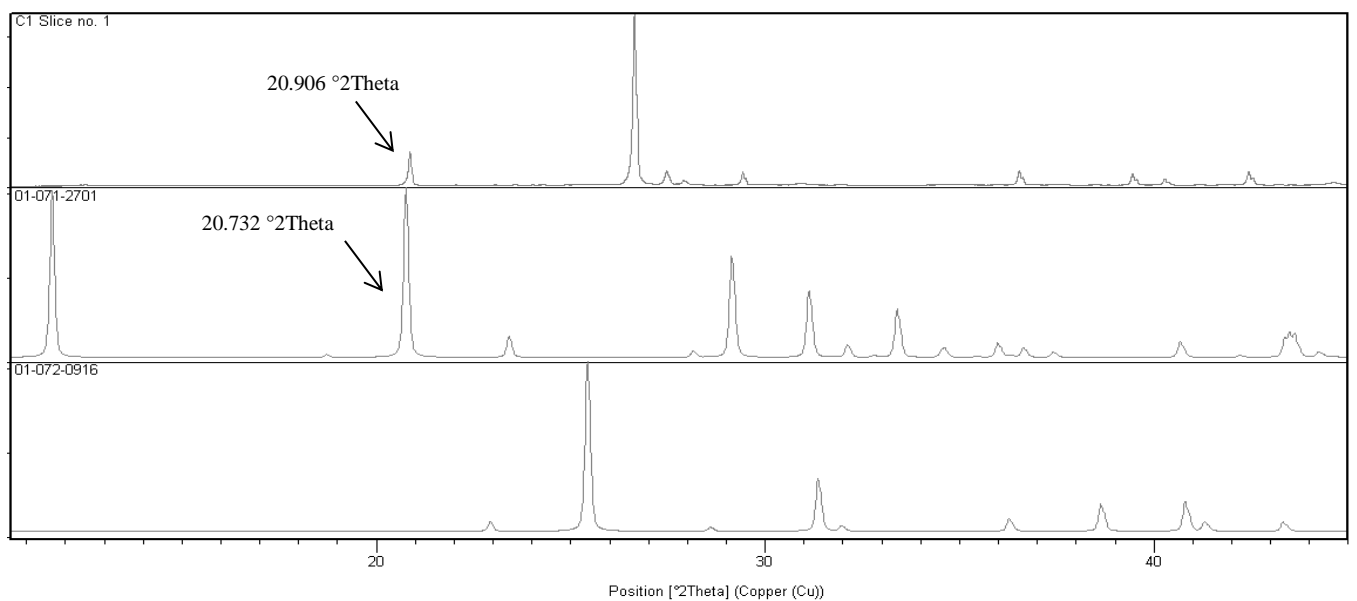Figure 6: XRD graphs for segment no.1 from A1 (Reference), B1 (with poultice) and C1 (without poultice).

Figure 7: XRD graphs for segment no. 1 from C1 and the simulated pattern from scan of gypsum (reference code in X'Pert High Score Plus are 01-071-2701, Boeyens and Ichharam 2002) and anhydrite (Reference code in X'Pert High Score Plus are 01-072-0916, Kirfel and Will 1980), respectively.
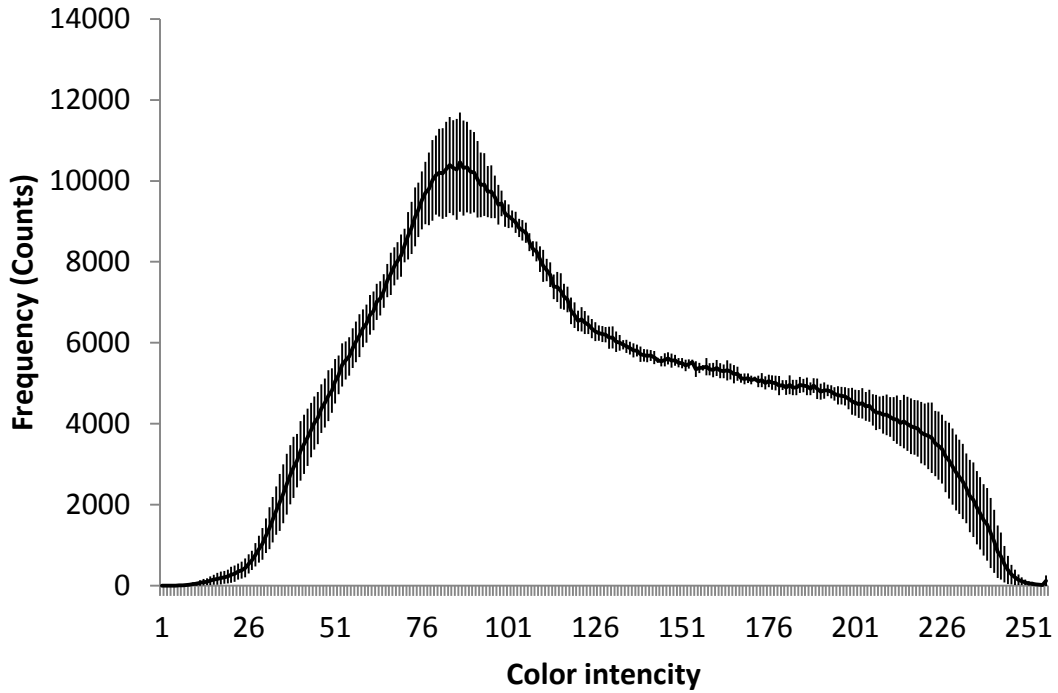
Figure 8: Histogram for the average of five images from the thin section for the reference (Sample A2) with standard deviation.
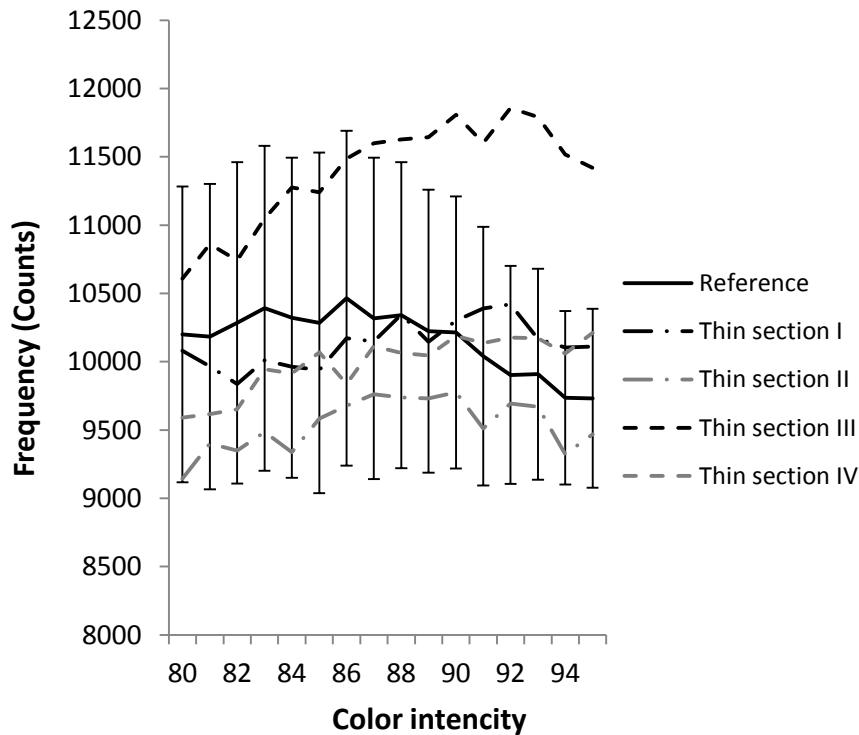

Figure 9: Part of histogram (from intensity 80-95) for thin sections I and II (ED with poultice, B2) and thin sections III and IV (ED without poultice, C2) including the reference with deviations.

Appendix F

Electrodialytic decomposition of the clay mineral illite

Gry Skibsted

Additional experiments

Electrodialytic decomposition of the clay mineral illite

(Additional experiments)

Purpose

Evaluate the impact of EDR on the matrix of the clay mineral illite.

Materials and methods

Clay shale of the mineral illite from Ward's Natural Science was used as matrix. Before use the dry shales were crushed in a mechanical mortar (Vibrating Cup Mill PULVERISETTE 9) for 30 seconds into a fine powder.

Analytical methods

The water content was measured and calculated as weight loss after drying at 105 °C for 24 h. Analysis of cations were made on dried powder samples (105 °C, 24 h). The Danish Standard (DS 259) was used to extract acid soluble cations from the samples: 1 g of powdered clay mineral was added 20 mL 7 M HNO_3 and autoclaved (120 °C, 200 kPa) for 30 min. After cooling, the samples were filtered through a 0.45 μm filter and cations in the extract were analyzed by ion coupled plasma – optical emission spectroscopy (ICP-OES, Varian 720-ES). The target elements were Al, Fe and Si. The total content of the elements in the matrix was determined by X-ray fluorescence (XRF).

Electrodialytic treatment

Two EDR experiments were made, EDR-I and EDR-II (Table 1). The EDR experiments were made in cylindrical Plexiglas cells with three compartments and an internal diameter at 8 cm (Figure 1). Illite with a moisture content of 22 % (adjusted with distilled water) was placed in the center compartment and separated from the two electrode compartments by Ionics(R) ion exchange membranes (AR204SZRA and CR67 HVY HMR427); an anion-exchange membrane separated the anolyte and the clay, and a cation-exchange membrane separated the catolyte from the clay. Platinum coated rod electrodes were used (0.3 cm in diameter, 7 cm long). The center compartment with soil was 3 cm long and the two electrode compartments were 5 cm. Anolytes and catolytes were distilled water adjusted to pH 2 with HNO_3, continuously circulated between the electrode compartment and a glass flask. A constant current of 10 mA or 20 mA (corresponding to 0.2 or 0.4 mA/cm^2) was applied and the voltage was monitored. During EDR, pH of the anolyte and catolyte was periodically adjusted with 1 M HNO_3 or 5 M NaOH, respectively, to maintain pH 2.

During EDR samples were taken from anolyte and catolyte approximately every second day to follow the cation concentrations. After EDR the electrodes were cleaned in 5 M HNO_3 for approximately 12 hours, to dissolve the electro-precipitated material and the membranes were

cleaned for approximately 12 hours in 1 M HNO_3, and the cation concentrations were then analyzed in the extracts.

The illite was divided into 3 slices perpendicular to the length of the compartment (numbered from the anode). Each slice was divided into two parts; one for analysis of XRF (only for EDR-II) and one for determination of cation concentrations.

Table 1: Experimental conditions

		EDR-I	EDR-II
Dry matter	g	248	252
Water content	%	22.2	22.1
Current density	mA/cm^2	0.2 (a), 0.4 (b)*	0.4
Voltage	V	4.1-11.7	5.2-17.2
Treatment time	Days	2 (a), 6 (b)*	35
Electrolyte volume (AN)	mL	500	2000
Electrolyte volume (CAT)	mL	500	1000

* EDR-I was first applied 0.2 mA/cm^2 for 2 days (a) and then the current density was raised to 0.4 mA/cm^2 (b).
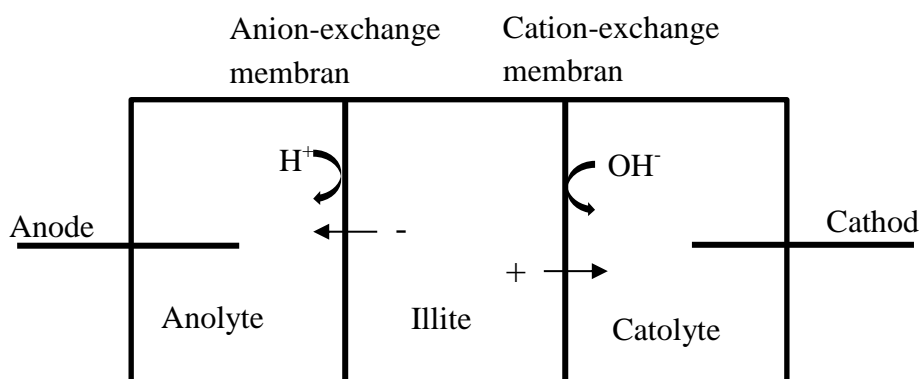

Figure 1: Illustration of the EDR setup.

Results and conclusions

- The two electrodialytic experiments showed that weathering of minerals occurred during EDR, since some Al, Fe and Si was recovered in the electrolytes.
- The removed fraction constituted 3.3 % (Al), 23 % (Fe) and 0.5 % (Si) of the total initial content, see Table 2.
- The acid soluble concentration of Al increased during EDR-II (Figure 2), which is undesired due to the toxicity of soluble Al.
- The acid soluble concentration profiles of Al (Figure 3) were almost identical in all three slices of both EDR-I and EDR-II, indicating that a kinetic equilibrium between the rate of electromigration of Al towards the electrolytes and the rate of Al mobilization from the matrix was established.

Table 2: Total concentration measured by XRF, the acid soluble fraction measured by DS 259, the initial amount of acid soluble element in the matrix and the amount removed into the electrolytes during EDR.

Element	Total (XRF) (mg/kg)	Acid soluble (DS 259) (mg/kg)	Acid soluble EDR-I (mg)	Removed EDR-I (mg)	Acid soluble EDR-II (mg)	Removed EDR-II (mg)
Al	95,000	9,660	2,400	10	2,430	798
Fe	37,000	12,900	3,220	154	3,260	2,114
Si	260,000	94	23	39	24	329

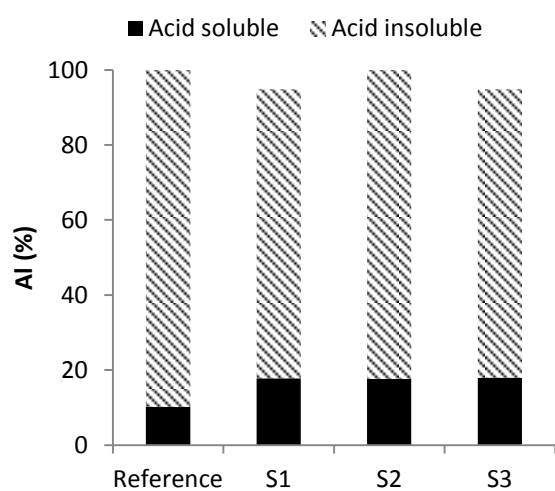Amount of dry matter: 248 g (EDR-I) and 252 g (EDR-II).

Figure 2: Distribution between acid soluble and acid insoluble fraction of Al in the initial matrix and in the three slices from EDR-II (named S1, S2 and S3). After the electrodialytic treatment the fractions is calculated on basis of the initial total content to visualize the reduction.
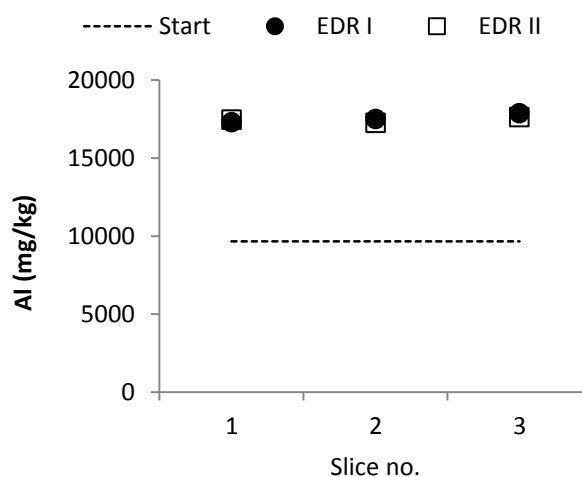

Figure 3: The profile of the acid soluble concentration of Al in the three illite slices numbered from the anode

Conference contributions

- EREM 2010, 9th symposium in electrokinetics, Taiwan. Title: The impact of the pore volume in sandstone on the electrochemical desalination rate. (Poster: Electrochemical desalination of sulfate from stone and the impact of calcium ions).

- Annual meeting of the Danish Electrochemical Society, October 2010, DTU, Denmark. Title: The impact of calcium ions on the electrokinetic desalination of sulfate from stone: Preliminary results. (Poster: The impact of calcium ions on the electrokinetic desalination of sulfate from stone: Preliminary results).

- EREM 2011, 10th symposium in electrokinetics, Belgium. Title: Test of a non-destructive method for determination of moisture changes in particulate materials during electrokinetic treatment. (Poster: Test of a non-destructive method for determination of moisture changes in particulate materials during electrokinetic treatment).

The impact of the pore volume in sandstone on the electrochemical desalination rate

Gry Petersen*, Lisbeth M. Ottosen

Department of Civil Engineering, Technical University of Denmark, 2800 Kgs. Lyngby, Denmark

ABSTRACT

Weathering caused by salt decay is undesirable. Electrochemical desalination can be an effective method for salt removal from sandstone and brick masonry and an alternative to application of absorbent poultices, which is the most widely, used method today. The rate of the electrochemical desalination is dependent on the amperage of the electrical DC field and to a great extent on the structure of the material (pore volume, and pore size distribution), and how the salts is distribute in the stone. This study is to investigate the impact of the porosity (pore volume) to the rate by which Na_2SO_4 can be electrokinetically removed from three different sandstones. The pore volume is increasing in the following order for the three sandstones; Øland < Nexø < Bremer. The experimental program is ongoing, but the preliminary results have indicated that the desalination rate of sodium sulfate will increase in the same sequence as the pore volume for the three sandstones.

KEYWORDS: Porosity, Desalination, Electrochemical, Diffusion, Rate

* Corresponding author. Tel.: +45 45251816
Email: gryp@byg.dtu.dk

INTRODUCTION

Weathering caused by salt decay of porous building materials like sandstone is a problem to cultural heritage and monuments. The source of salt may be different; most comes from de-icing salts with NaCl, sulfates and chlorides of Na and Mg; from rising groundwater, salt from ocean spray, and deserts dust (Winkler, 1987). The salts are transported into the material by moisture. The site of salt crystallization in the porous material is determined by the dynamic balance between the rate of escape of water from the surface and the rate of resupply of solution to that site (Lewin, 1982). The damaging effect of salts depends on the kind of salts present, on the size and shape of the capillary system, on the moisture content, and on the exposure to the solar radiation (Winkler, 1987). NaCl crystals grow on the stone surface, producing efflorescence while mirabilite-thenardite crystals grow inside the stone, producing subflorescence (Benavente et al, 2004). Subflorescence is considerably more damaging than efflorescence (Ioannis, 2008), which is more a visual problem.

In accordance to the Austrian ÖNORM '*Trockenlegung von feuchtem Mauerwerk; Bauwerksdiagnostik und Planungsgrundlagen*' the critical level for sulfate in masonry is above 0.25 % (2500 mg/kg). In a concentration below 0.10 % (100 mg/kg) sulfate is not expected to have any harmful effect and in the range in between, it is depend on an individual assessment. The most widely used methods for desalination of stones is by application of absorbent poultices (Vicente & Vicente-Tavera, 2001). A more efficient and time reducing methods is desirable and it is shown by Ottosen and Rörig-Dalgaard (2009) that electrochemical desalination is an efficient method for removal of salts from bricks. It is expected that the same method can be used for removal of salts from sandstone. The rate of the electrochemical desalination is dependent on the applied current of the electrical DC field and to a great extend on the structure of the material (pore volume, and pore size distribution), and how the salts is distribute in the stone. This (ongoing) study is to investigate the impact of the porosity to the rate by which Na_2SO_4 can be electrochemically removed from three different sandstones.

MATERIALS AND METHODS

The three stone used for the laboratory tests are Øland, Nexø, and Bremer sandstones. Øland is a red/brown sandstone, with a density at 2590-2680 kg/m^3 and a low porosity (0.52-1.82 %) (Suensen, 1942). The Nexø sandstone is a violet/red sandstone and the sample is visual inhomogeneous in separate layers (Figure 1). The Bremer sandstone is grey with brown spots and is the one with the largest porosity. The measured characteristics of the stone are listed in Table 1.

Fig. 1 The inhomogeneous Nexø sandstone.

Table 1 The density, pore volume, and the water absorption coefficient measured by capillarity of the test stones give as an average of three samples. The water absorption coefficient is measured in two directions; parallel and transverse to the direction of the applied electric DC field.

Stone	Density (kg/m^3)	Porosity (%)	Water absorption coefficient (g/(m^2·s$^{0.5}$))	
			Parallel	*Transverse*
Øland	*	*	*	*
Nexø	2424,74	8,32	8,421	13,122
Bremer	2097,93	20,88	40,860	38,336

*Not yet measured

Three samples (10.5 x 10.5 x 3.5 cm) of the three different sandstones are saturated in a solution of Na$_2$SO$_4$ to a concentration of 2500 mg sulfate/kg stone. After the saturation one of the samples is wrapped in plastic and used as a reference, one is for identify if diffusion can be neglected and the third sample is for the electrochemical treatment. The experimental set-up is inspired by (Ottosen and Rörig-Dalgaard, 2009) and is identical with the picture in Figure 2. On each side of the stone there are an electrode compartment filled with clay with water content at app. 30 %. Between clay and stone a piece of thin paper is placed. In each electrode compartment the two holes are closed with rubber corks. A platinum electrode is placed through one of the corks, the other hole is not used in this experiment. The stone is covered in plastic during the experiment to avoid evaporation. The experimental time is 3 days and the applied current is 10 mA. After the electrochemical treatment the sandstone is cut into three slices; anode end, cathode end, and the middle part. Water content, the sulfate concentration and the sodium concentration are measured in all samples from the stone and from the clay.
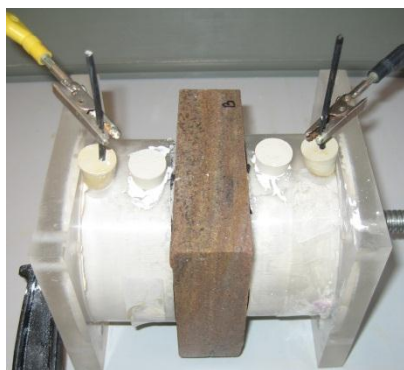

Fig. 2 The laboratory set-up. On each side of the stone there are an electrode compartment filled with clay. The stone was covered in plastic during the experiment to avoid evaporation of moisture.

EXPECTATIONS

The laboratory work is not finished yet but the preliminary results indicate that the simple diffusion in this case can be neglected compared to the desalination effect of the electric field. The sodium sulfate is not ~~removed~~ completely from the stone due to the short duration but a pattern of the desalination rate between the three sandstones is expected. Bremer has a high pore volume and is the stone with the highest water absorption coefficient which indicate that it is the stone with the largest amount of smallest capillary pores and it is likely that it will be the one with the highest desalination rate. It is expected that the desalination rate of sodium sulfate will increase in the following order for the tree stone; Øland < Nexø < Bremer.

REFERENCES

Benavente, D., M. A. García del Cura, J. Gracía-Guinea, S. Sánchez-Moral and S. Ordóñez, "Role of pore structure in salt crystallization in unsaturated porous stone", Journal of Crystal Growth, 260, pp. 532-544 (2004).

Ioannis, I., "Studies of salt crystallization in natural building stones" in Salt Weathering on Buildings and Stone Sculptures, Proceedings from the International Conference 22-24 October 2008, The National Museum Copenhagen, Denmark.

Lewin, s.Z., "The mechanism of masonry decay through crystallization", Conservation of Historic Stone Buildings and Monuments, Washington, D.c.: National Academy of Sciences, pp. 120-144 (1982)

Ottosen, L. M., and I. Rörig-Dalgaard, "Desalination of a brick by application of an electric DC field", Materials and Structures, 42, pp. 961-971 (2009).

Sawdy, A., A. Heritage, and L. Pel, "A review of salt transport in porous media, assessment methods and salt reduction treatments" in Salt Weathering on Buildings and Stone Sculptures, Proceedings from the International Conference 22-24 October 2008, The National Museum Copenhagen, Denmark.

Suenson, E., "Bygningsmaterialer, 3. bind: Natursten", Jul. Gjellerups Forlag, pp.117-139 (1942).

Vicente, M. A., and S. Vicente-Tarera, "Clay Poultices in salt extraction from ornamental stones: a statistical approach", Clays and Clay Minerals, Vol. 49, No. 3, pp. 227-235 (2001).

Winkler, E.M., "Weathering and Weathering Rates of Natural Stone", Environ Geol Water Sci Vol 9. No. 2, pp.85-92 (1987).

Authors:

Gry Skibsted*, Lisbeth M. Ottosen, Pernille E. Jensen
Department of Civil Engineering
Technical University of Denmark
Brovej, building 118
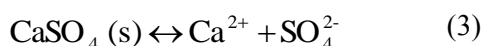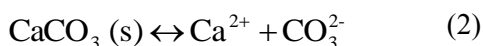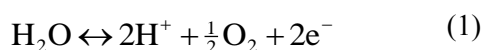2800 Kgs. Lyngby
Denmark

Title:

The impact of calcium ions on the electrokinetic desalination of sulfate from stone: Preliminary results

Abstract:

Salt can produce damage on porous materials like sandstone and bricks. The salts are transported into the pores in the material with moisture and due to the evaporation, the solution becomes super saturated and the salt can precipitate. Na_2SO_4 is particularly damaging because of its increasing volume caused by hydration leading to a crystal pressure high enough for the material to crack.

In laboratory, an experimental setup with a clay containing CaCO3 in the electrode compartments is used. The advantage of using clay with a relative high content of $CaCO_3$ in the electrode compartments is the buffer capacity. The production of acid at the anode (1) can decrease the pH in the part of the sample nearest to the anode. The carbonate containing clay (2) can avoid the pH drop by formation of bicarbonate and calcium ions are released and they will be the ions that can be transported into the sample instead of the protons. A side effect of the buffering from the anode compartment can be the generation of a calcium front in the stone sample and, as consequence; it can produce precipitation of $CaSO_4$ in the pores of the material (3). In this study it was evaluated if the calcium front can be a limiting factor for the desalination of sulfate from porous stone materials due to precipitations of $CaSO_2$ ($K_{sp} = 4.93 \cdot 10^{-5}$). For the experiments 3 different stones were used.

$$H_2O \leftrightarrow 2H^+ + \tfrac{1}{2}O_2 + 2e^- \qquad (1)$$

$$CaCO_3 \ (s) \leftrightarrow Ca^{2+} + CO_3^{2-} \qquad (2)$$

$$CaSO_4 \ (s) \leftrightarrow Ca^{2+} + SO_4^{2-} \qquad (3)$$

By the current setup with $CaCO_3$ containing clay in the electrode compartments for the electrokinetic desalination of SO_4 the Ca concentration in the stone increased due to electrokinetic treatment. Voltage during the electrokinetic desalination is highest in samples with the highest pore concentrations of Ca and SO_4 and can be explained by precipitations of $CaSO_4$. A significant increase in Ca combined with the unchanged SO_4 content for prolonged electrokinetic treatment indicates that precipitation of $CaSO_4$ can be the limiting factor for the effectiveness of the electrokinetic desalination of SO_4. Nevertheless, the sodium reduction is increased with the prolonged duration for the electrokinetic treatment so; this limiting factor does not stop the electrokinetic process itself. It only affects to the sulfate reduction.

Acknowledgements

Test of a non-destructive method for determination of moisture changes in particulate materials during electrokinetic treatment

Gry Skibsted[1,*], Lisbeth M. Ottosen[1], Henryk Sobczuk[2], Pernille E. Jensen[1]

[1]Department of Civil Engineering, Technical University of Denmark, 2800 Kgs. Lyngby, Denmark
[2]Institute of Environmental Protection Engineering, Faculty of Environmental Engineering, Lublin University of Technology, 20-618 Lublin, 40B Nadbystrzycka St., Poland

E-mail: gryp@byg.dtu.dk

Introduction

Moisture changes during electrokinetic treatment are often detected by the destructive weigh/drying method. The non-destructive method Time-Domain Reflectrometry (TDR) has provided a powerful tool for real-time, simultaneous measurement of soil water (Topp et al. 2000), but the method has not been tested in combination with electrokinetic treatment until now. A screening of the electroosmotic flow in two particulate materials during electrokinetic treatment is made by TDR. The TDR method is based on application of an electric pulse signal propagation in a two rods probe immersed in a material and the reflected signal is monitored. The moisture content decision is based on a standard curve established for the specific material. Calibrations consist in determination of moisture content by a reference method and comparison with the data measured by the TDR probe (Grunewald & Sobczuk, 2005). In this particularly case, the reference method was the weigh/drying method. The advantage of the TDR method for moisture measurement is that it is a non-destructive method and allows monitoring moisture change during experiments. Once the probe is installed it must be left intact in the material for as long as necessary and removed at the end of the experiment (Grunewald & Sobczuk, 2005).

Experimental Section

Two different experimental setups were used. Setup A consist of a box with the dimensions; length 25 cm, height 12 cm and depth 8 cm. In each end an electrode mesh was placed and the first 5 cm in each end was filled with clay. The clay had a high content of $CaCO_3$ to ensure a good buffering capacity to avoid extreme pH changes in the soil near the electrodes. In the middle part of the box (15 cm in length) soil was placed only separated from the clay with a thin filter paper. The soil was an unpolluted soil with a grain size below 2 mm. Setup B was similar to Setup A but instead of using soil and $CaCO_3$ containing clay in the electrode compartments, clay from Wewers brickwork was used in the hole volume. The electrode mesh was placed directly in the clay. The dimensions of setup B were; length 19 cm, height 12 cm and depth 8 cm. For the moisture measurement during the electrokinetic treatment FP[1]-time domain reflectometry (TDR) probes were used (Figure 1) in both experimental setups. The lengths of the rods were 100 mm and the distance between the two rods was 15 mm. In both experimental setups, the three TDR probes were placed with a distance of 5 cm in the middle of the box. Table 1 present the experimental details. After the electrokinetic treatment, the tested material was cut into slices (setup A: 5 cm each and setup B: 1 cm each) and the moisture content was analyzed by the weigh/drying method as a control.

---

[1] Field Probe

Table 1: Experimental details

	Exp. 1	Exp. 2	Exp. 3
Setup	A	A	B
Current (mA)	10 mA (first 4 days), 20 mA	20	0-142
Voltage (V)	6-38	7-20	40
Duration (days)	8	14	1
Moisture – start (%)	27.1	33.2	20.0
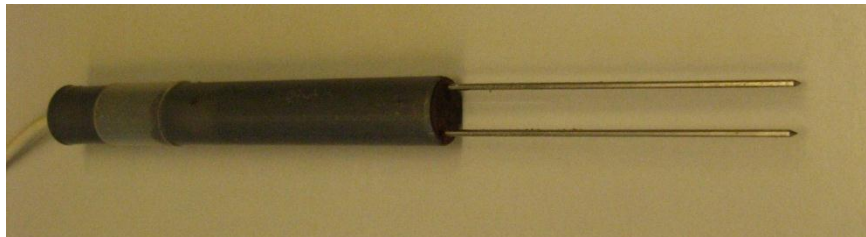
Figure 1: FP-time domain reflectometry (TDR) probe

Discussion

The screening of the TDR method showed advantages and disadvantages. The major disadvantage of TDR in combination with electrokinetic treatment is the narrow moisture interval in which the calibration curve is acceptable for the two tested materials. For the specific soil (Setup A) the calibration curve was only linear in the interval 20-27 % moisture content and for the clay it was 18-25 %. In this interval the deviation between the TDR measurement and the moisture content from the weigh/drying method at the end of the experiment was below 8 %. Outside this interval a deviation of 37 % was calculated for the soil with moisture content at 15.4 %. Topp et al. (2000) reported that a problem with the TDR method can arise in materials with significant electric conductivity. During the electrokinetic treatment the conductivity is even changing, which can cause the initially made calibration curve not to be acceptable to the same material after application of current for a period.

The advantages with the TDR method are that it is non-destructive and can be used during the electrokinetic treatment. It can be used for detection of electroosmotic flow, but the calibration needs to take conductivity changes into account.

References
Grunewald J, Sobczuk H (2005) Development of insulation materials with specially designed properties for building renovation. Chapter 5. Lublin, Polish Academy of Sciences, ISBN 83-89293-21-8

Topp GC, Zegelin S, White I (2000) Impacts of the Real and Imaginary Components of Relative Permittivity on Time Domain Reflectometry Measurements in Soils. Soil Sci. Soc. Am. J. 64:1244-1252